Master Thesis

What will a hub-based offshore network in the North Sea look like by 2050?

Author

Emma Larsson Ström
MSc. Energy Science
(9235914)

Word count

13,979

Guidehouse Supervisors

Marissa Moultak
Lennard Sijtsma

Utrecht University Supervisor

Dr. Matteo Gazzani

16th of August 2023

Contents

Abbreviations

CAPEX Capital Expenditure
CF Capacity Factor
DV Decision Variable
EEZ Exclusive Economic Zone
HVAC High Voltage Alternating Current
HVDC High Voltage Direct Current
LCOE Levelized Cost of Electricity
LCP Low Carbon Pathways
NUTS Nomenclature of Territorial Units for Statistics
NSEC North Sea Energy Cooperation
NSWPH North Sea Wind Power Hub
OPEX Operational expenditures
OWF Offshore Wind Farm
TSO Transmission System Operator
TYNDP Ten-Year Network Development Plan

Acknowledgements

This project could not have been completed without the unwavering patience of Marissa Moultak. Her support in answering my never-ending questions about LCP and her knowledge of energy system modelling has been crucial in helping this project come to life. Marissa- You are the LCP goddess! Equally important has the support of Lennard Sijtsma been, his knowledge of the offshore wind industry and overall calming presence have made this project better. When I spent weeks pulling my hair out and trying to get the model to work, your sharp minds and encouragement kept me going. I look up to you both.

Even though these past few months have been challenging, the experience of being an intern in the Energy Providers team at Guidehouse has been amazing. From coffee chats, countless ping pong games, encouraging words and willingness to help I have had a great time with you all!

And to Nino, thank you for letting there be three parts to our relationship these past months: you, me and LCP.

Abstract

In light of climate change and energy security issues, ambitious decarbonisation targets have been set across Europe. A cornerstone of realising these goals is a massive expansion of offshore wind power located in the North Sea. This area is one of the most favourable locations for successful wind projects in the world, due to a reliable wind resource and shallow waters. Considering announced plans to build upwards of 300 GW of offshore wind in the North Sea, how to best integrate this into the existing onshore energy system remains uncertain. A possible solution that has gained momentum in recent years is the build-out of an integrated transmission network placed offshore. This could transport the energy generated from offshore wind farms via a hub-based system to several nations. The hub-based network can comprise both power and hydrogen transmission infrastructure, as well as electrolysers placed offshore.

This project investigated potential configurations of such a hub-based offshore network in the North Sea by 2050, using a linear optimisation model. 2030 and 2040 were set as intermediate simulation years to monitor developments across the time horizon. The results indicate substantial build-out of both power and hydrogen transmission infrastructure, across all modelling runs. It predominantly consists of electricity connections, but hydrogen connections are also present. The electricity network displays both hub-to-hub as well as hub-to-shore connectivity. Major connection points across the offshore power network were found to be the areas around offshore wind farms (OWF) East Anglia, Nederwiek, Dogger Bank, and German search areas N 17-20. The 2050 offshore hydrogen network exhibits hub-to-hub connections between OWFs East Anglia and Nederwiek, and far-from-shore German OWF search areas N 17-20 and British Dogger Bank respectively. All other offshore nodes display the build-out of hydrogen pipelines which are radially connected to the shore.

1 Introduction

1.1 Societal & Scientific Background

Through the well-known Paris Climate Agreement, a vision was set for Europe to decrease greenhouse gas emissions by 55% in 2030, compared to 1990 levels [1]. This vision is driven by the threat of global warming, which is to be limited close to 1.5°C compared to pre-industrial levels [1]. Emission reduction efforts within the European Union are led by the 'Fit for 55%' package launched by the European Council, making it legally binding for all member states to comply [2]. This package will be the backbone of the decarbonization efforts that will need to occur across Europe. Steering the energy supply away from fossil fuel combustion and towards less polluting energy sources like wind and solar-based technologies will be an important cornerstone in decreasing emissions. Renewables have been rapidly growing, and are projected to account for 95% of all global power capacity growth to 2026 [3]. This will be essential for emission reduction.

Currently, close to 42% of European electricity is produced by fossil fuel combustion, and a quarter is produced in nuclear reactors [4]. Renewable sources together account for 33% of the European electricity supply, predominantly from wind-based technologies[4]. Energy is however not only consumed in the form of electricity, but also in fuels for transport and heat for industrial, commercial and residential purposes. At a global level, the total energy consumption is shared between 50% for heat, 30% for transport and 20% for electricity [5]. Fossil fuels constitute an even larger part of the former two, 60% of the global heat supply comes from fossil sources [5] and 91% of the final energy consumed within transport is oil-based [6]. Hence it is important to investigate ways to decarbonise all three segments by also looking beyond just decarbonising electricity.

Decarbonising the European energy supply is however not solely a climate conservation effort, but more recently also about ensuring a stable and secure energy supply. Geopolitical tensions as a consequence of the invasion of Ukraine have highlighted the European over-dependence on foreign fossil fuels, particularly from Russia [7]. This caused gas prices to soar over the past year, leaving businesses and households struggling to pay their energy bills [8], [9] and exacerbating energy poverty [10]. Prior to the war, 40% of all gas consumed in the EU came from Russia [11]. To escape this situation the European Union has responded with the REPowerEU plan, which states that independence from Russian fossil fuels can come through energy savings, diversifying of supply and an acceleration of the development of renewables [7]. REPowerEU plans have also shifted the role that natural gas can have as a bridging fuel for decarbonising Europe, adding further complexity to the European energy transition [7]. The plan emphasises the need for offshore wind energy to play a key role in the transition, as it is seen as a stable, clean and abundant resource [7].

1.2 The Role of Offshore Wind in the European Energy Transition

Offshore wind technology provides an immense opportunity to deliver affordable, clean electricity through harvesting kinetic energy found in wind to generate electrical power [3], [12]. The technical potential for offshore wind in 2040, when accounting for both floating and bottom fixed turbines, is 11 times greater than the expected global electricity demand in the same year [13]. This gives an indication of the scale of the opportunity. Offshore wind has seen a 30% annual growth rate between 2010-2018 [13], and is expected to be the fastest growing renewable technology until 2026 [3]. State-of-the-art offshore wind projects deliver capacity factors around 40-50%, thus matching capacity factors of power plants running on coal and gas [13]. This is crucial to reach high system integration and reliability while limiting curtailment. Neither onshore wind nor solar photovoltaics can achieve this high capacity factor [13].

Unlike traditional power generation such as coal and gas combustion is offshore wind reliant on a more variable resource, but its' output is less variable than other renewables. This makes it a favourable addition to power systems as it can help with providing baseload power [13]. It has even been referred to as a 'variable baseload technology', a class of its own, because of the increased dependency a system can place on it to maintain energy balance [13]. Offshore wind is further beneficial as it tends to generate more power during the winter season, thus matching the season with the greatest electricity demand in Europe [14]. There is less public opposition to Offshore Wind Farm (OWF) developments than to land-based renewable projects, as noise, shading and the visual impact of the installed wind turbines have less of an effect on humans [7], [12], [13]. Prioritising projects with higher public acceptance could be important to keep the pace of the energy transition sufficiently high.

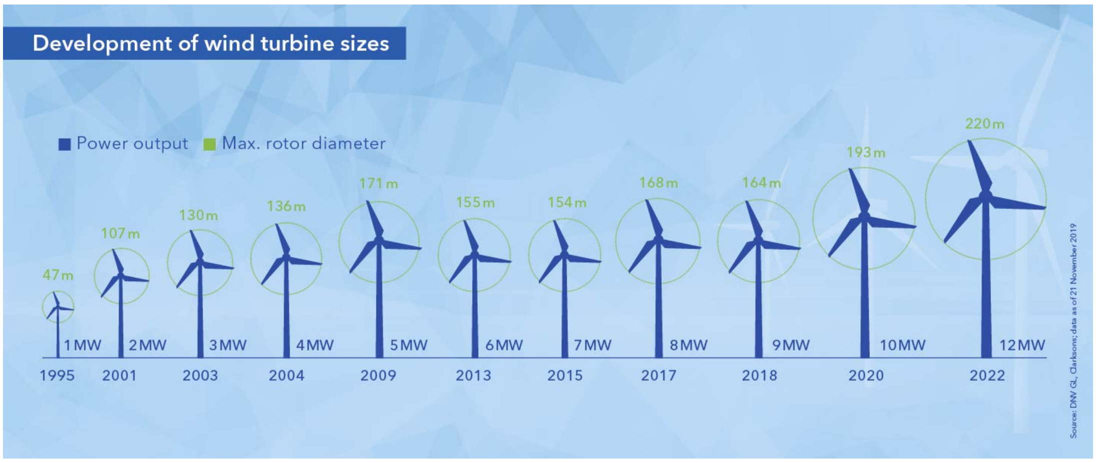

Figure 1.1: Size developments of commercially available wind turbines [15].

Apart from the technical advantages of offshore wind, financial advantages linked to a low Levelized Cost of Electricity (LCOE) competitive with fossil fuels are also reported in recent years [13]. Decreased costs are mainly linked with the development of larger, more powerful wind turbines [13]. The size evolution of wind turbines is presented in Figure 1.1. Larger turbines come at a higher investment cost, but the benefits of decreased operational costs across the turbine's lifetime and increased capacity factors provide positive net benefits and lead to an overall lower LCOE [13]. LCOE predictions for new offshore wind farms indicate that it will drop from 140 $ per MWh in 2018 to 70 $ per MWh in 2040 [13]. Offshore wind farms can transmit their generated power to shore via High Voltage Direct Current (HVDC) or High Voltage Alternating Current (HVAC) cables, the former being the most financially competitive when connecting wind farms located far from shore due to transmission losses [13].

One of the best European locations for offshore wind lies within the North Sea, surrounded by the Netherlands, Belgium, Germany, the United Kingdom, Denmark, Sweden and Norway (Figure 1.2). The North Sea offers shallow water depths and high wind speeds, making the conditions very favourable for successful offshore wind projects [16]. Two-thirds of the total European technical potential for offshore wind lies within this region [13], justifying the special attention it receives. The favourable conditions are also reflected in the fact that Danish Ørstedt, German RWE and Swedish Vattenfall jointly cover over 25% of the global offshore wind market, thus leading developments and installations globally [13].

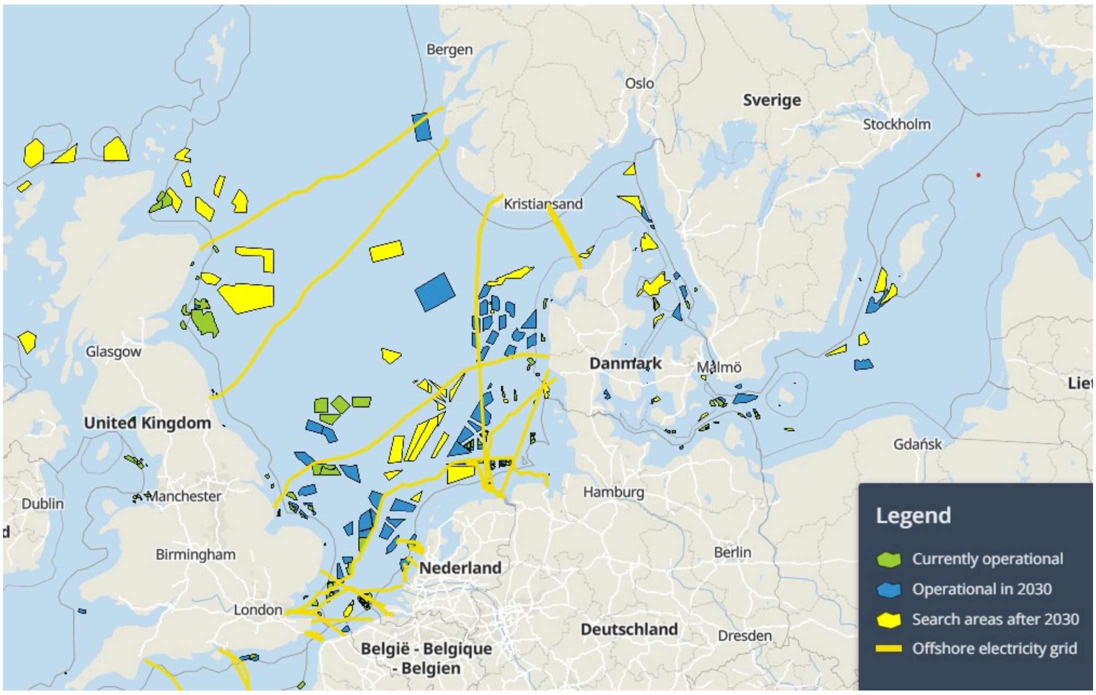

Figure 1.2: Map of North Sea offshore wind farms and current electricity grid [17].

When examining existing and planned offshore wind farms in the North Sea, presented in Figure 1.2, it can be seen that the number of operational wind farms by 2030 (blue) is far greater than those currently operational (green). This illustrates the expansive offshore growth that is expected in the North Sea in the coming decade. As suitable sites close to shores are becoming occupied, there is a trend towards wind farms being developed further from shore [13]. This allows for harvesting higher wind speeds and a more reliable wind resource, contributing to raising the capacity factor of offshore wind [13]. Developments of offshore energy infrastructure are however not discrete systems and they need to be interwoven with onshore energy infrastructure where consumers reside. Considering already existing issues of grid congestion [18]–[20], integrating additional large amounts of variable resources will be a challenge. This has led to the idea of a meshed offshore grid, whereby OWFs are connected via central points called 'energy hubs' to several countries to more efficiently distribute the produced power. An energy hub has been defined as a 'multi-carrier offshore energy system which encompasses production, conversion and/or storage' [21]. There is now a consensus among the majority of policymakers and the scientific community that building an interconnected offshore grid is important, both from a technical and financial standpoint, see e.g. [22]–[24]. Expanding offshore connections can also help relieve onshore grid congestion, such as those present in the UK [25]. A hub-based offshore grid is presented visually in Figure 1.3.

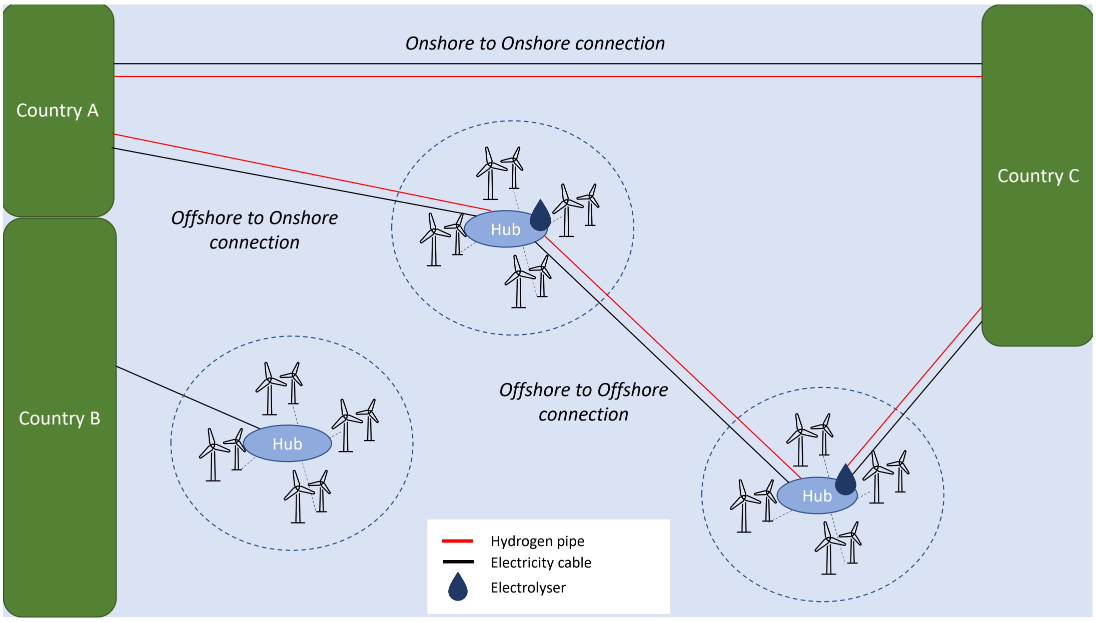

Figure 1.3: Visual representation of the offshore grid concept, adapted from [26].

Developing interconnected energy infrastructure in the North Sea, focused on large build-outs of OWF, was initially declared a goal for several countries in the region through the North Sea Energy Cooperation (NSEC) founded in 2016 [27]. In 2022 the NSEC collectively declared a target of 260 GW of offshore wind by 2050, representing 85% of the total European target [28]. More recently this ambition has been re-emphasised through the latest version of the Ostend Declaration announced in April 2023 [29]. Here the Netherlands, Belgium, Denmark, Germany, Norway, the United Kingdom, France, Ireland and Luxembourg together declared the goal of 300 GW of offshore wind by 2050, calling the North Sea the 'Green Power Plant of Europe' [30]. The North Sea Wind Power Hub (NSWPH) consortium initiated by Danish, Dutch and German electricity and gas TSOs further demonstrates the will to successfully develop integrated energy infrastructure in the North Sea [31]. The European Commission has also recognised an integrated North Sea grid as one of the prioritised infrastructure projects in Europe [22]. But achieving 300 GW of OWF by 2050 will require extensive infrastructure developments which is a complex task, as the North Sea is already home to fishing industries, gas and oil infrastructure as well as nature reserve areas [32]. There is therefore a growing body of research on North Sea offshore grid deployment, covered in further detail in section 1.3.

1.3 Previous Research & Literature Gap

Several previous studies have analysed North Sea offshore grid developments (e.g. [22], [25], [33], [34],), the majority focusing solely on the power system [35]. Hence, the interconnection with hydrogen and other energy sectors was often excluded [35]. Effects of coupling these sectors have albeit been explored on an EU level, but this has come at the expense of detailed results for the North Sea region [35].

Connecting wind farms individually to shore (radial connections) compared to creating an integrated offshore power grid was explored in [36] until 2050. It was found that an integrated power grid allowed for increased offshore wind investments, increased renewable generation and an overall lower system cost [36]. The decreased cost was mainly due to significantly lower fuel expenditures and CO_2 tax compared to the radially connected scenario [36]. Similar conclusions were drawn in [22] which analysed a UK-Benelux system consisting of three OWFs connected radially versus in an integrated manner. The researchers found that the integrated configuration produced both financial and environmental benefits compared to the radially connected system [22]. Other energy carriers than electricity were excluded [22]. In Ref. [37] research was conducted on the integration of offshore wind in the Netherlands, but import and export to neighbouring countries was assumed constant, no matter the weather conditions. Ref. [38] modelled a Dutch integrated energy system, but stated that future work is needed to include the remaining North Sea countries for more detailed results on offshore installations and hydrogen scenarios.

In an attempt to bridge this research gap Ref. [35] explored a North Sea energy system in 2050, using a linear optimisation model. The model included several energy carriers in Belgium, Denmark, Germany, The Netherlands, Norway, Sweden and the United Kingdom to optimise for technology investments and operation, based on radially connected OWFs [35]. The effect of different decarbonization scenarios to 2050 was also explored [35]. The results presented in [35] reveal that only the Netherlands and Germany reach their maximum OWF installed capacity potential in all scenarios, but the remaining countries do not. Through sensitivity analysis, it was investigated what the impact would be on British installed OWF capacities if the model was allowed to interconnect the UK, The Netherlands and Germany through offshore nodes [35]. This led to considerable increases in OWF investments and a build-out of offshore interconnections in the least cost solution [35], suggesting that allowing interconnections between the remaining countries could lead to similar beneficial results. The natural gas network was further assumed to be highly reliant on the imports from North Africa and Russia [35], the latter of which the EU now is doing its utmost to refrain importing from as a consequence of the war in Ukraine [7].

Ref. [34] explored possible North Sea offshore developments considering spatial limitations. Two main scenarios were investigated, the first being a solely power-based offshore system and the second allowing for both electricity and hydrogen transmission infrastructure build-out [34]. This was modelled using a linear programming methodology and optimised for simulation year 2050 [34]. Cost savings resulting from the build-out of an offshore grid were found in both cases, spanning from 1-7% relative to a system where no offshore grid developments were allowed [34]. This study allocated the location of their nine offshore nodes based on a k-means clustering algorithm of some of the existing and planned OWF in the North Sea. Only OWF areas which were deemed to possess a high degree of certainty in the realisation of their plans were included. This meant that several announced search areas for future OWF instalments were disregarded.

Furthermore is the economic and technical feasibility of integrating hydrogen production into an offshore network a contested topic. Ref. [26] found the inclusion of offshore electrolysis to lead to increased system costs while [39] found that generating hydrogen offshore rather than onshore lead to a lower Levelized Cost of Hydrogen (LCOH). Ref. [40] showed that offshore hydrogen can play a part of the optimal solution for a Dutch energy system, but stated that this is highly sensitive to levels of hydrogen demand, biomass availability and carbon capture and storage (CCS). In [41] the importance of building out hydrogen production offshore is highlighted, due to onshore spatial limitations that could make it difficult to expand cable landing points further. Considering the varying conclusions drawn in previous literature, more research into the topic is needed.

Further discussion and a comprehensive overview of the challenges that offshore energy systems have, and will face, focusing on the North Sea can be found in [32]. At their core these challenges mainly pertain to the lack of sufficiently detailed data and expertise across all the sectors researchers are trying to integrate, and a lack of computational power able to handle the complexities of an integrated energy system [32]. In light of the research gaps identified across the existing body of literature, more research is needed.

1.4 Research Question

As detailed in sections 1.1,1.3, further research is needed into possible future configurations of a North Sea offshore grid covering multiple energy carriers. This project undertook that endeavour, with a special focus on enhancing the granularity of the North Sea while maintaining cross-border interactions across mainland Europe. Considering this, the main research question was formulated to be:

> **"What will a hub-based offshore network in the North Sea look like by 2050?"**

In order to answer the main research question, three sub-questions were defined:

1. *What are the locations, functionalities, key characteristics and connection patterns of the offshore energy hubs?*
2. *What are the key characteristics and utilisation rates of the connection infrastructure to and from the offshore energy hubs?*
3. *What is the impact of varying electrolyser pricing on the resulting modelled offshore grid developments?*

To answer the main research question, along with the three sub-questions, Guidehouse's Low Carbon Pathways (LCP) model was employed. A description of LCP along with the theoretical background of energy system modelling is discussed in more detail in the next chapter, chapter 2. The methodology is thereafter outlined in chapter 3 followed by the results in chapter 4. A discussion of the results is provided in chapter 5 and conclusions of the study are summarised in chapter 6.

2 Theoretical background

2.1 Energy system modelling

As the European energy system becomes increasingly interconnected, the need for cross-border planning also increases. This has led to the Ten-Year Network Development Plan (TYNDP) initiative, whereby European power and gas Transmission System Operator (TSO)s jointly agree on a vision for how to develop the energy system over the coming decade [42]. This has become necessary as the expansion of energy supply technologies and its' related infrastructure is an investment intensive endeavour with long lead times which could require significant multi-national collaboration. As a result there is a growing body of research on energy system modelling which attempts to solve for the 'optimal' build-out; the configuration which fulfils the imposed requirements at the lowest cost to the system. Such requirements can be levels of emission reduction or self sufficiency.

Using models for investigating potential development paths is now common practice, as this allows for 'testing' the implications of varying policies and targets on the final outcome [25]. There are many types of energy system models which focuses on different aspects of an energy system, such as power dispatch modelling and capacity expansion modelling. Some well known examples of energy system models are EnergyPLAN [43], Plexos [44] and IESA-Opt [45].

2.1.1 Low Carbon Pathways model

This project employed Guidehouse's internal energy model Low Carbon Pathways (LCP), written in R programming language. LCP is a capacity expansion model, whereby the user can investigate how an energy system develops over a specified time horizon considering techno-economic detail, demand fluctuations, and imposed constraints. This is done by looking at how the installed capacity of energy supply technologies and their associated infrastructure will develop over time, guided by the main objective to minimise the present-day value of the total system costs. LCP is constructed to observe the energy flows of three main carriers, namely electricity, hydrogen and natural gas/methane. These three are the only forms of energy allowed to pass across the interconnection stage of the model, from the point of supply to the point of demand. This is illustrated in Figure 2.1, where all input fuels will need to be converted into either electricity, hydrogen or methane on the supply side before reaching the interconnection phase. After passing through the interconnection stage the three energy carriers are consumed in accordance to their respective specified demand. This simplification allows for decreasing the computational complexity significantly, compared to a real-life energy system. LCP is based on a linear optimisation methodology, which will now be covered in further detail.

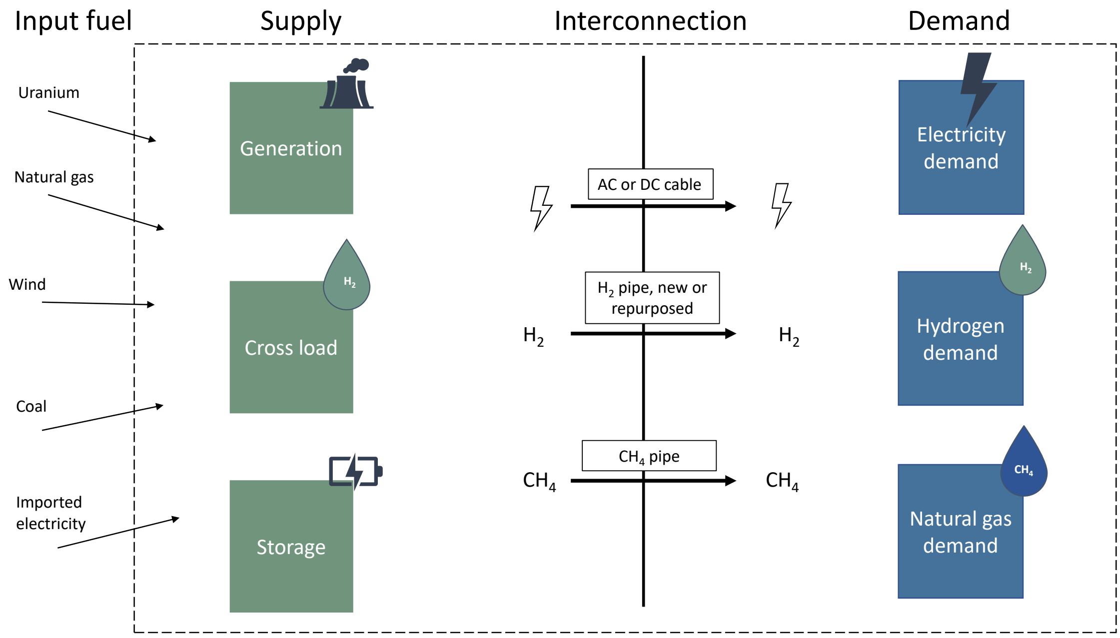

Figure 2.1: Simplified overview of energy flows in LCP at each node.

2.1.2 Linear optimisation

Linear optimisation, or linear programming, is a methodology to investigate optimal solutions to complex problems, where the optimum is defined as the solution that is associated with the lowest overall costs. Linear optimisation models have been employed extensively in energy systems literature, e.g. [35], [38], [46], as it allows for a manageable computational time through problem simplification, while still producing valuable results [47]. They can be adapted to investigate different problems, but at their core, they consist of three parts: decision variables, constraints and an objective function. Decision variables are those that the model will need to determine endogenously, which in capacity expansion modelling mainly pertains to the installed capacities of different supply and infrastructure technologies. Constraints define the computational space within which the optimal solution can be found. This can, for example, be the allowed CO_2 emissions, the maximum allowed build-out of a particular technology, or limits to allowed retrofitting. The objective function analyses the total set of decision variables, along with their associated cost coefficients, to find the optimal solution while still abiding by the constraints.

Mathematical formulation of LCP model

Figure 2.2 illustrates how the decision vector in LCP is formulated. At a high level, the matrix is firstly divided up by technology. This is can be either a supply technology such as a coal plant, an infrastructure technology such as a HVDC cable or a storage technology such as a battery. Each technology is optimised over several properties, for example, its' capacity, dispatch or charging. Figure 2.2 only displays the former two for simplicity. It can be seen that the capacity is optimised on an annual level, once per simulation year 2030, 2040 and

2050 respectively. Hence the Decision Variable (DV) size is equal to one per simulation year. The dispatch is however optimised on a more granular level, whereby LCP has to determine what quantity of energy should be dispatched from each technology in a specific hour on a specific day in a specific simulation year. This can for example be the energy dispatched in the first hour on the second representative day in the simulation year 2030. With 24 hours per day and 13 representative days per year, the DV size per annual dispatch becomes 312. The total set of DVs, i.e. the capacity and dispatch DVs for every technology (n) in every node (a) is known as the decision vector.

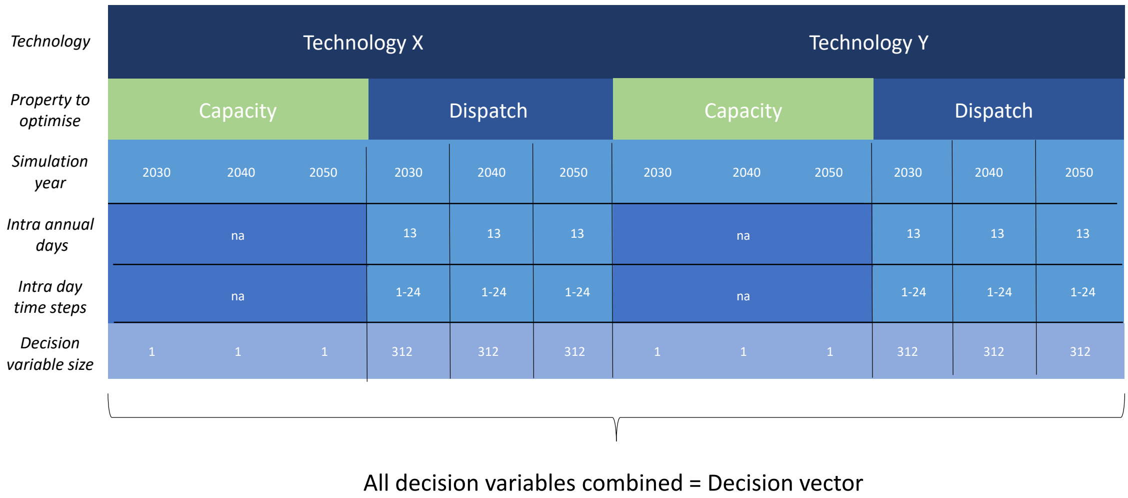

Figure 2.2: LCP decision matrix.

Each DV is associated with a cost, for the capacity-based DVs this pertains to their respective CAPEX values, while for the dispatch DVs this relates to the OPEX corresponding to the energy dispatch. For other optimising properties the corresponding costs may be other factors such as emission costs, and charging costs. The total set of cost variables is known as the cost objective vector, which combined with the decision vector forms the objective function, displayed in Equation 2.1. The objective function aims to minimise the present value of the total system cost.

Table 2.1: Variable explanation

Variable	Description	Unit	Variable	Description	Unit
t	Hourly time step	hour	F	Fuel demand/ use	MWh
T	Total set of time steps	n	E	Energy in/out	MWh
a	Node	n	DV	Decision variable	n
A	Total set of nodes	n	C_{new}	New capacity built	MW
n	Technological unit	n	C_{max}	Maximum capacity built	MW
N	Total set of technological units	n	$C_{retrofit}$	Retrofitted capacity	MW
D	Dispatch	MWh	C_{ret}	Retired capacity	MW
Y	Demand	MWh	R_{max}	Maximum replacement	MW

Objective function LCP

$$Minimise = \sum_{n \in N, a \in A} (DV1_{n,a}(t) \times Cost_{n,a}(t) + ... + DV_{n,a}(t) \times Cost_{n,a}(t)) \tag{2.1}$$

The costs associated with each DV can for example be Capital Expenditure (CAPEX) or Operational expenditures (OPEX) which can in turn consist of expenditures such as fuel costs, emission costs, commissioning and de-commissioning costs, and infrastructure costs.

Several constraints are imposed to ensure a feasible cost-optimal solution determined by LCP. Firstly, an energy balance constraint is imposed to ensure that the energy demand per energy carrier, node and time step is fulfilled. This is displayed in Equation 2.2.

$$D_{f,a}(t) = Y_{f,a}(t), f \in F, a \in A, t \in T \tag{2.2}$$

To account for system losses, the energy balance is further divided into an energy balance at the points of energy supply and energy demand (Equation 2.3). These are linked via an interconnection step. The supply side energy balance consists of input fuels such as upstream fuels like coal, biomass and natural gas together with natural resources like wind and solar irradiance. For each node on the demand side, three demand profiles are specified: one for electricity, one for methane CH_4 and one for hydrogen H_2. This means that across the interconnection step, moving from the energy supply to the demand, only the three energy carriers of electricity, CH_4, H_2 are considered to limit computational complexity. All input fuels thus have to be converted to one of the three energy carriers before reaching the interconnection step.

$$\sum E_{in} = \sum E_{out} \tag{2.3}$$

There are also several constraints placed on the capacity expansion. Firstly a constraint on the annual allowed capacity build-out is enforced, Equation 2.4, to ensure that LCP does not expand the capacity of a technology faster than what is realistic.

$$C_{n,a,new}(t) \leq C_{n,a,max}(t), a \in A, n \in N, t \in T \tag{2.4}$$

The total allowed capacity build-out across the entire simulation period was also constrained through Equation 2.5.

$$C_{n,a,new}(t) - C_{n,a,retrofit}(t) - C_{n,a,retired}(t) \leq C_{n,a,max}(t), a \in A, n \in N, t \in T \tag{2.5}$$

As this model contained the option to retrofit natural gas pipes to transport hydrogen, this was limited through Equation 2.6.

$$C_{retrofit} \leq R_{max} \tag{2.6}$$

A constraint was also placed on the energy dispatch, to ensure that it does not exceed the installed generation capacity (Equation 2.7).

$$D(t) + C_{retrofit}(t) - C_{new}(t) \leq C_{known}(t) \tag{2.7}$$

To restrict model fuel usage, the following constraint was imposed on the objective function:

$$\sum(F_{input,a}) \leq F_{max,annual} \tag{2.8}$$

2.1.3 Spatial granularity

In order to analyse a large geographical region certain simplifications are often made. One of these is the division of a geographical area into smaller regions, which can then be represented using a single point, or 'node' in the modelling. A nodal approach allows for assigning all the input data associated with a region to a single point, so geographical complexities can be disregarded. There is however a trade-off between decreasing spatial granularity and how well the modelled outcomes represent real-life behaviour. Being mindful of this balance is particularly important as intermittent renewables grow in prominence, as their energy outputs can be highly location-specific due to their weather dependency [48].

Despite this, a common methodology to divide Europe into smaller geographical regions is the Nomenclature of Territorial Units for Statistics (NUTS) methodology, where NUTS-0 represent entire countries while NUTS-2 are smaller areas where regional politics apply [49]. The benefit of this methodology is that it can be applied to a vast range of research, also beyond those which are energy-related. An approach that is more targeted toward energy-related research is to use electrical bidding zones as the defining border of each node. This methodology was for example applied in the Ten-Year Network Development Plan (TYNDP) created by ENTSO-E [50].

2.1.4 Temporal resolution

With increased variable renewable generation, the importance of temporal detail also becomes more prominent [48], [51]. This is because intermittent renewables are dependent on ever-changing weather patterns, making it difficult to accurately forecast their power output. To decrease the computational complexity of capacity expansion modelling, the temporal resolution is often limited to a set of 'time slices' [52]. Time slices represent periods of time with similar characteristics, such as those with similar variable renewable generation or extraordinarily high energy demand [52]. Together, the complete set of time slices should represent the majority of situations that the energy system will likely face throughout the simulation horizon, as this outlines the boundaries within which the energy system needs to be functional. An overview of different approaches applied to time slicing while modelling energy systems with high variable renewable penetration is presented in [52].

Moreover, the temporal resolution of a capacity expansion model is also dependent on whether a static or dynamic approach is chosen [53]. In a static modelling exercise, the system configuration of the target year is solely considered, with no regard to how the system developed over time to get there. A dynamic modelling exercise on the contrary considers how the capacity expansion unfolds across the entire simulation horizon, and hence produces more detailed results. These detailed results however come at the expense of increased computational complexity, meaning that they are often limited in their scope [53]. A hybrid approach was taken within this project, whereby the system configuration in three simulation years was investigated, namely 2030, 2040 and 2050. Capacity developments for the time between these simulation years were disregarded. This provided some detail into how the energy system developed over time, while still keeping the computational complexity relatively low.

For capacity expansion exercises the temporal resolution is mainly dictated by two parts; the energy demand profiles and the renewable supply curves. The demand profile specifies an hourly energy demand at each node, which can fluctuate across the entire set of time steps. The renewable supply curves convert wind speed or solar irradiation fluctuations to power output curves. These fluctuations come about as a result of the time of day, season and location. To find a balance between capturing variability and limiting computational time 'representative days' can be used.

Representative days

To decrease computational complexity in the temporal domain is the selection of representative profiles to represent a larger set of time steps often used [52], [54], [55]. The aim of the representative days methodology is to choose a set of days which represent the behaviour of a larger data set, without having to include the full data set with all the time steps.

Within the context of energy system modelling, this can be a smaller set of daily profiles that are used to represent an entire year. The need for representative days has risen with the increased integration of intermittent renewables within the energy system [51]. Energy system modelling is reliant on appropriately encapsulating the variability of renewables, system costs are otherwise underestimated and renewable technology expansion is overestimated [54]. Their intermittent nature means that their electricity generation is changing with the weather and is hence less predictable than that of fossil-based generation. As weather patterns are highly location-specific, there is also a need for spatial granularity.

Representative days are used to create time slices, where a single value is placed on demand and supply [54]. There is no singular method for selecting representative days, which makes it difficult to determine the suitability of the selection [52], [54]. The literature review conducted in [52] revealed that the majority of previous literature used a demand variation-based selection method, which cannot be used on models that include intermittent renewables [52]. The timing of the renewable generation is also important to consider with respect to the timing of the demand, as this will determine curtailment levels and the economic value of the renewable generation assets, as well as their environmental impact from avoided emissions [54]. Ideally, the correlation between demand profiles and supply profiles across different regions is maintained throughout the representative day selection [54].

In [52] an analysis was conducted to determine a suitable number of representative days, as the optimised power generation mix was significantly different when using one representative day, versus one hundred representative days. This is especially important to consider for wind power as a 30% higher installed capacity was seen in the one-day run compared to the 100-day run [52]. By using only one representative day the system was not able to capture the output variability of the wind power, making it seem more favourable and dependable than in reality [52]. This also negatively affected the installed capacities of nuclear and natural gas turbines, which in reality are needed for balancing services and to provide base load power [52]. Ref. [52] ultimately found six representative days to be sufficient to get results closely resembling that of the hundred representative day run, reporting a 4% difference in system costs and 2.5 % difference in the installed capacity of intermittent renewables.

There are two main approaches in literature to selecting representative days; heuristics or creating a set of time slices which together form the best combination according to predefined success criteria [54]. The heuristic approach relies on the fact that even though there is significant variability in the weather patterns on each day, there are similarities in the wind behaviour across many days of the year [54]. Hence, in order to represent all the possible weather scenarios only a smaller number of days are needed.

3 Methodology

This chapter describes the steps taken in order to answer the main research question. Firstly the model topology was constructed in order to create system boundaries in LCP. Extensive data collection and processing were thereafter performed to prepare the input data for LCP modelling. An overview of the LCP modelling process is provided in Figure 3.1. The robustness of the results was lastly tested through a sensitivity analysis. Each step of the methodology will now be covered in further detail.

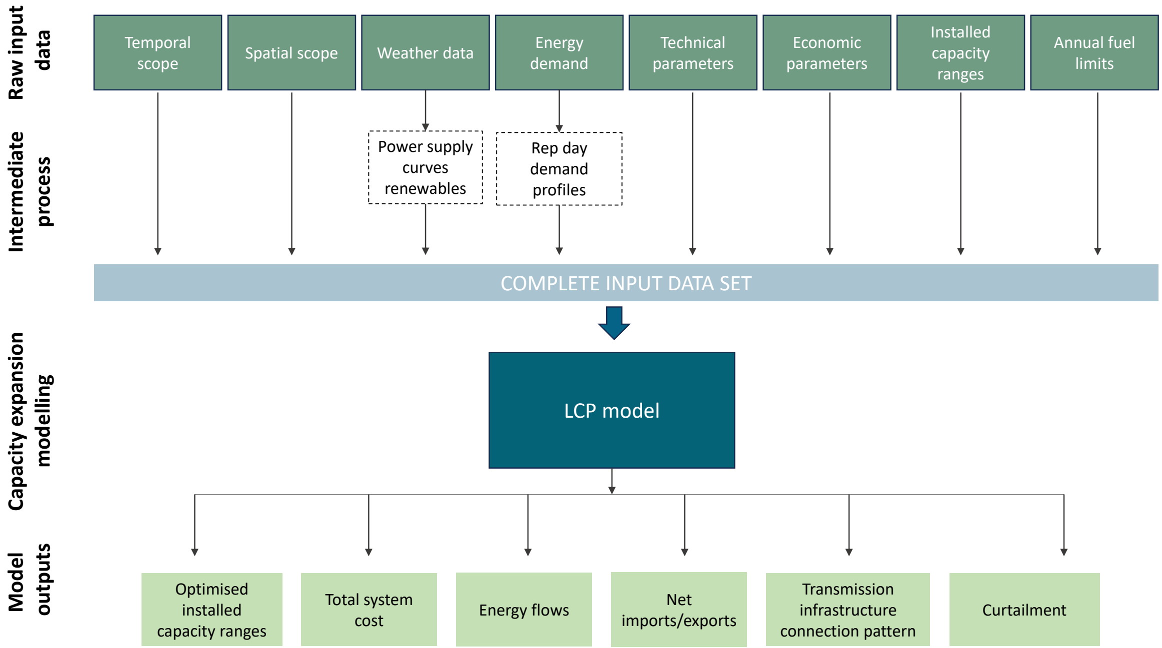

Figure 3.1: LCP modelling process overview

3.1 Model topology

In order to employ LCP for the use case determined in this project, a model topology was firstly constructed. This consisted of setting up the spatial granularity and the temporal resolution.

3.1.1 Spatial granularity

The importance of including European cross-border interactions throughout an energy modelling exercise has been discussed in [56], where the researchers state that it improves the reliability of the results. Hence, a large geographical scope was deemed necessary in order to determine the configuration of a North Sea offshore energy system in 2050. This included the entirety of onshore Europe, together with the North Sea region, as developments in the North Sea are likely highly affected by the vastly interconnected onshore energy systems. To computationally cope with this, a nodal approach was used. Within this project, the area within a node is assumed to operate under a copper plate assumption, i.e. there is no restriction to the energy flows within the region.

Onshore nodes

All onshore nodes, with the exception of the Netherlands, were assigned to be the same as those defined in the TYNDP data set created by [42]. These are defined as the geographical midpoint of each electricity bidding zone in Europe [50], shown in Figure 3.2. It can be seen that for all European countries, besides Sweden, Norway and Italy, the electricity bidding zones represent the entire country (NUTS-0 level). Keeping these identical to those used in [42] increased the repeatability of this project.

Figure 3.2: TYNDP nodes marked on map.

In order to expand on previous work on this topic, [38], the Netherlands was dis-aggregated further than its' singular TYNDP node, to instead consist of three onshore nodes. Building on the work performed in [57], Dutch NUTS-2 segregated data (Figure 3.3) was clustered into

3 onshore regions for the Netherlands, with 4 NUTS-2 regions in each. These 3 regions were referred to as NLN for Netherlands North, NLM for Netherlands Middle and NLS for Netherlands South. A major landing point for offshore energy infrastructure is located within each of these three regions; NLN with Eemshaven, NLM with Beverwijk and NLS with Maasvlakte.

Figure 3.3: NUTS map of the Netherlands, with NLN, NLM and NLS marked on map. Adapted from [49].

Offshore nodes

As this research focused on offshore developments in the North Sea, this region was investigated with enhanced spatial granularity to the rest of Europe. National development plans for offshore wind were analysed for the Dutch, German, Danish, Norwegian, Belgian and British parts of the North Sea through desk research. A selection of these development maps can be found in Table 2 in the Appendix. This was done in an effort to identify major OWF locations within each Exclusive Economic Zone (EEZ) that could act as offshore nodes. Their currently installed capacities, planned future installed capacities and de-/commissioning years were collected to serve as the basis for the allowed optimisation ranges (section 3.2). The data was primarily obtained from governmental websites, as these plans are usually set on a national level.

As an example of this process, the Dutch planned offshore developments can be used. As reported by [58] three OWF areas stand out, namely Nederwiek/IJmuiden Ver (6 + 6 GW), Doordewind (4 GW), and search areas 6-7 (10 + 6 GW). An energy hub in search area 6-7 is further stated as a planned development in [59]. Considering their large expected installed capacities and distant location to shore (between 62-100 km), these OWFs are assumed to be possible locations for future energy hubs and were therefore chosen as the 3 offshore Dutch nodes within this project. The identified OWFs and their respective sources for each country's offshore wind development plans are displayed in Table 3.1, with the full list of considered OWFs available in Table 2 in Appendix 1. OWFs located in the proximity of each other within the same EEZ were clustered together to jointly form a node. The midpoint of each OWF zone was determined as the nodal coordinate, and thus hub location, all mapped out in Figure 3.4. To visualise the entire spatial topology applied in this project, Figure 3.5 combine all onshore and offshore nodes.

Table 3.1: North Sea planned offshore wind developments and sources

Country	Major OWF identified	Data source
The Netherlands	Ijmuiden Ver, Search areas 6-7, Doordewind	[58]
The United Kingdom	Hornsea, East Anglia, Dogger Bank	[60]–[66]
Belgium	Princess Elizabeth energy island	[67]
Denmark	Nordsøen energy island	[68]
Germany	Search areas N 3.5-17	[69]
Norway	Sørlige Nørdsjo II	[70]

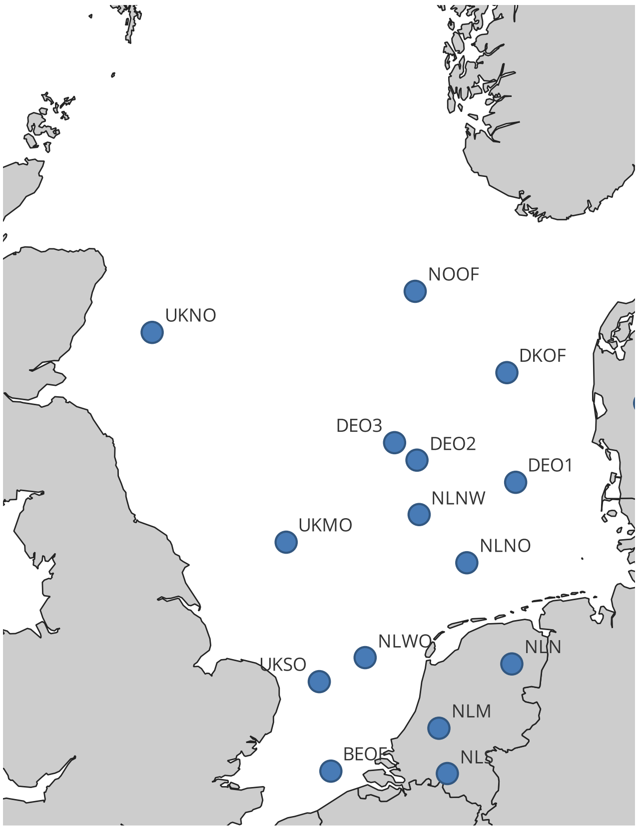

Figure 3.4: North Sea offshore nodes marked on map

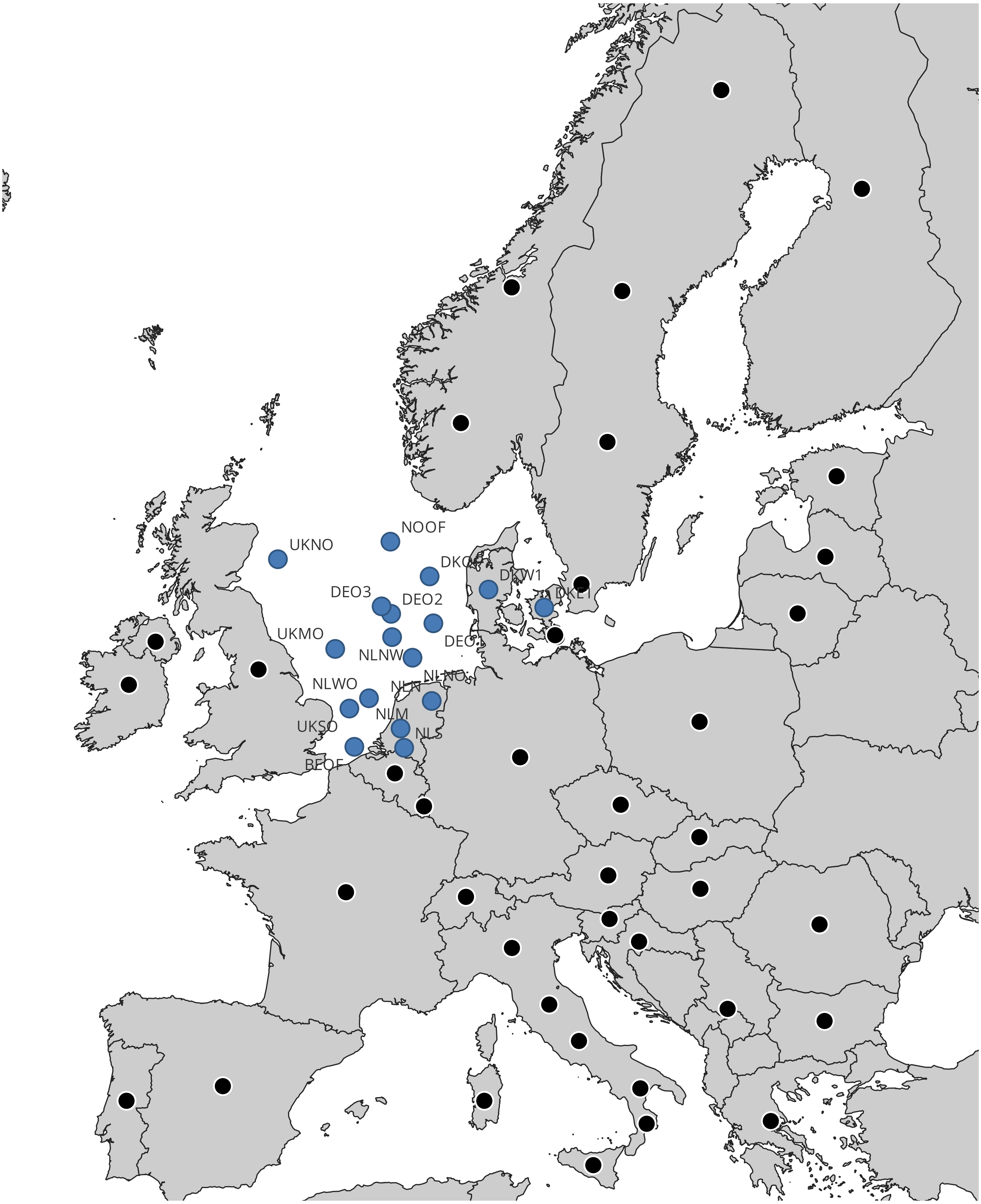

Figure 3.5: Overview of all nodes analysed in the project.

Table 3.2: Node abbreviations and coordinates.

Model Nodes	Representing	Latitude	Longitude
BE00	Belgium	50.8	4.7
CH00	Switzerland	47.0	8.1
DE00	Germany	51.3	10.7
DEKF	Germany offshore Baltic sea	54.7	12.4
DKKF	Denmark offshore Baltic sea	54.8	12.3
FI00	Finland	65.2	26.9
FR00	France	47.1	2.4
GR00	Greece	39.2	22.6
IE00	Ireland	53.4	-7.9
LU00	Luxembourg	49.8	6.1
NO00	Norway, cluster	61.8	9.3
PL00	Poland	52.3	19.2
SE00	Sweden, cluster	63.5	15.9
UK00	United Kingdom	53.8	-1.8
UKNI	Northern Ireland	55.0	-7.0
DKOF	Denmark Offshore	56.3	6.4
DKW1	Denmark West	56.0	9.2
DKE1	Denmark East	55.5	11.8
NLN	The Netherlands North	52.9	6.5
NLM	The Netherlands Middle	52.1	5.0
NLS	The Netherlands South	51.6	5.2
NLNO	The Netherlands North Offshore	54.1	5.6
NLNW	The Netherlands North West Offshore	54.7	4.6
NLWO	The Netherlands West Offshore	53.0	3.5
UKNO	United Kingdom North, Offshore	56.8	-0.8
UKMO	United Kingdom Mid, Offshore	54.4	1.9
UKSO	United Kingdom South, Offshore	52.7	2.6
DEO1	Germany Offshore 1	55.1	6.5
DEO2	Germany Offshore 2	55.3	4.5
DEO3	Germany Offshore 3	55.5	4.1
NOOF	Norway Offshore	57.2	4.5
BEOF	Belgium Offshore	51.6	2.8
BALT	The Baltics	57.0	24.9
EAST	Hungary, Romania, Slovakia, Slovenia	46.4	18.9
ESPT	Spain and Portugal cluster	40.2	-5.7
IT00	Italy, cluster	41.1	13.1

3.1.2 Temporal resolution

Simulation period

This project aimed to investigate a North Sea offshore grid by 2050, with 2030 and 2040 set as intermediate simulation years. 2020 was set to be the current year, in line with the Ten-Year Network Development Plan (TYNDP) [71]. LCP was hence tasked with solving the capacity expansion for each of the simulation years 2030, 2040 and 2050. The installed capacities in the years between the simulation years were assumed to be constant. Within each simulation year, the computational complexity was further decreased by cycling through thirteen representative daily profiles instead of using 365 unique daily profiles. These 13 days represented each calendar month together with an additional peak demand profile. The number of days that each representative day characterises is shown in Table 3.3, equivalent to the weighting applied to each representative profile when forming the annual profile.

Table 3.3: Representative days and their respective weighting

Representative day name	Weight [days]
January	27 (-4 given to peak)
February	28
March	31
April	30
May	31
June	30
July	31
August	31
September	30
October	31
November	30
December	27 (-4 given to peak)
Peak day	8

Representative energy demand profiles

The capacity expansion explored within this project is driven by the aim to serve the specified hourly energy demand for each energy carrier, at each node. This means that at every time step, there is a specific amount of electricity, methane and hydrogen required at each location. LCP must compute a solution that can fulfil this demand, as the energy balance must always hold. For the European nodes which were identical to those used in the TYNDP the demand profiles were obtained from [42], where they were provided on an annual basis covering 8760 hours. For the nodes placed onshore in the Netherlands (i.e. NLN, NLM, NLS) the demand profiles were prepared in a different manner. Using the Dutch demand profile provided by [42] this was further dis-aggregated using the clustered demand shares presented in Table 3.4, based on the work from [57]. The 2040 demand shares were assumed to also apply in 2050.

Applying the demand shares from [57] allowed for capturing regional differences across the Dutch mainland, in terms of industrial clustering and residential energy demands. A similar methodology was also applied in [72]. It can be seen in Table 3.4 that the energy demand across all three energy carriers is highest within node NLS, corresponding to the industrial areas located in this part of the country.

Table 3.4: Demand shares of Dutch regions, average across all seasons and time steps. Based on work from [57].

	Electricity [%]			Hydrogen [%]			Methane [%]		
Node	2020	2030	2040	2020	2030	2040	2020	2030	2040
NLN	18.62	10.68	10.88	0	1.77	2.13	18.49	17.80	15.13
NLM	28.23	17.06	25.58	0	0.77	6.30	11.94	16.09	19.10
NLS	53.16	72.26	63.54	0	97.46	91.57	69.56	66.11	65.77

In order to transform the annual demand profiles into ones consisting of 13 representative days the following approach was taken:

For every calendar month (e.g. January, February) the same time step across every day was averaged to give the representative day's energy demand for the same time step. Taking January as an example, the energy demand for every first hour of each day in January (i.e. hour 1 January 1st, hour 1 January 2nd, hour 1 January 3rd etc.) was averaged to give a single value for the energy demand in hour 1 in the representative day named *January*. Similarly, this was done for every hour 2 on every day of January (i.e hour 2 January 1st, hour 2 January 2nd, hour 2 January 3rd etc.), every hour 3 and so forth until there were 24 time steps with specified energy demand for the representative day of *January*. This was replicated for every calendar month until the demand profiles for the 12 representative days of *January, February, March, April,....., December* were constructed. The day with the highest energy demand in the 8760 hourly profile was also determined and assigned to the representative day denoted as *Peak day*.

Representative supply curves

In order to determine the energy generated by the intermittent renewable technologies of offshore and onshore wind, power supply curves were determined. Firstly, sample wind turbines were chosen to represent the existing and future installed offshore/onshore wind turbines. Different models were chosen for the currently installed and those installed in the future to reflect expected technological advancements. Selecting the representative wind turbines was needed as this provided the power curves with which the capacity factors across the simulation years could be determined. In Table 3.5 the selected technologies can be found, along with their sources. The selection was made considering the current average sizes of wind turbines placed offshore versus onshore, and the likely average sizes of their counterparts in the future. For other renewable technologies, such as solar PV or solar thermal, power curves were already determined by Guidehouse for all TYNDP nodes.

Table 3.5: Selected representative models for currently existing and future installed wind turbines, along with key technical parameters.

	Key parameters		
Technology	Rated power [MW]	Hub height [m]	Source
Offshore wind existing	10	119	IEA 10 MW ref. turbine [73]
Offshore wind new	15	150	IEA 15MW ref. turbine [74]
Onshore wind existing	2.3	80	Siemens SWT-2.3-108 [75]
Onshore wind new	3.6	115	Siemens SWT-3.6-130 [76]

Each selected wind turbine is associated with a specific power curve, which shows the turbine power output behaviour as a function of wind speed. An example of a power curve is shown for the 10 MW IEA reference turbine in Figure 3.6 below.

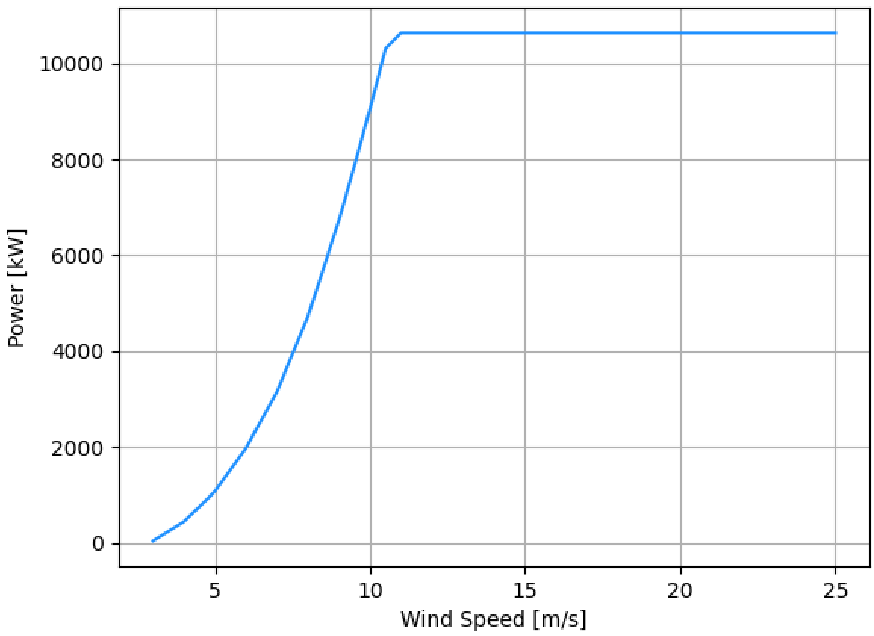

Figure 3.6: Power curve for the IEA 10 MW reference turbine [73]

After the representative technology selection was made, the annual Capacity Factor (CF) fluctuations were determined using the Windatlas.xyz online tool [77]. This tool takes the power curve and hub height of a selected turbine and computes the CF output as a function of wind speed for a specified location and climatic year. In this project 2009 was selected as the weather year, as this is the most representative climate year according to [50]. Detailed documentation for how the annual CF profiles are made in Windatlas.xyz is provided in [78]. In Figure 3.7 the wind speed fluctuations across a year at node NLNO can be seen, and in Figure 3.8 the resulting annual CF profile for a 10 MW turbine placed at the same node is shown.

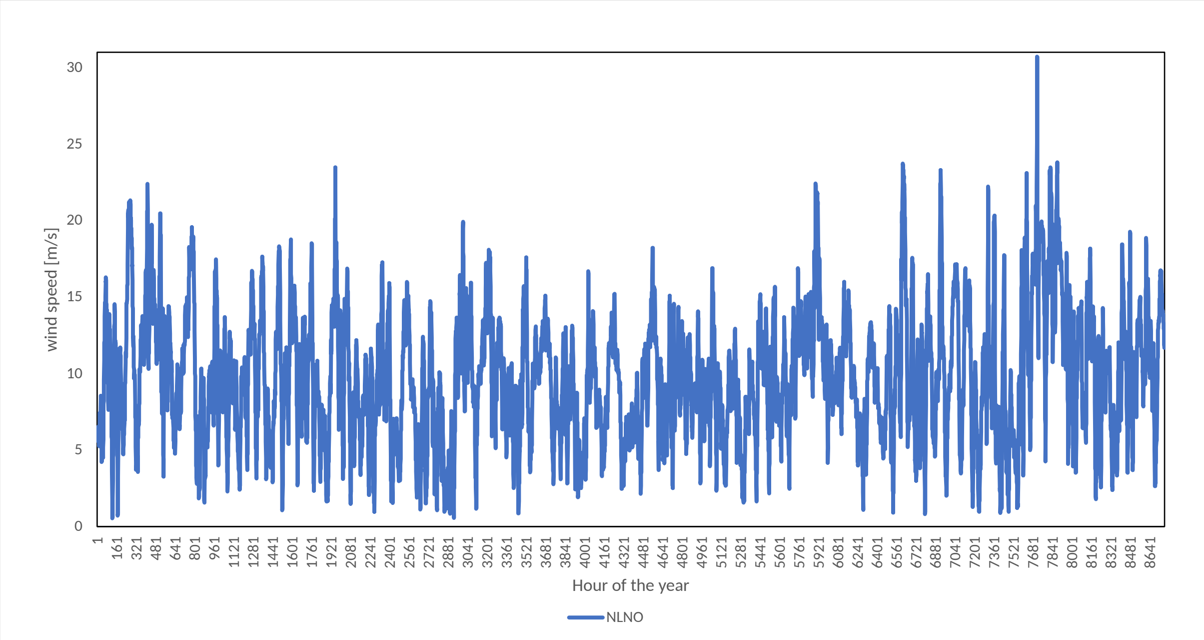

Figure 3.7: Annual wind speeds fluctuations at node NLNO.

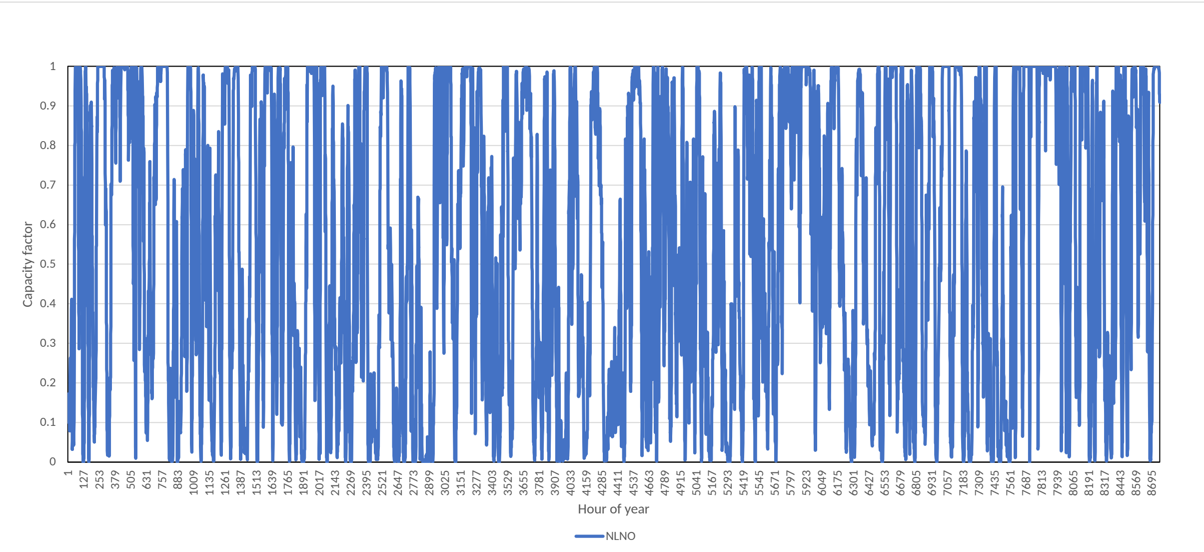

Figure 3.8: Annual capacity factor fluctuations for a 10 MW turbine located at offshore node NLNO.

This process was repeated for all applicable nodes and corresponding renewable technologies. The importance of maintaining the spatial granularity at this step can be seen in Figure 3.9 where the CF of the same 10 MW turbine placed at different nodes significantly varies across different points in time.

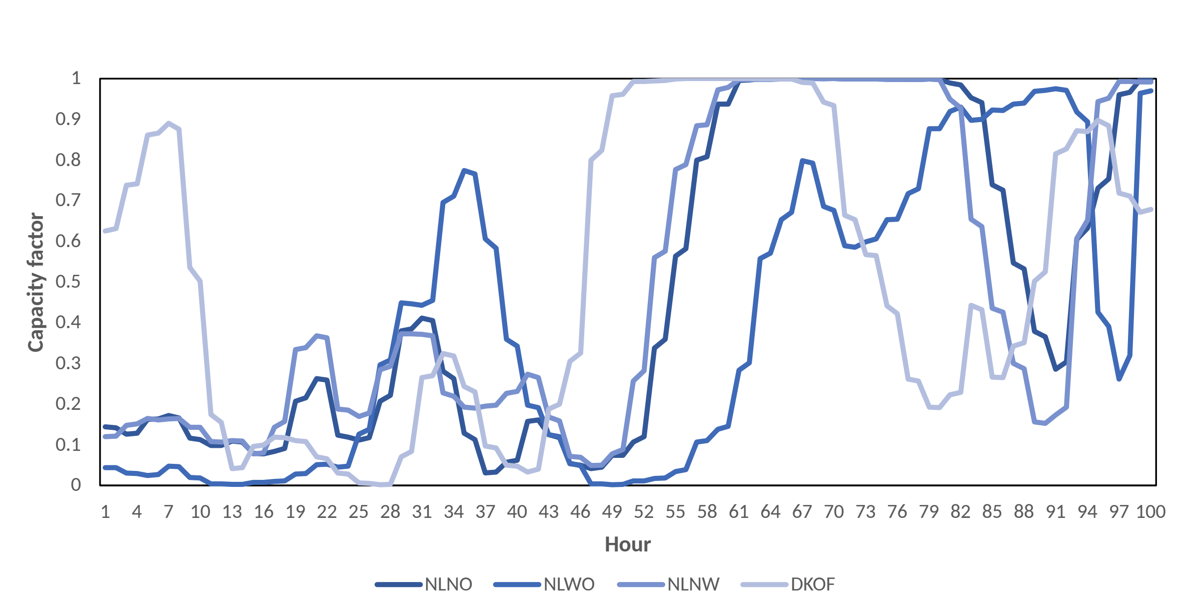

Figure 3.9: Capacity factor variations across 100 time steps, for a 10 MW turbine located at four different offshore nodes.

The main objective when creating the supply profile curves was to find a balance between creating a representative profile for the yearly production, while still being able to capture the power output variability. Finding monthly averages like previously done for the demand profiles could not be used for the representative supply curve, as this could mask extreme weather events during which the renewables experience exceptionally high or low production. Therefore, the following methodology was applied.

Using the yearly capacity factor profiles, including 8760 hourly time steps, obtained from the Windatlas.xyz tool [77] the data sets were treated to firstly calculate, per node, the annual, seasonal (i.e. monthly) and daily average CFs using Equation 3.1, Equation 3.2 and Equation 3.3. The yearly average is used to benchmark that the selected representative days together constitute a yearly output which is close to the yearly average. The same logic was applied to the seasonal averages, where these values were used to ensure that the selected days were close to the seasonal average.

$$CF_{avg,annual} = \frac{\sum_{annual} CF}{8760hrs} \tag{3.1}$$

$$CF_{avg,season} = \frac{\sum_{season} CF}{(\sum_{season} Days \times 24hrs)} \tag{3.2}$$

$$CF_{avg,daily} = \frac{\sum_{Dayx} CF}{24hrs} \tag{3.3}$$

Daily average CFs were filtered by month to only keep the days that fell within +/- 10% of the seasonal averages for that same season and node. From this set of filtered days, the daily fluctuations were determined by Equation 3.4.

$$\Delta CF_{daily} = CF_{daily,max} - CF_{daily,min} \tag{3.4}$$

Determining daily fluctuations for each filtered day was done in an effort to select days that have a high degree of wind speed variability, in order to capture the intermittent nature of these technologies. The day with the highest daily CF fluctuation within each season was assigned to be equivalent to the maximum seasonal fluctuation. To capture the variability across the course of a day hourly fluctuations per node were calculated according to Equation 3.5. These hourly fluctuations were thereafter normalised through Equation 3.6 and the average hourly CF fluctuations per day were determined by Equation 3.7.

$$\Delta CF_{Hourly} = CF_{hour,n} - CF_{hour,n+1} \tag{3.5}$$

$$\Delta CF_{Hourly,normalised} = \frac{\Delta CF_{Hourly}}{\Delta CF_{Hourly,Max}} \tag{3.6}$$

$$\Delta CF_{Avg,hourly} = \frac{\sum(\Delta CF_{Hourly,norm.})}{24hrs} \tag{3.7}$$

After doing this on a node-by-node level, the entire group of offshore nodes was clustered together to determine the group average, minimum, and maximum daily CFs. Group daily fluctuations were also determined, and normalised using the maximum daily fluctuation across the group.

From the set of hourly and daily fluctuations per node and per group, a weighted average was determined (Equation 3.8). The day within each season with the highest weighted average daily fluctuation was selected as the representative day. This methodology ensured that the selected days had a high degree of variability hour by hour but also on a daily level per node, and that they were days which were variable across the whole group.

$$\overline{\Delta CF}_{DayX} = \frac{(\Delta CF_{Hourly,norm,node} + 2\Delta CF_{Daily,norm.,node} + \Delta CF_{Daily,norm.,group})}{4} \tag{3.8}$$

Once the selection of the representative days was made, the mean of their raw CFs was determined. The representative day CFs were scaled through Equation 3.9, and any resulting scaled CFs above 1 were assumed to be equal to 1.

$$CF_{scaled,t} = \frac{CF_{avg,season}}{CF_{avg,repday,season})} * CF_t \tag{3.9}$$

Extremely unfavourable weather events for renewable power production, i.e. days with very low wind speeds and direct irradiance can occur up to 50-100 hours per month in November, December and January across the North Sea region [79]. These weather events are commonly known as 'Dunkelflaute' and usually occur in seasons with high energy demand, making them particularly challenging for an energy system with high renewable integration to cope with [79]. It is imperative that an energy system has sufficient resilience and flexibility to handle these events, and that they are included in energy systems modelling to accurately estimate their associated costs [80]. To simulate 'Dunkelflaute' events within this project, the day with the lowest daily CF per node was assigned to the representative *Peak day*.

3.2 Energy Supply

There are 145 energy supply technology categories available within LCP, representing both fossil and renewable technologies. Input data on the already existing installed capacities of each technology, as well as the planned build-out (has to be built in LCP) and the minimum and maximum potential capacity expansion levels (determined endogenously by LCP) was therefore collected. The majority of this data was retrieved from the nodal breakdown in the Distributed Energy scenario of the TYNDP, published by [42]. This scenario's underlying story line is one where there is a high societal drive for energy security based on domestic renewable sources, thus maximising European renewable energy production [42]. This corresponds with the underlying ambition of this project; to massively expand renewable power generation in the North Sea to support the European energy transition.

3.2.1 Onshore nodes

The installed capacities of all the supply technologies located onshore were assigned fixed expansion capacities in line with TYNDP [71], to limit computational complexity. LCP was therefore not left with any degrees of freedom to optimise the capacity expansion of these. The only exception to this was the expansion of onshore electrolysers as this should be coupled to the optimised levels of OWF and offshore electrolyser build-out. Technology categories included at each onshore node are presented in Table 3.6. It can be seen that a range of pipelines, both for H_2 and CH_4, were modelled as cross-load technologies and are assumed to have no losses across their transportation (100% efficiency). Russia is abbreviated as RU, Norway as NO, the Middle East as ME, North Africa as NA and UA stands for Ukraine. The technology categories that are listed in Table 3.6 with an efficiency range instead of a singular value are constructed by several sub-categories in LCP.

Table 3.6: Supply and cross-load technologies, electricity, hydrogen, and methane included for onshore nodes. These were retrieved from [50], [81].

Technology	Input	Output	Lifetime	Efficiency
Nuclear PP	Nuclear	Electricity	50	0.33-0.35
Biomass PP	Biomass	Electricity	30	0.34-0.41
Heavy Oil PP	Heavy Oil	Electricity	30	0.36
ICGG	Hard Coal	Electricity	30	0.39
CH_4-CCGT	CH_4	Electricity	30	0.41-0.6
H_2-CCGT	H_2	Electricity	30	0.6
LightOil	Light Oil	Electricity	30	0.37
OilShale PP	Oil Shale	Electricity	30	0.29
ST Hard Coal	Hard Coal	Electricity	30	0.35-0.43
ST Lignite	Lignite	Electricity	30	0.35-0.43
ST waste heat	Waste heat	Electricity	30	0.33
Wind onshore	Wind	Electricity	30	Determined by power curve
Wind offshore	Wind	Electricity	30	Determined by power curve
Solar PV	Solar	Electricity	40	Determined by power curve
Solar Thermal	Solar	Electricity	30	Determined by power curve
Hydro	Hydro	Electricity	100	1
Electrolyser-ONW	Wind	Hydrogen	25	0.69-0.74
Electrolyser-OFW	Wind	Hydrogen	25	0.69-0.74
Electrolyser-PV	Solar	Hydrogen	25	0.69-0.74
H_2 - Pipeline - NO	H_2 NO	Hydrogen	31	1
H_2 - Pipeline - ME	H_2 ME	Hydrogen	31	1
H_2 - Pipeline - NA	H_2 NA	Hydrogen	31	1
H_2 - Pipeline - UA	H_2 UA	Hydrogen	31	1
H_2 - Pipeline - RU	H_2 RU	Hydrogen	31	1
H_2 - Shipped	H_2 - Shipped	Hydrogen	31	1
Biomethane	Biomethane	Methane	31	1
Domestic Natural Gas	Natural Gas	Methane	31	1
CH_4 - Pipeline - NO	CH_4- NO	Methane	31	1
CH_4 - Pipeline - ME	CH_4 ME	Methane	31	1
CH_4 - Pipeline - NA	CH_4 NA	Methane	31	1
CH_4 - Pipeline - RU	CH_4 RU	Methane	31	1
CH_4 - Pipeline - ME	CH_4 ME	Methane	9	1
CH_4 - Pipeline - NA	CH_4 NA	Methane	9	1
CH_4 - Pipeline - RU	CH_4 RU	Methane	9	1
CH_4 - Pipeline - ME	CH_4 ME	Methane	31	1
CH_4 - Pipeline - NA	CH_4 NA	Methane	31	1
CH_4 - Pipeline - RU	CH_4 RU	Methane	31	1
CH_4 - Shipped	CH_4 - Shipped	Methane	9	1

3.2.2 Offshore nodes

Two technologies, namely offshore wind power and offshore electrolysers, were the only two supply technologies allowed to be built at the offshore nodes. Their technical parameters are presented in Table 3.7. The offshore electrolysers are constructed using three sub-categories within LCP; those installed in 2030 (69% efficiency), 2040 (71% efficiency) and 2050 (74%). The efficiencies are assumed to increase due to expected technological improvements over the coming decades. LCP was allowed to freely optimise the electrolyser capacities without restrictions, but the build-out of the offshore wind power was restricted to ensure realistic results.

Table 3.7: Technologies included at offshore nodes.

Supply Technology	Input	Output	Lifetime	Efficiency
Offshore wind	Wind	Electricity	30	Determined by power curve
Offshore electrolyser	Electricity	Hydrogen	25	0.69-0.74

In order to determine suitable optimisation ranges for each offshore node, the national offshore wind targets and published governmental site plans for offshore wind developments were investigated. The result of this endeavour is presented in Table 3.8 and an example of a site plan is provided in Figure 3.10. It can be seen that the overall targets and the announced site plans rarely align, with a discrepancy as high as 93 GW for the United Kingdom in 2050. To combat this ambiguity in OWF capacity expansion targets , the difference was allocated between the nodes to allow LCP to have the option to build out until the highest target. For the Netherlands this was done by allocating 1/4 of the difference to nodes NLNO and NLWO each, and the rest to NLNW due to its far from shore location. For Germany and the United Kingdom the difference between the targets were equally distributed between their respective offshore nodes. For Denmark, half of the difference was allocated to the Danish offshore node DKOF while the rest was assumed to be in other areas than the North Sea and was thus allocated to the DKW1 node. Differences in the Belgian targets was all allocated to the offshore node BEOF, while for Norway the discrepancy was all assumed to be built out in other locations than Sørlige Nordsjøand was thus allocated to the NOS0 node.

Table 3.8: Announced national OWF targets and site plan targets, North Sea offshore wind. * denotes values that have been calculated by taking the average of the targets in the surrounding years.

	Overall targets [GW]			Site plan & TYNDP values [GW]			Difference [GW]		
	2030	**2040**	**2050**	**2030**	**2040**	**2050**	**2030**	**2040**	**2050**
NL	22	50	70	6.3	54.8	54.8	15.7	0.0	15.2
DE	30	40	70	21.0	34.5	34.5	9.0	5.5	35.5
DK	12.9	23.95*	35	12.6	24.5	16.7	0.3	0.0	18.3
UK	50	108.5*	125	31.2	31.2	31.2	18.8	77.3	93.8
BE	8	8	8	5.8	5.8	5.8	2.2	2.2	2.2
NO	-	30	30	3.0	3.0	3.0	0.0	27.0	27.0

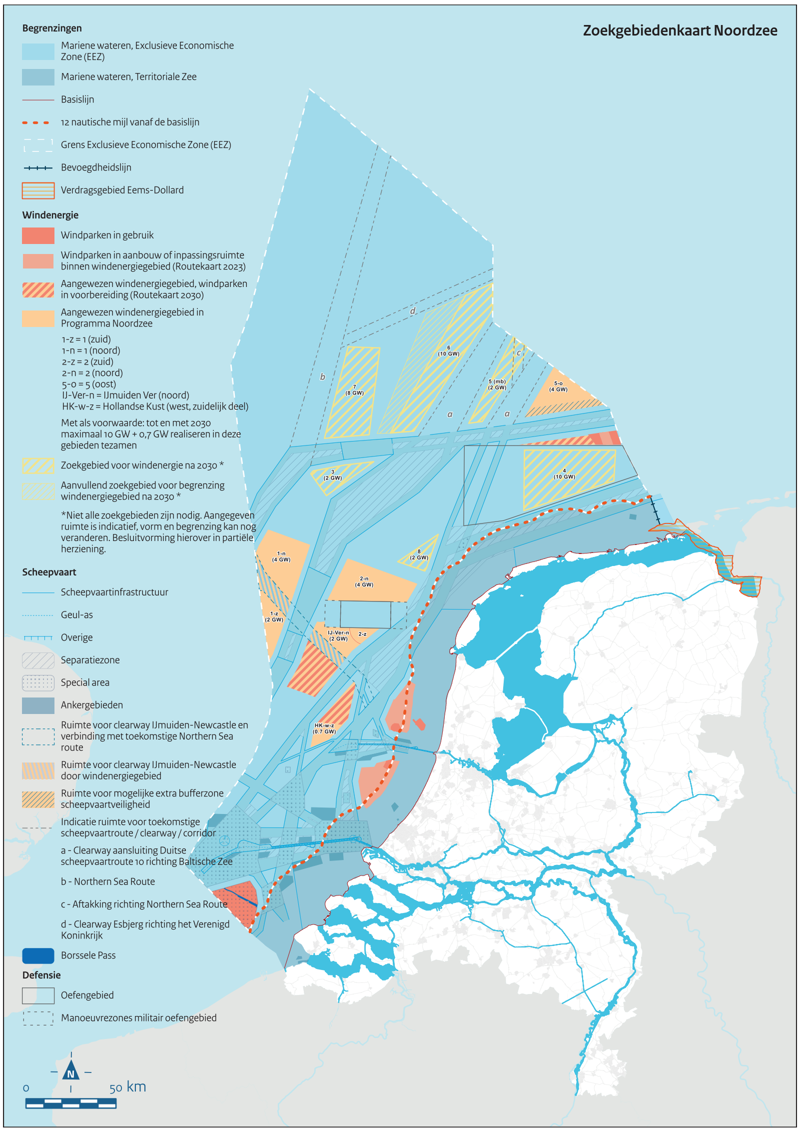

Figure 3.10: Planned Dutch offshore wind developments [82].

To ensure that the development path optimised in LCP resembled the national targets, a minimum OWF build out of 75% of the announced site plans was enforced. The maximum OWF expansion was capped at 100% of the announced overall governmental plans, as these were seen as highly ambitious and not likely not be surpassed. The resulting optimisation ranges for each offshore node are presented in Table 3.9. The installed capacities of the offshore electrolysers were allowed to be freely optimised, as the build-out of these is coupled to the offshore wind developments. All the offshore wind turbines located at the offshore nodes were assumed to be fixed bottom turbines, due to the lower water depth of the North Sea [83].

Table 3.9: Optimisation ranges for offshore wind [GW]

		Existing	Total max			Total min			Planned retirement		
Country	**Node**	**2022**	**2030**	**2040**	**2050**	**2030**	**2040**	**2050**	**2030**	**2040**	**2050**
NL	NLNO	0.6	4.6	14.7	18.5	0.7	11.2	11.2	0.0	0.0	0.0
NL	NLNW	0.0	7.9	24.0	31.6	0.0	18.0	18.0	0.0	0.0	0.0
NL	NLWO	3.4	9.5	16.1	19.9	5.0	12.9	9.9	0.0	0.0	3.0
DE	DEO1	6.6	22.9	27.3	37.3	16.6	20.7	20.7	0.0	0.0	0.0
DE	DEO2	0.0	3.0	7.8	17.8	0.0	4.5	4.5	0.0	0.0	0.0
DE	DEO3	0.0	3.0	3.8	13.8	0.0	1.5	1.5	0.0	0.0	0.0
NO	NOOF	0.0	3.0	3.0	3.0	2.3	2.3	2.3	0.0	0.0	0.0
BE	BEOF	2.3	8.0	8.0	8.0	4.9	4.9	4.9	0.0	0.0	0.0
UK	UKNO	0.0	14.1	33.6	39.1	5.8	5.8	5.8	0.0	0.0	0.0
UK	UKMO	2.5	18.7	38.2	43.7	9.9	9.9	9.9	0.0	0.0	0.0
UK	UKSO	1.2	10.6	30.1	35.6	3.5	3.5	2.3	0.0	0.0	1.2
DK	DKOF	0.0	3.2	10.0	19.1	2.3	7.5	7.5	0.0	0.0	0.0

3.3 Storage technologies

Energy storage technologies are crucial for large-scale integration of renewable technologies [84]. These will also play an important part in building European energy security and were hence included in the model. The included types of storage technologies are listed in Table 3.10. Technology categories that are listed with a range instead of a singular value for the hourly storage duration consist of several sub-categories in LCP.

Table 3.10: Storage technology overview

Technology	Input/Output	Lifetime [yrs]	Duration [hrs]	Seasonal?	Efficiency
Battery	Electricity	25	4	No	0.92
DSR-loadShift	Electricity	31	1	No	1
Hydro	Electricity	100	4-24	No	0.8
Hydro storage	Water	100	200-1000	Yes	1
Line packing	Hydrogen	50	3	No	0.999
AGS	Hydrogen	30	48	No	0.9
Salt Cavern - new	Hydrogen	50	180-1200	Yes	0.995
Salt Cavern - repurp.	Hydrogen	50	180-1200	Yes	0.995
Depl. Gas Field - repurp.	Hydrogen	50	900-2400	Yes	0.995
Rock Cavern - new	Hydrogen	50	200	Yes	0.995
Line packing	Methane	50	3	No	0.999
AGS	Methane	30	48	No	0.9
Depl. Field - existing	Methane	50	900-2400	Yes	0.995
Other UGS - existing	Methane	50	250-2850	Yes	0.995

3.4 Economic input values

In order for the optimisation to be run, each supply and storage technology was assigned a Capital Expenditure (CAPEX), a fixed and a variable Operational expenditures (OPEX). These values are presented in Table 3.11. The CAPEX is specified per unit of installed capacity (i.e. €/MW), while the fixed and variable OPEX are in €/ MWh. A discount rate of 5% was used to determine the present-day system costs of the capacity expansion.

Further, the cost of each fuel unit was prepared as input data for the model, based on [50]. To reflect the expected price fluctuations across seasons and simulation years, as a consequence of demand-supply interactions over the simulation period, these were specified for each time step.

Table 3.11: Economic input values for CAPEX, variable and fixed OPEX for all storage and supply technologies. Values given in €$_{2020}$*Retrievedfrom*[71], [81]

SupplyTechnology	**CAPEX [€/MW]**			**Fix. OPEX [€/MW-year]**			**Var. OPEX [€/MWh]**		
	2030	2040	2050	2030	2040	2050	2030	2040	2050
Nuclear PP	0	0	0	0	0	0	9	9	9
Biomass PP	0	0	0	0	0	0	3.3	3.3	3.3
Heavy Oil PP	0	0	0	0	0	0	3.3	3.3	3.3
ICGG	0	0	0	0	0	0	1.1	1.1	1.1
CCGT	830000	800000	800000	27800	26900	26000	1.6	1.6	1.6
OCGT	435000	424000	412000	7700	7600	7400	1.6	1.6	1.6
LightOil	0	0	0	0	0	0	1.1	1.1	1.1
OilShale PP	0	0	0	0	0	0	3.3	3.3	3.3
ST Hard Coal	0	0	0	0	0	0	3.3	3.3	3.3
ST Lignite	0	0	0	0	0	0	3.3	3.3	3.3
ST waste heat	0	0	0	0	0	0	3.3	3.3	3.3
Wind onshore	915000	817000	758000	10500	9100	8600	1.4	1.3	1.3
Wind offshore	2076000	1954000	1851000	38800	35900	33900	2.8	2.6	2.5
Wind offshore fixed	1817000	1710000	1620000	38800	35900	33900	2.8	2.6	2.5
Solar PV	333000	281000	250000	6000	5400	5000	0	0	0
Solar Thermal	0	0	0	0	0	0	0	0	0
Hydro power	0	0	0	0	0	0	0	0	0
Electroyser-Offshore	616250	475000	337500	27500	22500	17500	0	0	0
Electroyser-Grid	493000	380000	270000	22000	18000	14000	0	0	0
Electroyser-ONW	1586323	1331113	1125668	32817	27217	22822	2.1	1.8	1.7
Electroyser-OFW	2760000	2439000	2132000	74000	65000	57000	4.1	3.7	3.4
Electroyser-PV	810000	643000	504000	26000	22000	18000	0	0	0
Hydrogen - Pipeline - NO	0	0	0	0	0	0	0	0	0
Hydrogen - Pipeline - ME	0	0	0	0	0	0	0	0	0
Hydrogen - Pipeline - NA	0	0	0	0	0	0	0	0	0
Hydrogen - Pipeline - UA	0	0	0	0	0	0	0	0	0
Hydrogen - Pipeline - RU	0	0	0	0	0	0	0	0	0
Hydrogen - Shipped	432000	353000	273000	10800	8825	6825	5	4	3
Biomethane	0	0	0	0	0	0	0	0	0
Domestic Natural Gas	0	0	0	0	0	0	0	0	0
Methane - Pipeline - NO	0	0	0	0	0	0	0	0	0
Methane - Pipeline - ME	0	0	0	0	0	0	0	0	0
Methane - Pipeline - NA	0	0	0	0	0	0	0	0	0
Methane - Pipeline - RU	0	0	0	0	0	0	0	0	0
Methane - Shipped	0	0	0	0	0	0	0	0	0
Battery	764000	500000	378000	5670	5670	5670	1.9	1.8	1.7
DSR-loadShift	0	0	0	0	0	0	0.1	0.1	0.1
Hydro storage	360000	360000	360000	7200	7200	7200	0.1	0.1	0.1
H2 Line packing	241200	241200	241200	7200	7200	7200	0	0	0
H2 AGS	1598.4	1598.4	1598.4	32	32	32	0.1	0.1	0.1
H2 Salt Cavern - new	360000	360000	360000	7200	7200	7200	0.1	0.1	0.1
H2 Salt Cavern - repurp.	241200	241200	241200	7200	7200	7200	0	0	0
H2 Depl. Gas Field - repurp.	180000	180000	180000	3600	3600	3600	0	0	0
H2 Rock Cavern - new	7200000	7200000	7200000	9600	9600	9600	0	0	0
CH4 Line packing	0	0	0	0	0	0	0.1	0.1	0.1
CH4 AGS	0	0	0	0	0	0	0.1	0.1	0.1
CH4 Depleted Field - existing	0	0	0	0	0	0	0.1	0.1	0.1
CH4 Other UGS - existing	0	0	0	0	0	0	0.1	0.1	0.1

3.5 Transmission infrastructure

Integrating energy supply technologies into the existing energy system requires transmission infrastructure, to transport energy carriers from the point of generation to points of demand. In this project, five types of energy infrastructure were considered, namely High Voltage Direct Current (HVDC) and High Voltage Alternating Current (HVAC) power cables, H_2 pipes, CH_4 pipes and repurposed CH_4 pipes for H_2 transmission. To incorporate these into LCP was firstly the already existing cables and pipes across Europe mapped out and their installed capacities determined. For mainland Europe, this was predominantly retrieved from the TYNDP data set [71], with the exception of the Netherlands where the input values were based on numbers reported in [57], clustered together from a NUTS-2 level to be consistent with the three Dutch onshore nodes used in this project.

3.5.1 Cables

For LCP to be able to determine if it is more cost-efficient to build out HVAC or HVDC cables between two nodes, the CAPEX, variable and fixed OPEX cost of each potential cable connection was determined. To capture the difference in cable installation costs that come as a consequence of onshore versus offshore installations, their respective share [%] of each possible connection was estimated. Each connection-specific cost of building a HVDC or HVAC cable between two nodes A and B with an intra-nodal distance D, was thereafter determined using Equation 3.10 and Equation 3.11. The economic input data used for the calculations is available in Table 3.12.

Table 3.12: Economic input data used for power transmission infrastructure

Symbol	Category	Value	Unit	Comment	Source
$\%_{\text{offshore/onshore}}$	% of cable located offshore vs onshore	-	%	Own estimations	
D	Distance between nodes	-	km	Calc. based on nodal coordinates	
$C_{\text{trans, onshore}}$	Transport cost, onshore	3533	€/MW-km		[37]
$C_{\text{fixed, HVAC}}$	HVAC fixed cost	141000	€/MW	Incl. HVAC platform	[37]
$C_{\text{variable, HVAC}}$	HVAC variable cost	2000	€/MW-km	Incl. HVAC cable	[37]
$C_{\text{fixed, HVDC}}$	HVDC fixed cost	300000	€/MW	Incl. HVDC platform	[37]
$C_{\text{converter, HVDC}}$	HVDC converter cost	250000	€/MW	Incl. 2 HVDC converters	[37]
$C_{\text{variable, HVDC}}$	HVDC variable cost	1100	€/MW-km	Incl. HVDC cable	[37]
L_{HVAC}	HVAC line losses	0.70%	/100km		[50]
L_{HVDC}	HVDC line losses	0.35%	/100km		[50]
$O_{\text{HVAC/HVDC}}$	HVAC/HVDC OPEX	0.50%	of CAPEX	Own assumption	

$$C_{HVAC} = \%_{onshore}(DC_{trans,onshore}) + \%_{offshore}(C_{variable} + DC_{fixed}) \tag{3.10}$$

$$C_{HVDC} = \%_{onshore}(DC_{trans,onshore}) + \%_{offshore}(DC_{var.,HVDC} + C_{fixed,HVDC} + C_{conv.,HVDC}) \tag{3.11}$$

3.5.2 Pipes

Within this project, two types of gas infrastructure were allowed to be built out, namely new H_2 pipes and repurposed CH_4 pipes for H_2 transmission. Considering European ambitions to decrease reliance on fossil fuels (e.g. [7]), no new CH_4 pipes were allowed to be built. Existing installed capacities of CH_4 pipes were however accounted for in the model and a maximum of 80% of these were allowed to be retrofitted into H_2 pipes. The existing connections and their respective capacities were retrieved from [85]. The reported CAPEX values for onshore and offshore H_2 pipelines include costs for the necessary compressors [86].

Table 3.13: Economic input data used for H_2 transmission infrastructure. Retrieved from [87] and [86].

Symbol	Category	Value	Unit	Source
$\%_{offshore/onshore}$	% of pipe located offshore vs onshore	-	%	Own estimations
D	Distance between nodes	-	km	Calc. based on nodal coordinates
$C_{onshore,\ new}$	CAPEX H_2 onshore pipe	535	€/MW-km	[86], assuming medium pipelines (36 inch)
$C_{offshore,\ new}$	CAPEX H_2 offshore pipe	910	€/MW-km	[86], assuming medium pipelines (36 inch)
$C_{onshore,\ repurp.}$	CAPEX Repurp. pipe H_2 onshore	149	€/MW-km	[86], assuming medium pipelines (36 inch)
$C_{offshore,\ repurp.}$	CAPEX Repurp. pipe H_2 offshore	168	€/MW-km	[86], assuming medium pipelines (36 inch)
O_{H2}	OPEX H_2 cost	1%	of CAPEX	
L_{pipe}	Transmission losses	0	%	Own assumption

$$C_{pipe} = D(\%_{onshore}C_{onshore} + \%_{offshore}C_{offshore}) \tag{3.12}$$

3.6 Modelling in LCP

Once the input data files were prepared it was uploaded to the Posit workbench environment of LCP, and executed using the commercial program Gurobi as a solver. As the input data set is of significant size, it was divided into two main Excel files, one containing the TYNDP European data set, and one containing the North Sea specific data set. For each of these two main Excel files, CSV files were prepared which contained the respective set of demand and supply profiles.

3.7 Sensitivity analysis

In order to answer sub-question 3, "*What is the impact of varying electrolyser pricing on the resulting modelled offshore grid developments?*" a sensitivity analysis was performed. The aim of this sub-question was to test the robustness of the base results pertaining to sub-questions 1 and 2, in regards to the hub functionalities and connection infrastructure characteristics. The topic of placing electrolysers onshore or offshore for optimal integration of North Sea wind power has yielded different results throughout literature, see e.g. [26] or [39]. CAPEX cost assumptions for offshore electrolysers were therefore varied within a -15% to +30% range to investigate how the location of built-out electrolysers, either onshore or offshore, is dependent on their assumed investment costs. The results of the sensitivity analysis were analysed on both a system level, as well as on a nodal breakdown for the North Sea.

4 Results

4.1 Sub question 1: Locations, functionalities, key characteristics and connection patterns of the offshore energy hubs.

4.1.1 Base scenario

Base scenario modelling results are presented in this section. Firstly, Figure 4.1 displays the optimised installed capacities of OWF and electrolyser for North Sea offshore nodes in years 2030, 2040 and 2050. The exact installed capacities are listed in Table 4.1. These results show that a total of 287 GW of offshore wind will be installed in the North Sea in 2050, equivalent to the maximum allowed installed capacity across these nodes, as detailed in Table 3.8. Hence, LCP found it cost-efficient to build out all the allowed OWF. Over the entirety of Europe, 491 GW of offshore wind are installed by 2050 as part of the least-cost solution. In 2050, approximately 79 GW of electrolysers will be installed offshore, spread across all offshore nodes. Node UKSO has the greatest build-out of offshore electrolyser (16 GW), while UKMO has the greatest build-out of OWF (44 GW). The majority of the offshore electrolyser build-out occurs in simulation year 2050, corresponding to the year with the highest hydrogen demand.

Table 4.1: Installed capacities of wind power and electrolyser at each offshore node in the North Sea, base scenario.

Node	Offshore wind [GW]			Offshore electrolyser [GW]		
	2030	**2040**	**2050**	**2030**	**2040**	**2050**
DKOF	3.2	10.0	19.1	0.68	2.10	9.49
NLNO	4.2	14.7	18.5	0.00	4.63	7.99
NLNW	6.0	24.0	31.6	0.00	0.00	5.73
NLWO	8.2	16.1	19.9	0.00	0.00	3.18
UKNO	14.1	33.6	39.1	3.51	4.72	8.06
UKMO	18.7	38.2	43.7	0.00	8.20	10.81
UKSO	10.6	30.1	35.6	4.39	12.32	16.01
DEO1	22.9	27.3	37.3	3.67	3.67	9.50
DEO2	3.0	7.8	17.8	0.00	0.00	5.11
DEO3	2.3	3.8	13.8	0.00	0.00	3.03
NOOF	3.0	3.0	3.0	0.23	0.23	0.23
BEOF	8.0	8.0	8.0	0.00	0.00	0.58
Total	104.2	216.6	287.4	12.48	35.87	79.72

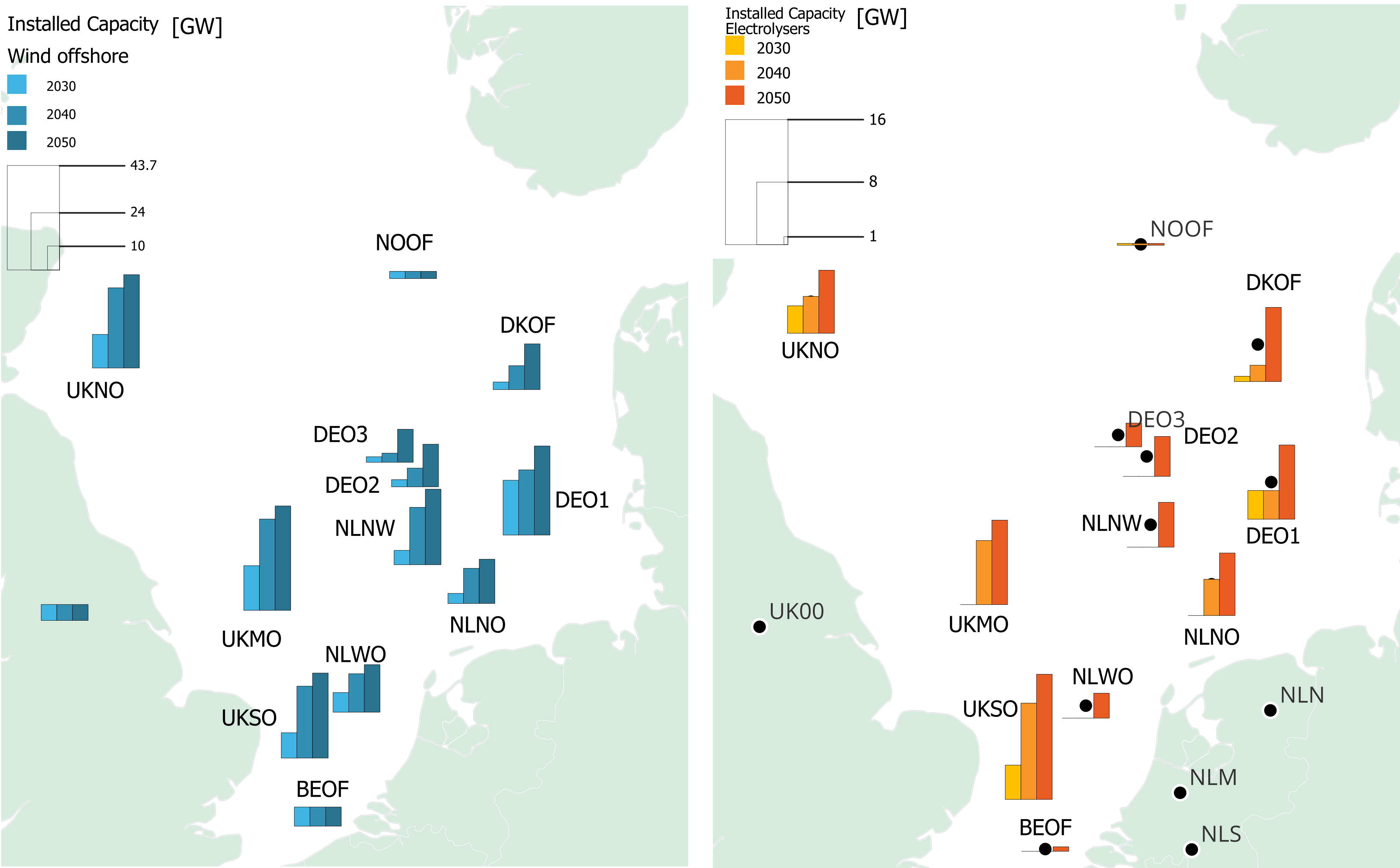

Figure 4.1: 2030, 2040 and 2050 installed capacities of offshore wind (left) and offshore electrolysers (right) in the North Sea, base scenario.

The resulting electricity transmission network configuration in 2050, as a consequence of the supply technology build-out, is presented in Figure 4.2. Net electricity energy flows in 2050 are displayed in Figure 4.3. The equivalent 2030 and 2040 results are located in Figure 3, Figure 5, Figure 4 , Figure 6, in the Appendix (section 6). It can be seen that there is a vastly interconnected electricity transmission network across Europe, and also across the North Sea. All offshore nodes connect to at least one other offshore node, while also all connecting directly to shore. The area surrounding nodes DEO2 & 3 exhibits several offshore node to offshore node connections. From the net electricity flows (Figure 4.3) it can be seen that large flows are directed towards Germany (DE00) and the UK (UK00), due to their large electricity demands. Nodes NLNW and NLWO provide the greatest electricity flows to mainland Netherlands, while nodes DEO1-3 export the majority of their power production directly to mainland Germany. Node UKSO only supplies a small share of the electricity it produces to mainland UK, while the majority of the produced electricity instead flows towards the Belgian offshore node BEOF and the Dutch offshore node NLWO to later feed into the respective mainlands.

Figure 4.4 demonstrates the optimised 2050 hydrogen transmission network across the entirety of Europe, and more specifically across the North Sea region. 2030 and 2040 configurations are presented in section 6. As a result of building out electrolysers offshore, offshore nodes are also connected via hydrogen pipelines. There is considerably less offshore-to-offshore hydrogen connectivity compared to electricity, with DEO2-3 connecting to UKMO, and UKSO-NLWO forming the only international hub-based transmission links. Net hydrogen flows in 2050 (Figure 4.5) indicate major quantities of hydrogen flowing into Germany from a wide range of locations, and the Spain and Portugal cluster (ESPT) being important hydrogen providers for central Europe. The two far German offshore nodes (DEO2 and 3) deliver a total of 55 TWh of hydrogen to mainland UK, via the offshore node UKMO. Node UKSO contributes to meeting mainland European hydrogen demand by exports via node NLWO. Notably, two out of three German offshore nodes do not possess hydrogen transmission connections to their own mainland, Germany. Node NLNO will feed 48 TWh of hydrogen into Northern Netherlands (NLN) in 2050, which in turn exports 171 TWh further to Germany. 2030 and 2040 net hydrogen flows are displayed in section 6.

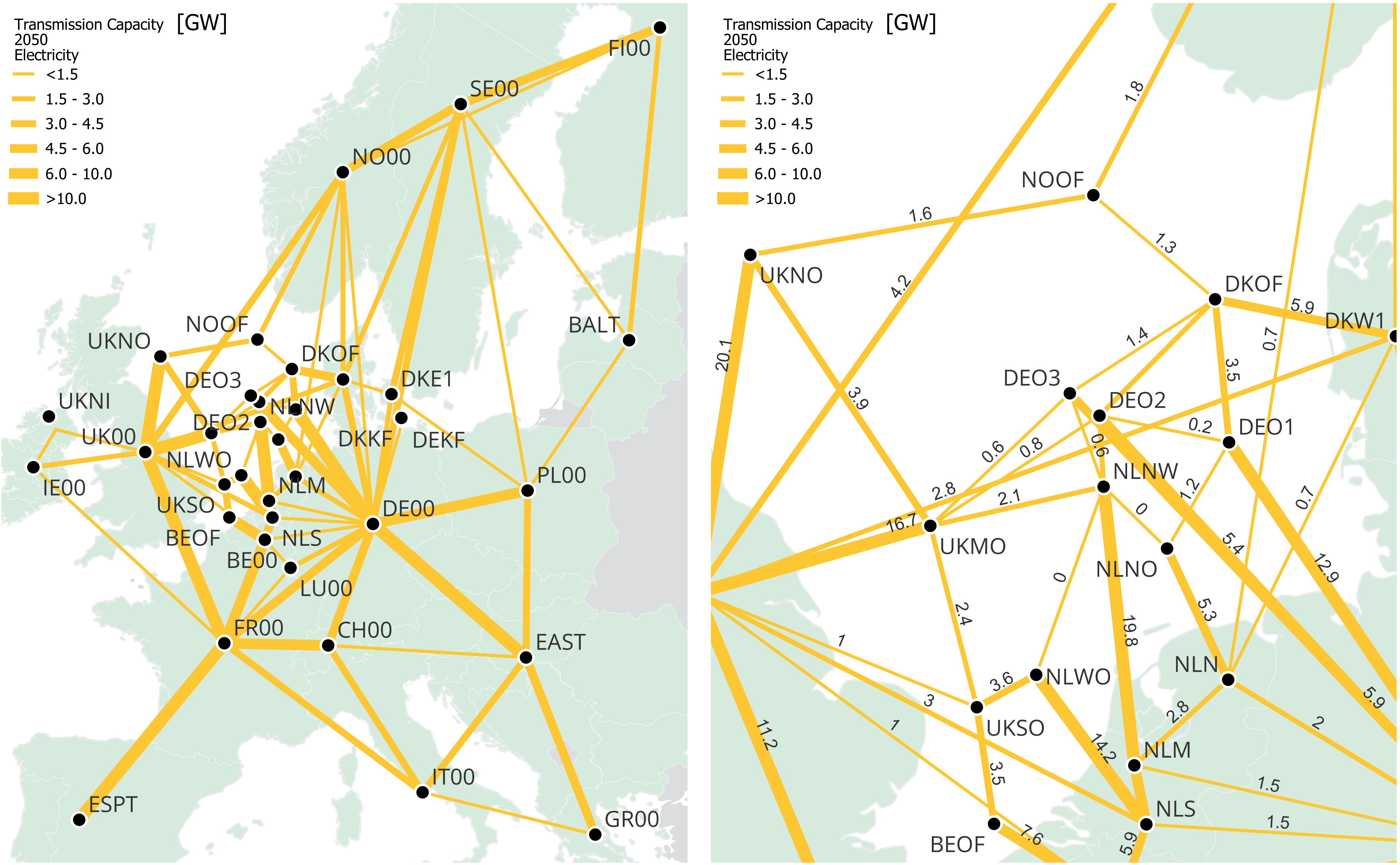

Figure 4.2: Electricity transmission network in 2050 in Europe (left) and North Sea (right), base scenario.

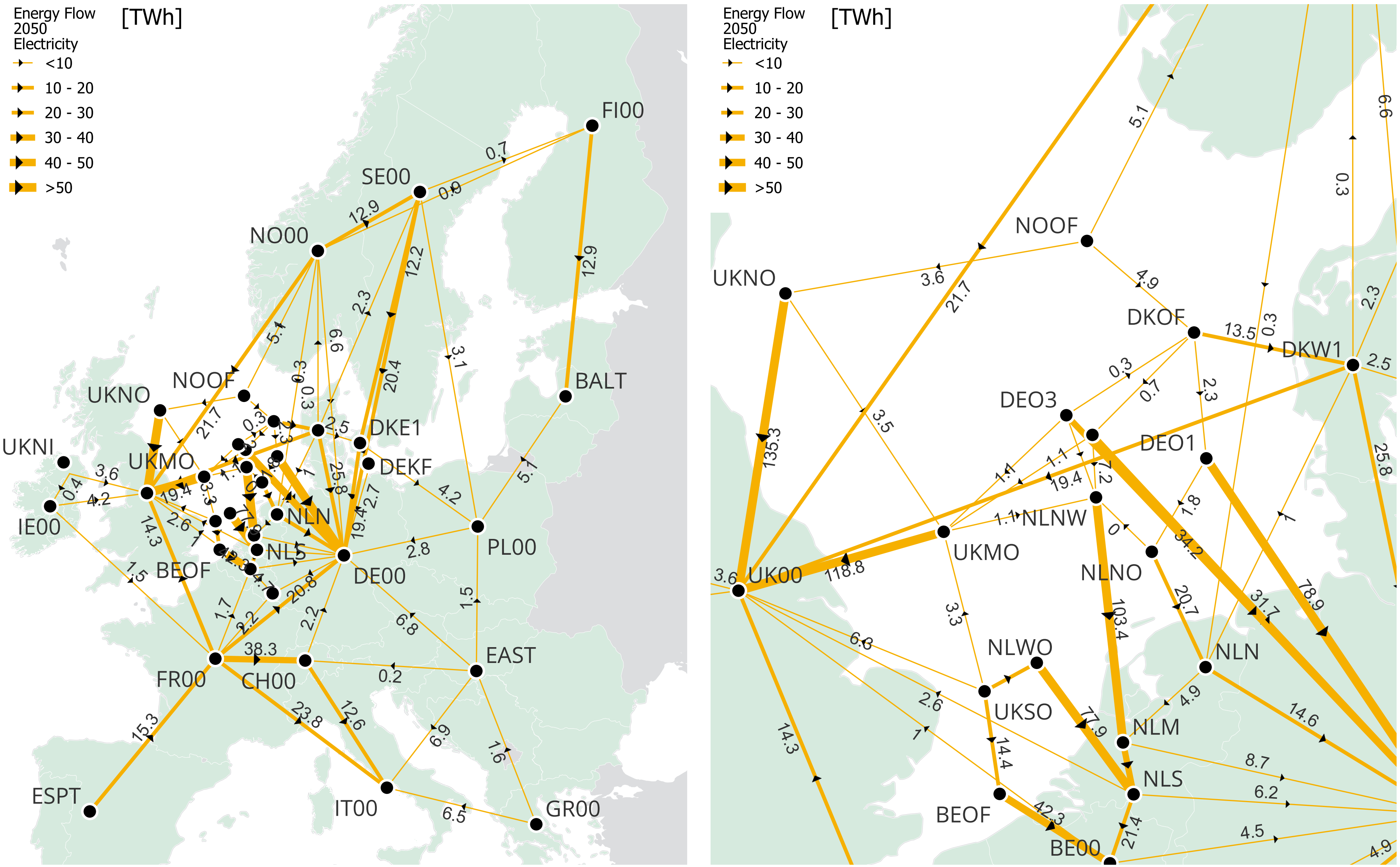

Figure 4.3: Electricity net energy flows in 2050 for Europe (left) and the North Sea (right), base scenario.

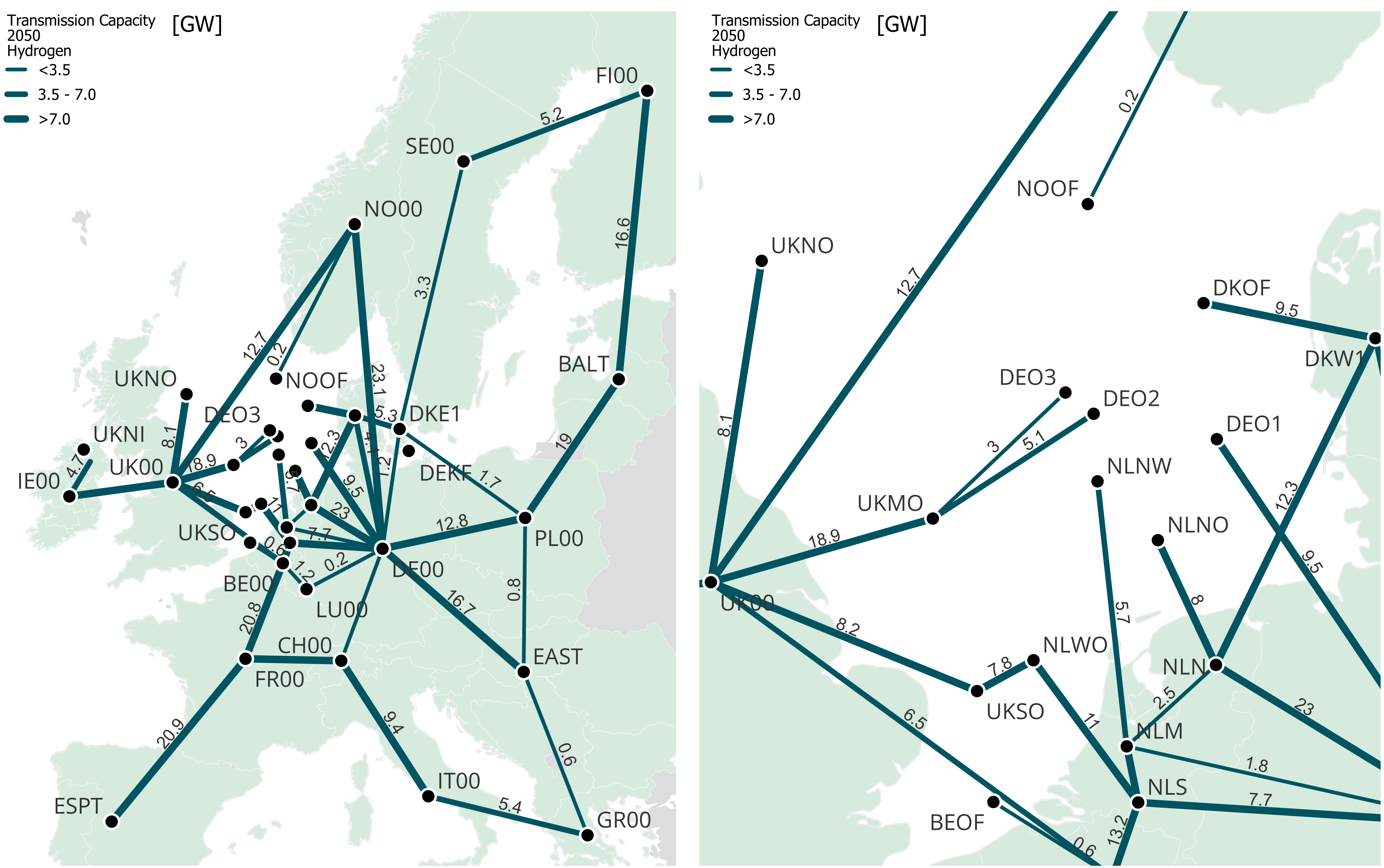

Figure 4.4: Hydrogen transmission network in 2050 for Europe (left) and the North Sea (right), base scenario.

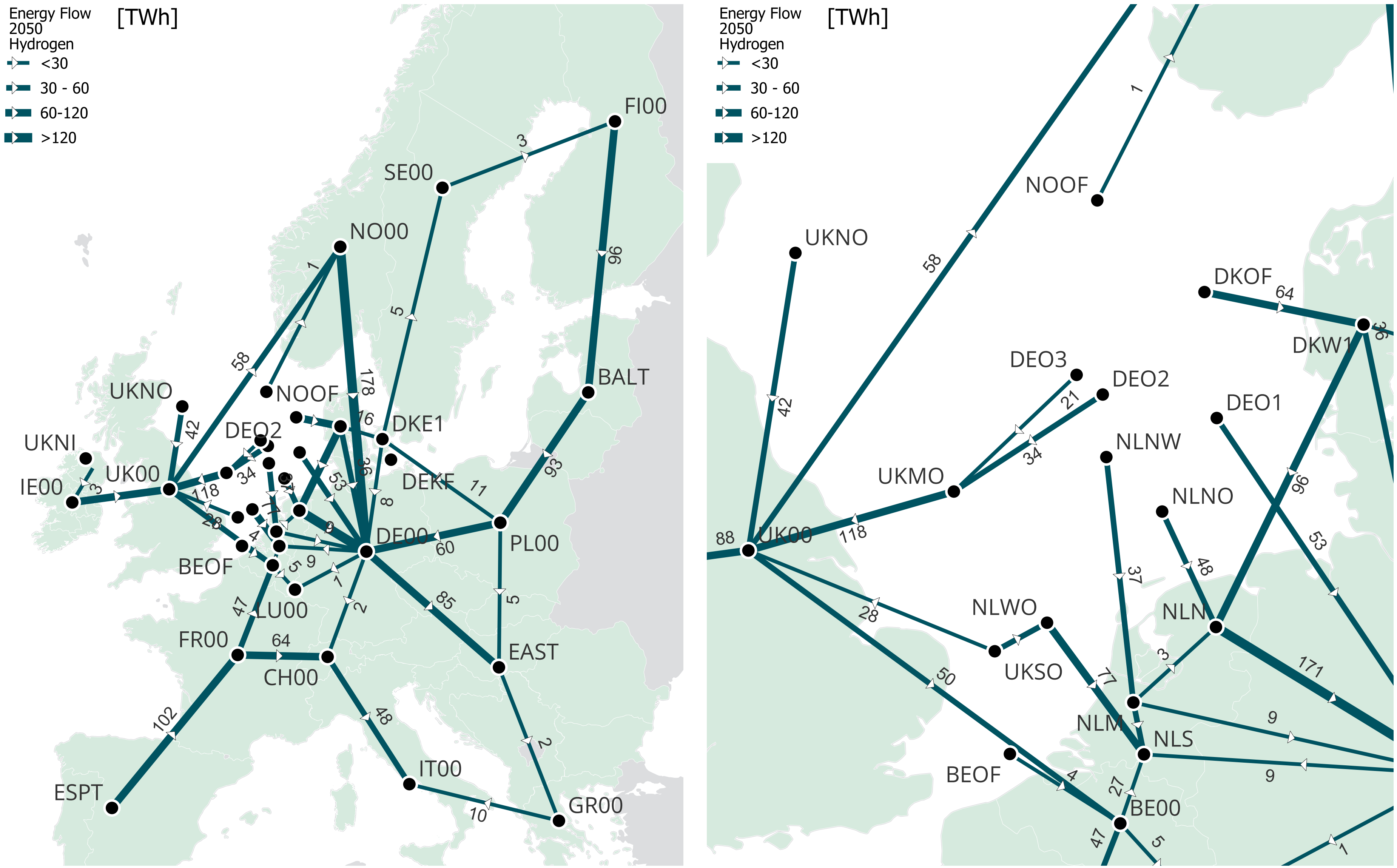

Figure 4.5: Net hydrogen energy flows in 2050 for Europe (left) and the North Sea (right), base scenario.

To get a more detailed understanding of what occurs at the offshore nodes throughout the course of the year, dispatch graphs for electricity and hydrogen are provided for node DEO1 for a December (Figure 4.6 and Figure 4.7) and a July day (Figure 4.8) in 2050. Throughout the course of the December day, it can be seen that the wind turbines are producing power during the early hours of the day, to slow down during the morning and later pick up again around 11 a.m. The majority of the power produced until 11 a.m. is exported via HVDC cable. Between 10-11 am offshore electrolysis significantly ramps up and thus 'consumes' electricity in Figure 4.6.The latest installed electrolyser (PtH2 Offshore inst. 2050) is favourably utilised to the equivalent technology installed in 2030, due to its assumed enhanced efficiency (74% versus 69%). The hydrogen produced by the electrolysers is all exported via hydrogen pipes (Figure 4.7).

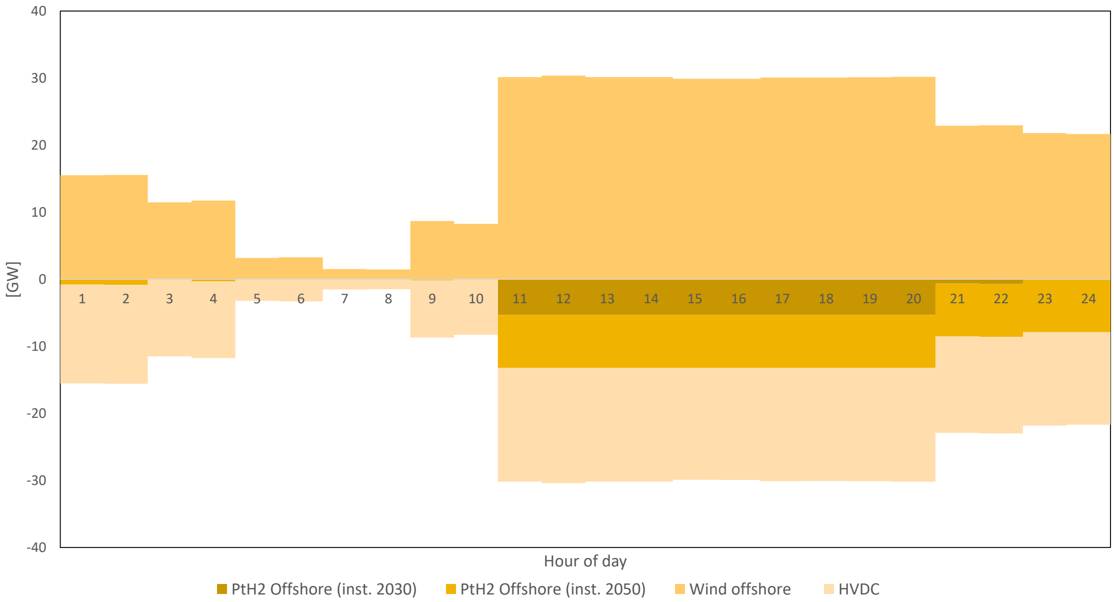

Figure 4.6: Electricity dispatch at node DEO1 during a December day in 2050, base scenario.

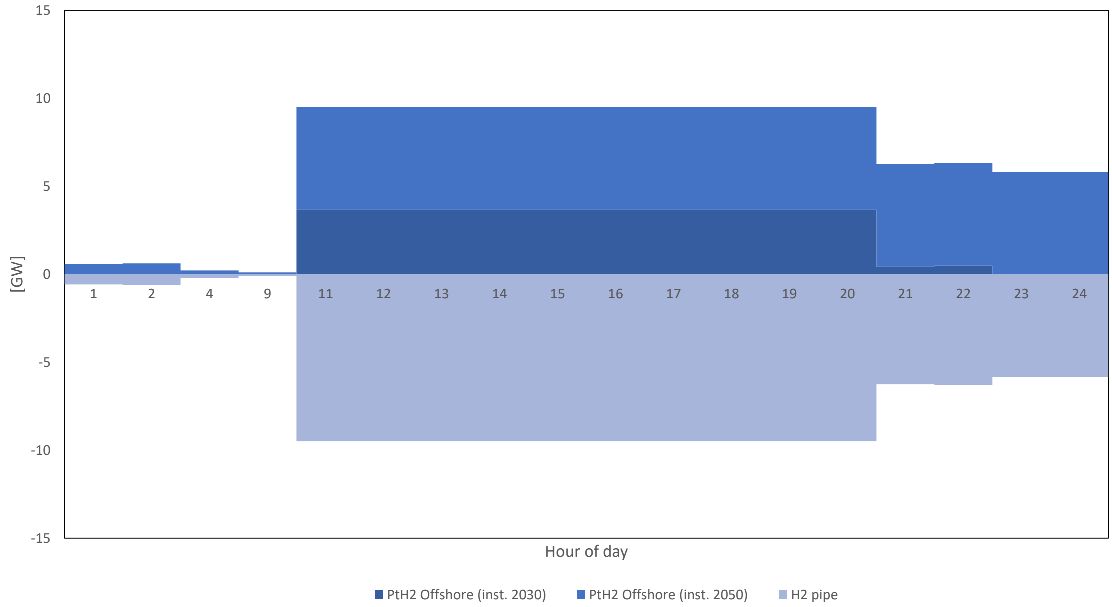

Figure 4.7: Hydrogen dispatch at node DEO1 during a December day in 2050, base scenario

The dispatch behaviour during the July day reveals that during hours 7-13 electricity is imported to node DEO1 to power the electrolysers (Figure 4.8). Examining the exact energy flows during hour 8 on this July day, as presented in Table 4.2, it can be seen that electricity is imported into DEO1 from offshore nodes DEO2 and NLNO together with mainland Germany (DE00). This electricity is converted to hydrogen which in turn is transported back to mainland Germany (DE00).

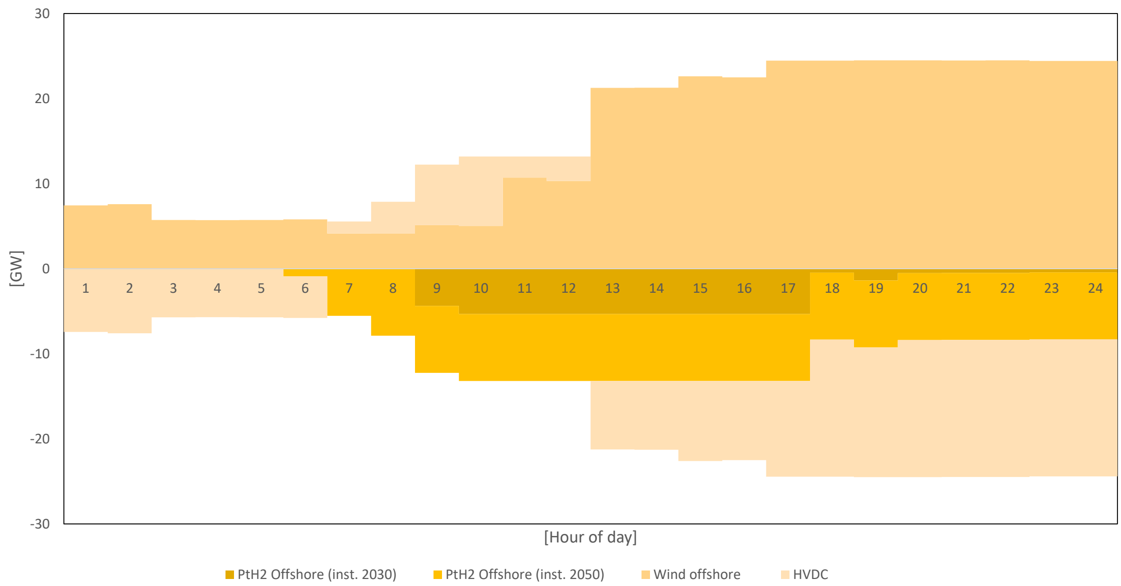

Figure 4.8: Electricity dispatch at node DEO1 during a July day in 2050, base scenario.

Table 4.2: Granular dispatch at node DEO1 during hour 8 on a July day in 2050, all energy carriers, base scenario.

Time step	Carrier	Dispatch [MW]	InfraType	Node from	Node to
Hour 8, July 2050	Hydrogen	5826	Pipe-H2-new	DEO1	DE00
Hour 8, July 2050	Electricity	729	HVDC	DKOF	DEO1
Hour 8, July 2050	Electricity	1620	HVDC	DE00	DEO1
Hour 8, July 2050	Electricity	169	HVDC	DEO2	DEO1
Hour 8, July 2050	Electricity	1238	HVDC	NLNO	DEO1

At first glance, this behaviour might seem peculiar, but a closer inspection of the dispatching behaviour of node DE00 during the July day 2050 (Figure 4.9 and Figure 4.10) provides an explanation. During hour 8 of a July day in 2050, all onshore electrolysers in mainland Germany (DE00) are operating at maximum capacity, with the exception of the grid-connected electrolysers installed in 2030 and 2040. Instead of using these to meet the remaining hydrogen demand, electricity is sent from mainland Germany (DE00) to the offshore node (DEO1) to be converted to hydrogen, which is then sent back to the mainland to fulfil the German hydrogen demand. This means that during this time step, LCP finds it more cost-efficient to send electricity from shore to an offshore location using the HVDC cable, with an assumed efficiency loss of 0.35% per 100 km, to use the offshore electrolyser with an efficiency of 74% and transporting the produced hydrogen back to shore rather than using the most efficient available onshore electrolyser which has 71% efficiency. This leads to a net efficiency gain of approximately 1.25% when considering the 500 km distance between DE00 and DEO1.

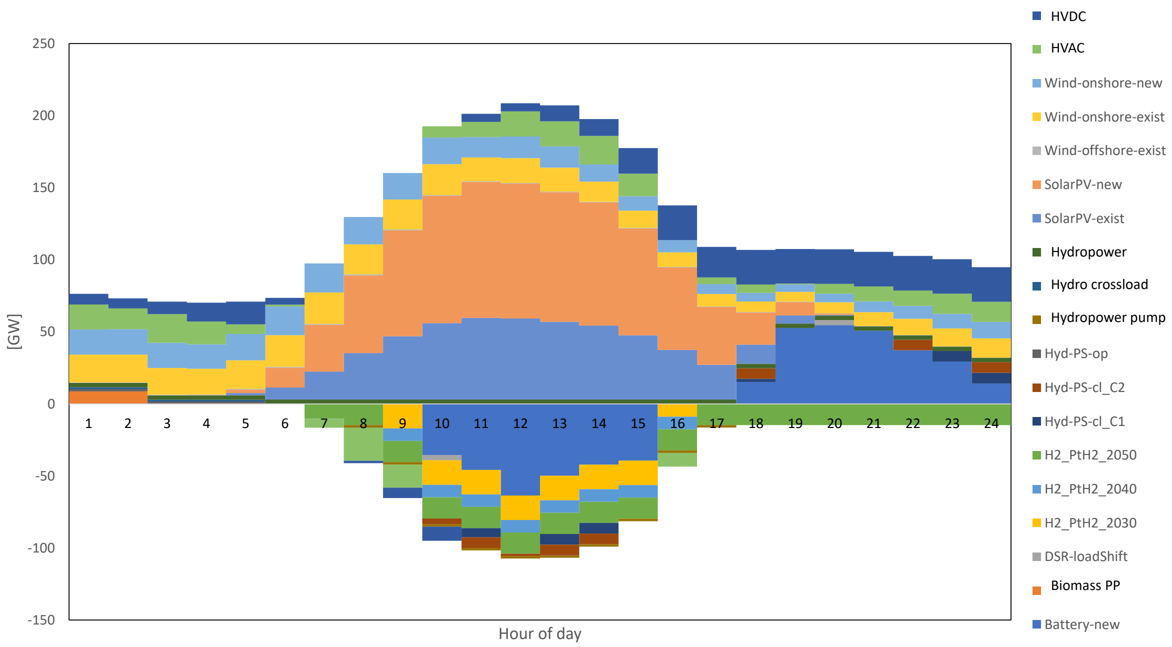

Figure 4.9: Electricity dispatch at node DE00 during a July day in 2050, base scenario.

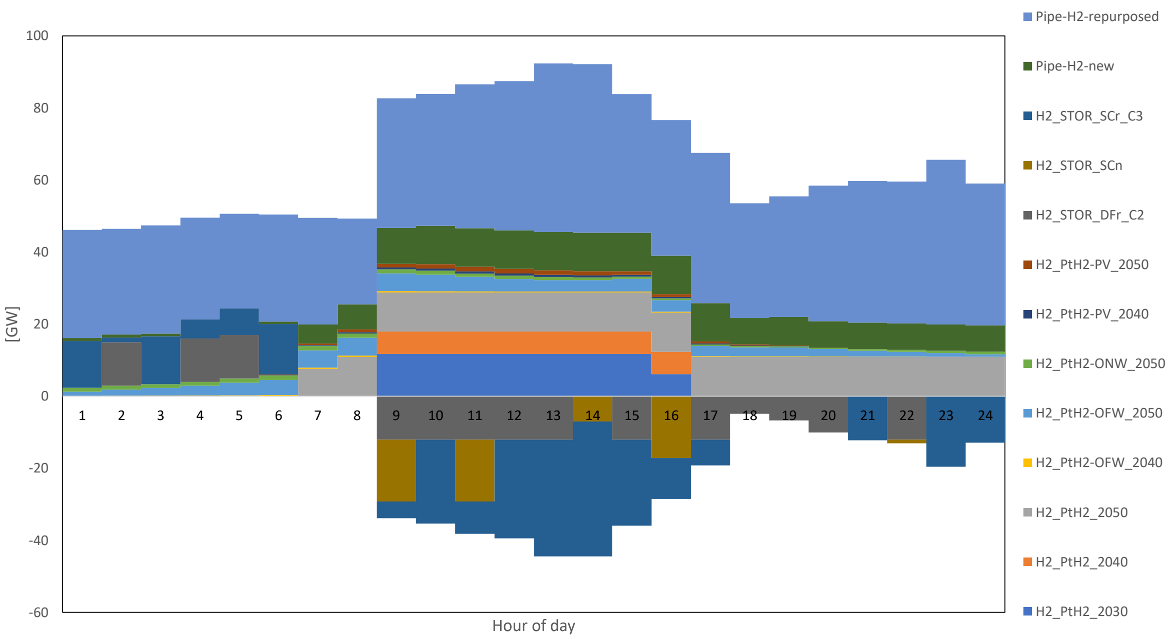

Figure 4.10: Hydrogen dispatch at node DE00 during a July day in 2050, base scenario.

4.1.2 Infrastructure 500MW scenario

Base scenario results revealed that the optimal solution contained several very small transmission connections, below 500 MW. These are listed in Table 4.3. The construction of these transmission connections is however not likely in practice, as the investment, environmental disturbance and operational effort incurred would likely not be deemed worth it for the small transmission gain. A subsequent LCP run was therefore performed, in which the possibility for LCP to build out these connections was removed. This scenario was named '*Infra500*', and represents this project's 'best estimate' of how the North Sea offshore network will develop by 2050. This two-step procedure was necessary as one is unable to specify minimum expansion capacities in LCP, due to its linear optimisation properties.

Table 4.3: Transmission infrastructure connections below 500 MW in base scenario results.

To node	From node	Installed capacity [MW]	Type
NLNW	NLWO	4.5	HVDC cable
NLNO	NLNW	27.8	HVDC cable
DEO1	DEO2	168.7	HVDC cable
DE00	DEKF	433.3	HVAC cable
DEKF	DKKF	433.3	HVAC cable
FR00	LU00	475.0	HVAC cable
NOOF	NO00	227.2	H_2 pipe
DE00	LU00	232.1	H_2 pipe

Infra500 scenario results reveal that identical capacities of OWF were installed across the North Sea, while the installed capacity of electrolysers located offshore decreased by 200 MW in 2050 Table 4.4. Total installed capacities of electricity and hydrogen infrastructure across the entirety of the system are presented in Table 4.5. It can be seen that the Infra500 scenario led to a 0.1% increase in electricity transmission and a 0.1% decrease in hydrogen transmission infrastructure in 2050 compared to the base scenario.

Table 4.4: Installed capacities of offshore wind and electrolyser [GW] across the North Sea, base versus Infra500 scenario

	OWF [GW]			Electrolyser [GW]		
Scenario	2030	2040	2050	2030	2040	2050
Base	104.2	216.6	287.4	12.5	35.9	79.7
Infra500	104.2	216.6	287.4	12.5	35.6	79.5

Table 4.5: Total installed electricity and hydrogen infrastructure in 2030, 2040 and 2050 for each scenario [GW], along with difference [%] compared to the base scenario.

	Total electricity infrastructure [GW]			**Total hydrogen infrastructure [GW]**		
Scenario	**2030**	**2040**	**2050**	**2030**	**2040**	**2050**
Base	197.4	297.3	323.8	103.6	241.6	385.3
Infra500	197.6 (+0.1%)	297.7 (+0.1%)	324 (+0.1%)	103.8 (+0.2%)	242 (+0.2%)	385 (-0.1%)

Comparing curtailment levels across the Infra500 and base scenarios (Table 4.6) showed a small decrease in curtailment for the Infra500 scenario in the years 2030 and 2040. On a system-wide level, there is a 0.4% curtailment increase in 2050. The majority of the curtailment across the North Sea occurred in December, February and March.

Table 4.6: Curtailment levels [TWh] for the base and Infra500 scenarios across all simulation years, along with difference [%] to base scenario results.

	System total [TWh]			**North Sea [TWh]**		
Scenario	**2030**	**2040**	**2050**	**2030**	**2040**	**2050**
Base	4.2	17.1	23.9	2.7	3.3	2.3
Infra500	4.1 (-2.4%)	16.9 (-1.2%)	24.0 (0.4%)	2.6 (-3.7%)	3.3 (0.0%)	2.3 (0.0%)

The resulting 2050 North Sea transmission network for electricity and hydrogen is presented in Figure 4.11. As expected, HVDC interconnections between NLNW-NLWO, NLNO-NLNW and DEO1-DEO2 are no longer present compared to the base scenario (Figure 4.2). This led to marginal reinforcements of other cable interconnections, such as NOOF-DKOF and NOOF-UKNO whose installed capacity increased by 200 MW respectively compared to the base results. The connection between DKOF-DEO1 was also increased by 100 MW compared to the base scenario. The connection pattern of the *Infra500* offshore hydrogen transmission network remained identical to the base scenario, with the exception of the Norwegian offshore node NOOF no longer being directly connected to mainland Norway NO00. The DEO3-UKMO connection was reinforced from 3 GW (base) to 3.2 GW (Infra500), further leading to downstream reinforcements through a 200 MW capacity increase of the UKMO-UK00 connection. The DEO1-DE00 hydrogen pipeline was increased by 100 MW compared to the base scenario. Figure 4.12 portrays net electricity and hydrogen flows across the North Sea in 2050.

The total annualised CAPEX and OPEX costs for the Infra500 scenario, across the simulation horizon 2030-2050, were 20 million €higher compared to the base scenario. This constituted a 0.002% increase and is thus very marginal.

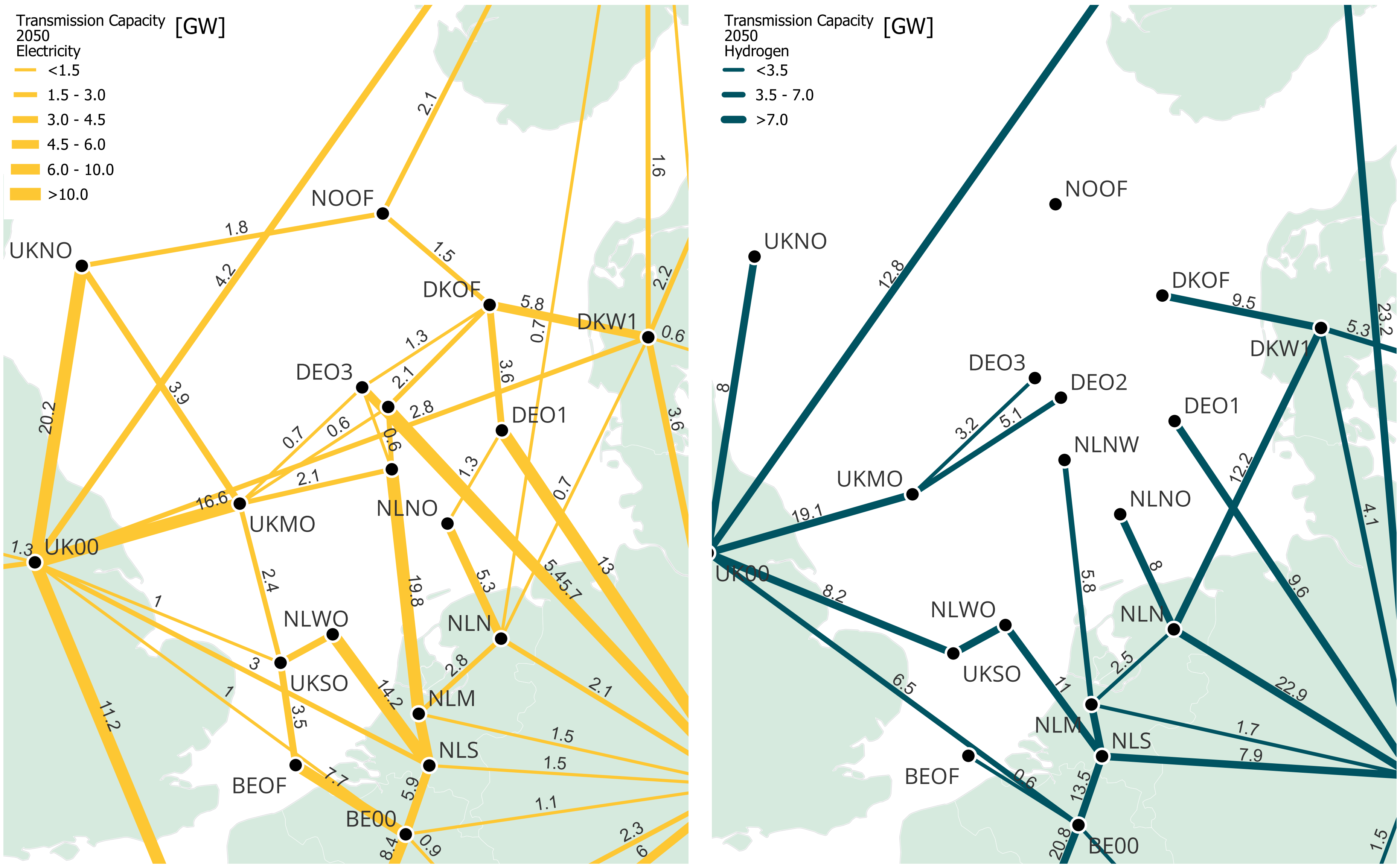

Figure 4.11: North Sea electricity (left) and hydrogen (right) transmission network in 2050, Infra500 scenario.

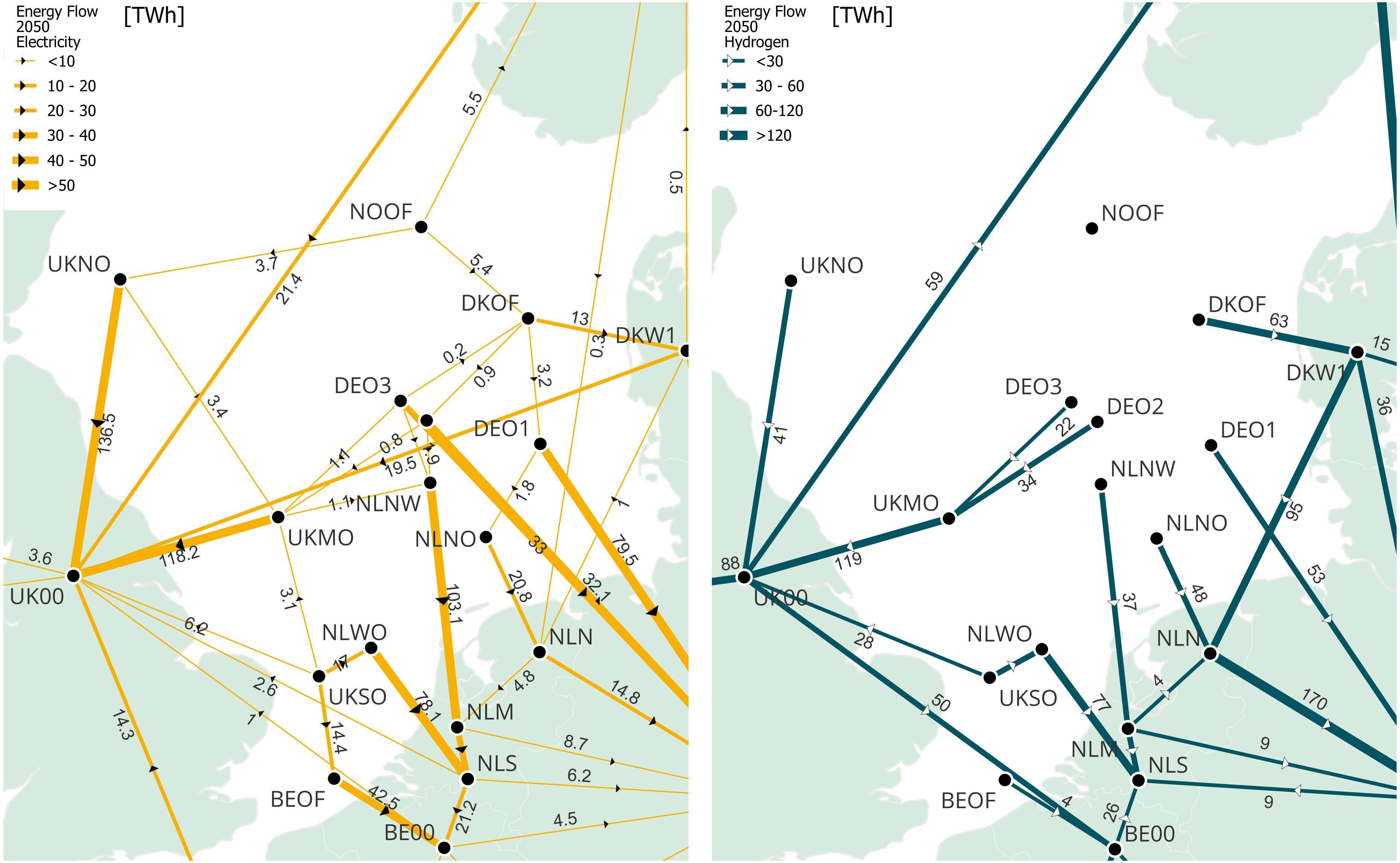

Figure 4.12: North Sea net energy flows for electricity (left) and hydrogen (right) in 2050, Infra500 scenario.

4.2 Sub question 2: Key characteristics and utilisation rates of the connection infrastructure to and from the offshore energy hubs

Figure 4.13 displays the characteristics of the electricity and hydrogen transmission infrastructure that is built out in the North Sea by 2050 under the Infra500 scenario. It can be seen that HVDC cables have been preferentially built out over HVAC to form the interconnected offshore network. The only HVAC cable that is present between an offshore node and shore is connecting NLWO to NLS, synonymous with the existing connection between the Dutch OWF Borssele and Southern parts of the Netherlands [88]. The hub-based network is also built up with new hydrogen pipelines, to transport the hydrogen which is produced at sea to shore. As there are no currently existing CH_4 pipes connecting the offshore nodes with the mainland, LCP was unable to re-purpose any CH_4 pipes into H_2 pipes. Thus only newly built H_2 pipes are present in the North Sea offshore network. However, when examining Figure 4.13 it can be determined that there is significant re-purposing of CH_4 pipes across mainland Europe, as the economic input parameters fed into LCP assumes that this is cheaper than constructing new H_2 pipes (see Table 3.13 for details). H_2 connections between the Iberian peninsula and the Nordics respectively to central Europe show that additional reinforcements of new H_2 pipe connections are needed beyond the repurposed infrastructure. This is linked to the their respective high regional potential for cheap hydrogen production; the Iberian peninsula with excess solar power generation and the Nordics with hydropower. Electricity connections across Europe are denoted as being a combination of HVDC/HVAC as this input data was retrieved from [71] which does not make a distinction between the two.

Utilisation rates of the 2050 North Sea offshore transmission network are listed in Table 4.7 (Infra500 scenario). The utilisation rates for the electricity cables all fall between 12-83% , with the average being 60%. Utilisation rates of North Sea hydrogen pipelines fall between 56-82% with an average of 69%. This is in line with the HVDC utilisation rates reported in [89]. The HVDC cable with the highest utilisation was the UKMO-UK00 connection, while the hydrogen pipeline with the highest utilisation was the connection between UKSO-NLWO.

Table 4.7: Utilisation rates [%] of North Sea offshore infrastructure in 2050, Infra500 scenario

Connection	Infrastructure type	**Utilisation**	Infrastructure type	**Utilisation**
BEOF-BE00	HVDC	12%	New H2 pipe	74%
DEO1-DE00	HVDC	73%	New H2 pipe	63%
DEO1-NLNO	HVDC	61%		-
DEO2-DE00	HVDC	67%		-
DEO2-NLNW	HVDC	55%		-
DEO3-DE00	HVDC	66%		-
DEO3-NLNW	HVDC	61%		-
DKOF-DEO1	HVDC	43%		-
DKOF-DEO2	HVDC	57%		-
DKOF-DEO3	HVDC	52%		-
DKOF-DKW1	HVDC	59%	New H2 pipe	76%
NLM-NLNW	HVDC	61%	New H2 pipe	73%
NLN-NLNO	HVDC	62%	New H2 pipe	68%
NLS-NLWO	HVDC	63%	New H2 pipe	79%
NOOF-DKOF	HVDC	63%		-
NOOF-NO00	HVDC	60%		-
UKMO-DEO2	HVDC	65%	New H2 pipe	77%
UKMO-DEO3	HVDC	62%	New H2 pipe	79%
UKMO-NLNW	HVDC	63%		-
UKMO-UK00	HVDC	81%	New H2 pipe	71%
UKNO-NOOF	HVDC	47%		40%
UKNO-UK00	HVDC	77%		59%
UKNO-UKMO	HVDC	38%		-
UKSO-BEOF	HVDC	76%		-
UKSO-NLWO	HVDC	79%	New H2 pipe	82%
UKSO-UK00	HVDC	79%	New H2 pipe	56%
UKSO-UKMO	HVDC	49%		-
Average	**HVDC**	**60%**	**New H2 pipe**	**69%**

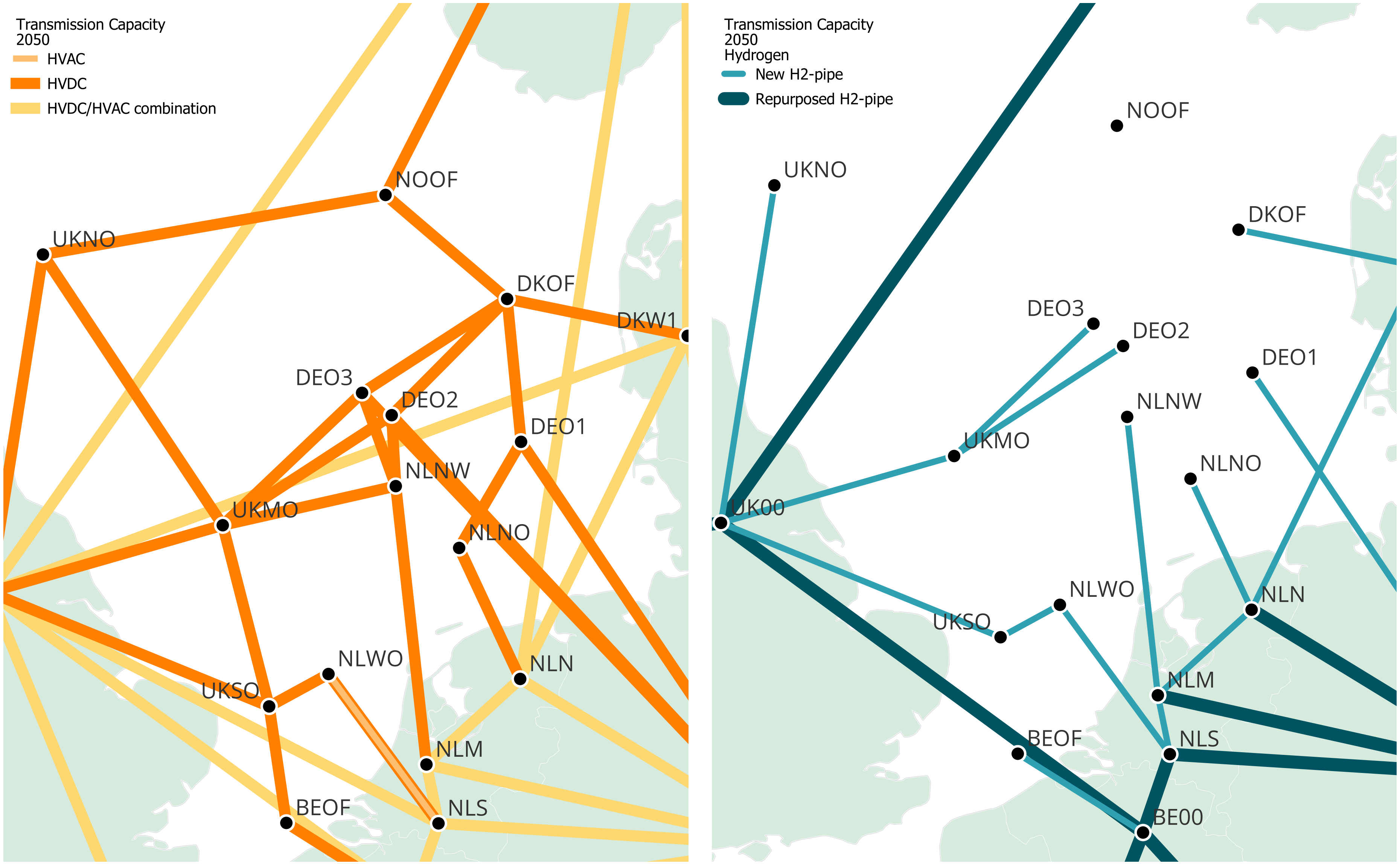

Figure 4.13: North Sea transmission infrastructure characteristics in 2050, electricity network (left) and hydrogen network (right). Infra500 scenario.

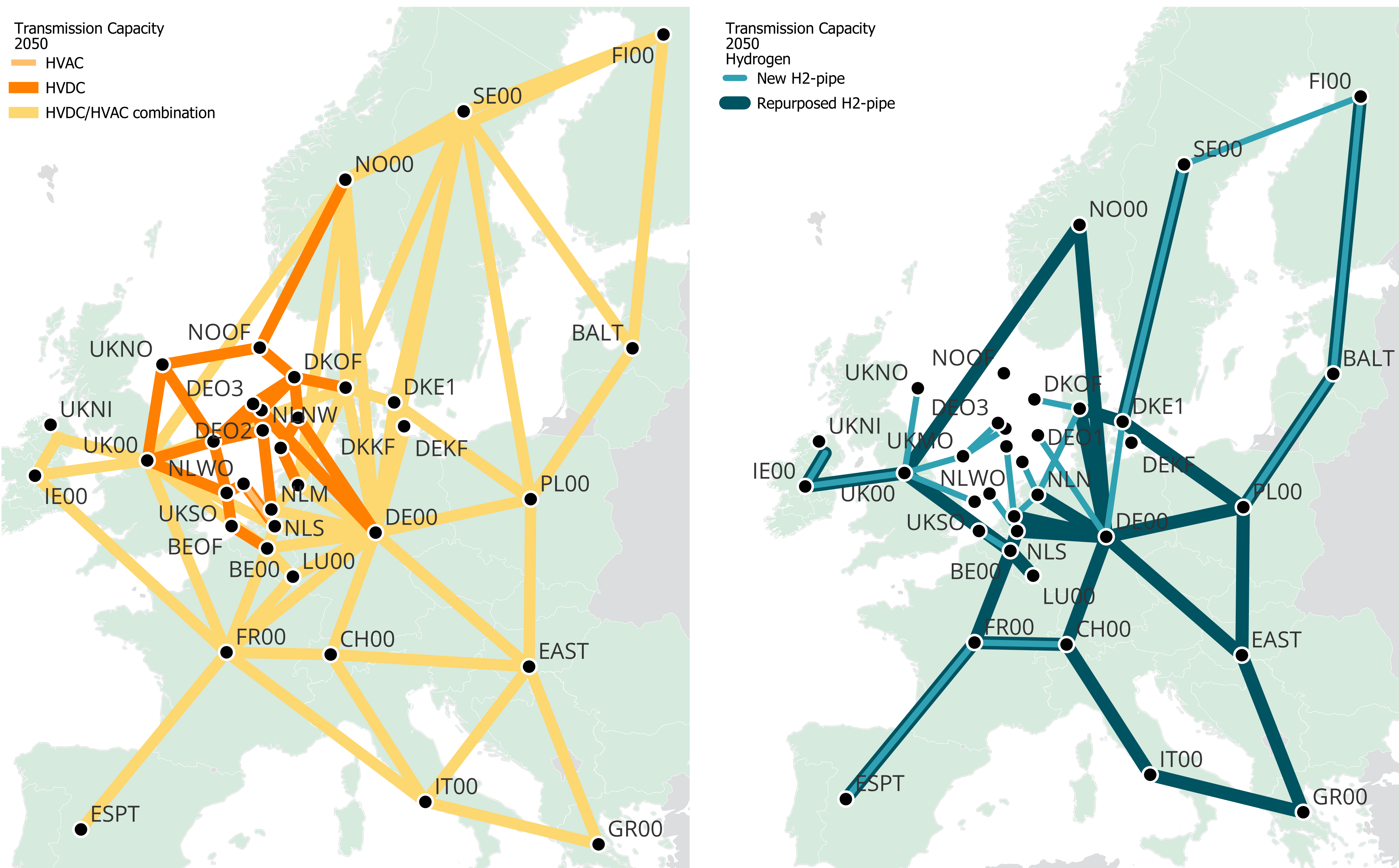

Figure 4.14: European transmission infrastructure characteristics in 2050, electricity network (left) and hydrogen network (right). Infra500 scenario.

4.3 Sub question 3: What is the impact of varying offshore electrolyser pricing on the resulting modelled offshore grid developments?

This section presents the results of the sensitivity analysis where the CAPEX assumptions for the electrolysers located offshore were varied within a -15% to +30% range. In Figure 4.15 the relative changes [%] compared to the base scenario in offshore electrolyser CAPEX and resulting installed capacities of offshore (PtH2 Offshore) and onshore (PtH2 Grid) can be seen. The technology categories are also split by their year of installation, where e.g. PtH2 Offshore inst. 2030 refers to the offshore electrolysers installed in 2030. It can be seen that the offshore electrolysers installed in 2030 are the most sensitive to CAPEX variations, with a 30% increase in CAPEX leading to a 54% decrease in their installed capacity compared to the base scenario. Conversely, a 15% decrease in the CAPEX leads to a 31% increase in offshore electrolyser installations in 2030. The CAPEX sensitivity for the installed offshore electrolyser decreases over the simulation horizon, as seen by the decreased slope of the PtH2 Offshore installed in 2040 and 2050. The results in Figure 4.15 further reveal that the installed capacities of electrolysers located onshore are only marginally impacted by CAPEX variations in the -15% to +30% range. A near-linear behaviour is displayed for all categories in Figure 4.15.

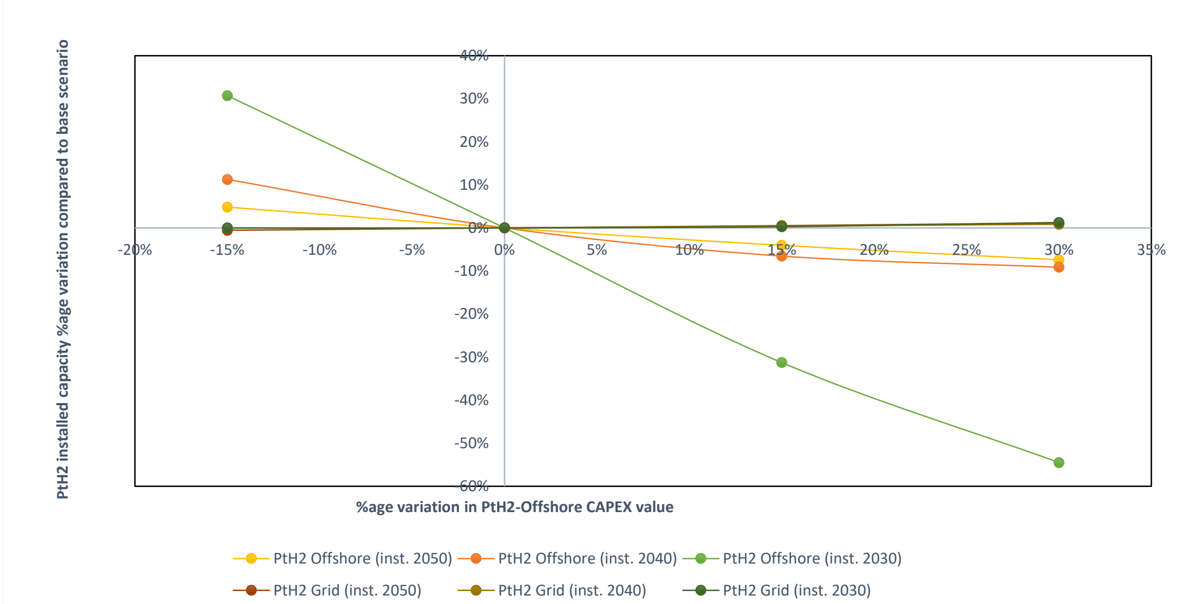

Figure 4.15: Installed capacity sensitivity of offshore and onshore electrolyser (PtH2) as a function of offshore electrolyser CAPEX variations

A closer examination of the offshore electrolyser sensitivity on a nodal level is provided in Figure 4.16, Figure 4.17 and Figure 4.18 for 2030, 2040 and 2050 respectively. The results reveal that there are large variations in the installed electrolyser capacity at nodes UKNO and DEO1 depending on the CAPEX assumptions, while the node UKSO displays a lower sensitivity. For node DEO3 the assumed CAPEX value is directly linked to whether any electrolysers at all get installed by 2030 or 2040. The same is true for node NLWO in 2040 (Figure 4.17). However, by 2050 all offshore nodes exhibit electrolyser build-out regardless of

CAPEX assumption Figure 4.18. This indicates that the resulting 2050 offshore network is not sensitive to offshore electrolyser CAPEX assumptions, within the tested range, and are thus robust.

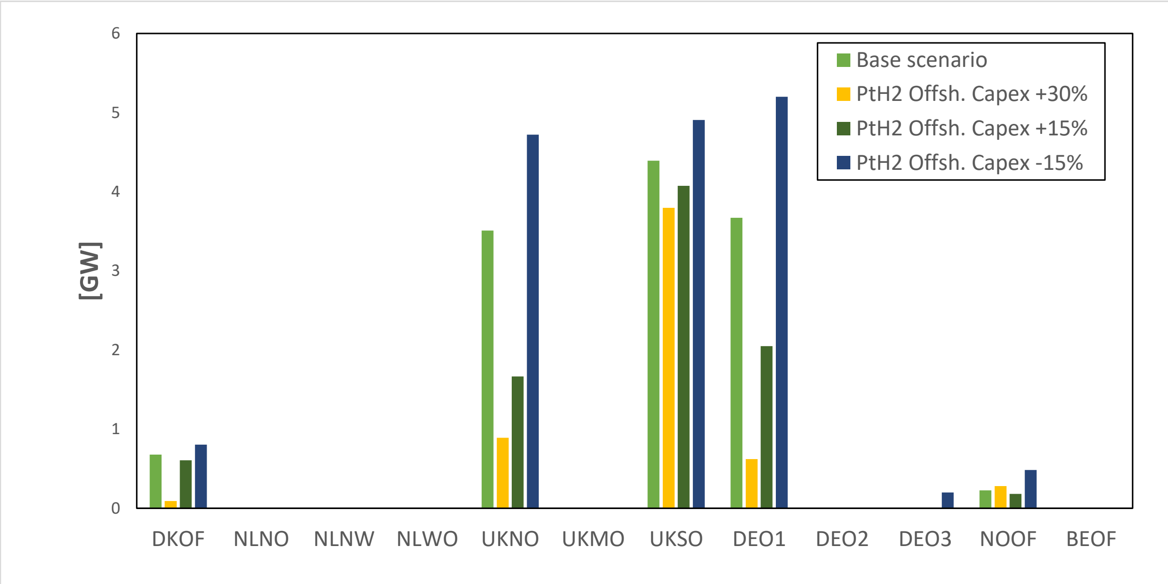

Figure 4.16: Installed capacities of offshore electrolysers at each offshore node in 2030.

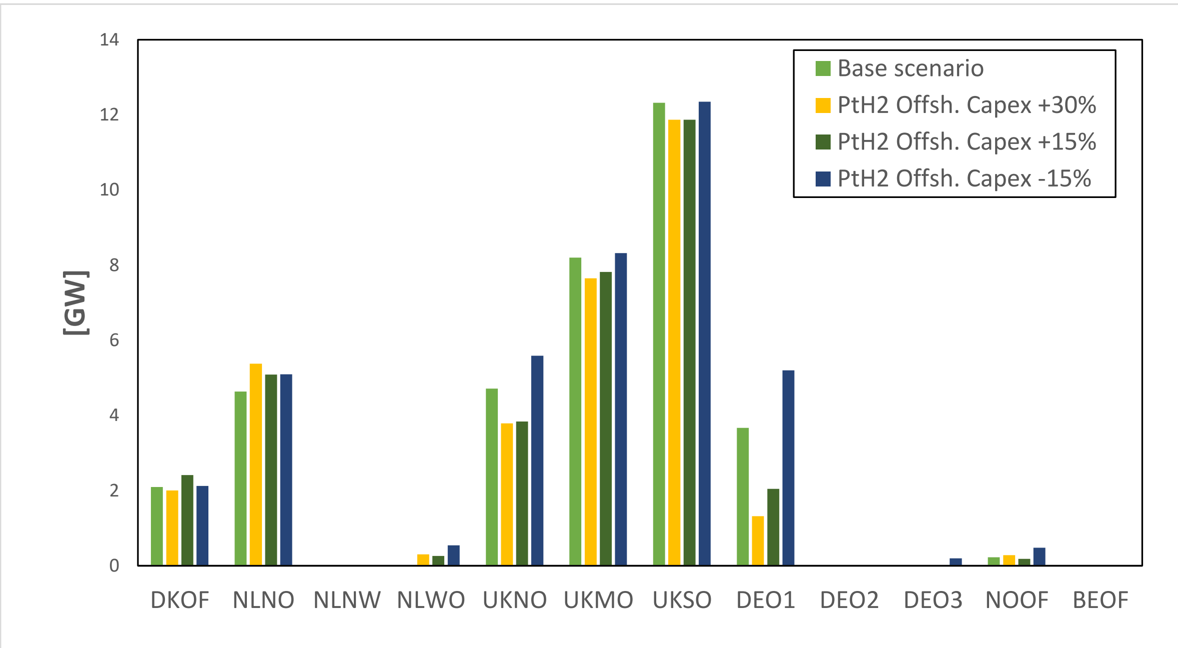

Figure 4.17: Installed capacities of offshore electrolysers at each offshore node in 2040.

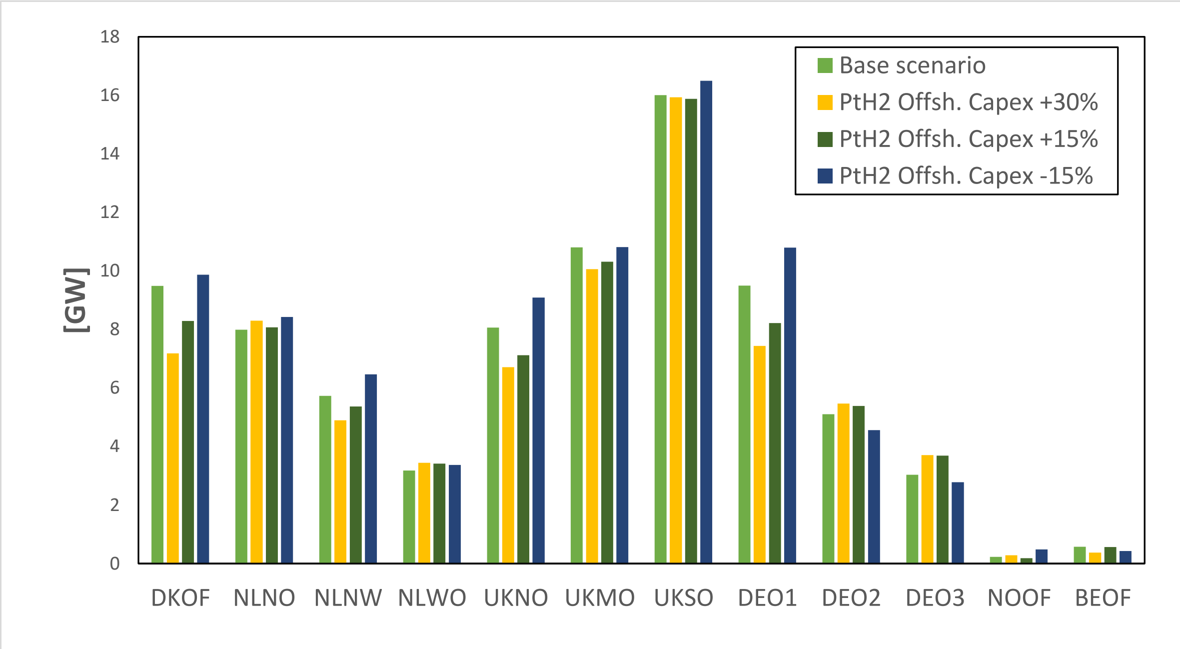

Figure 4.18: Installed capacities of offshore electrolysers at each offshore node in 2050.

The installed capacities of offshore wind across the North Sea in the base scenario and the three sensitivity scenarios are displayed in Table 4.8. It can be seen that the installations of OWF did not change throughout the sensitivity analysis, indicating that their expansion is not sensitive to this parameter. Absolute values of the installed offshore electrolysers are also shown in Table 4.8.

Table 4.8: Installed capacities of offshore wind and electrolyser [GW] across the North Sea.

	OWF [GW]			**Electrolyser [GW]**		
Scenario	2030	2040	2050	2030	2040	2050
Base	104.2	216.6	287.4	12.5	35.9	79.7
PtH2 Offshore CAPEX -15%	104.2	216.6	287.4	16.3	39.9	83.6
PtH2 Offshore CAPEX +15%	104.2	216.6	287.4	8.6	33.5	76.5
PtH2 Offshore CAPEX +30%	104.2	216.6	287.4	5.7	32.6	73.8

Table 4.9 shows the total installed electricity and hydrogen infrastructure in the base scenario and the three CAPEX sensitivity scenarios. As expected from examining the results in Table 4.8, an increased CAPEX value led to a decrease in hydrogen infrastructure build-out and an increase in electricity transmission infrastructure. This is because fewer electrolysers were built out and hence less hydrogen transmission infrastructure was needed. The opposite behaviour was found when the CAPEX was instead increased. The only exception to this behaviour was the 2050 values for the PtH2 Offshore CAPEX -15% scenario, which showed a slight decrease in hydrogen transmission infrastructure (-0.8%). This could be due to a higher utilisation of the pipelines. The resulting offshore hydrogen grid for the two extreme CAPEX scenarios are presented in Figure 4.19.

Table 4.9: Total installed electricity and hydrogen infrastructure in 2030, 2040 and 2050 for each scenario [GW], along with difference [%] compared to the base scenario.

	Total elec. infrastructure [GW]			**Total H_2 infrastructure [GW]**		
Scenario	**2030**	**2040**	**2050**	**2030**	**2040**	**2050**
Base	197.4	297.3	323.8	103.6	241.6	385.3
PtH2 Offsh. CAPEX -15%	-3.1%	-1.9%	-1.5%	+7.4%	+1.0%	-0.8%
PtH2 Offsh. CAPEX +15%	+3.0%	+1.1%	+1.3%	-8.4%	-1.3%	-1.0%
PtH2 Offsh. CAPEX +30%	+5.5%	+1.7%	+2.0%	-13.0%	-1.9%	-1.2%

Variations in offshore electrolyser CAPEX values also had an effect on levels of curtailment, as seen in Table 4.10. A 30% increase in the offshore electrolyser CAPEX led to a 48% increase in curtailment in the North Sea in 2050, but only a 1% increase when looking over the total system. The large difference in curtailment levels when looking at solely the North Sea compared to the whole system can be explained by the fact that the North Sea is only a small part of the overall European energy system. Hence, the onshore energy system was able to counteract the increased North Sea curtailment by expanding the amount of flexible assets onshore.

Table 4.10: Curtailment levels [TWh] across all scenarios and simulation years, along with difference [%] to base scenario results.

	System total [TWh]			**North Sea [TWh]**		
Scenario	**2030**	**2040**	**2050**	**2030**	**2040**	**2050**
Base	4.2	17.1	23.9	2.7	3.3	2.3
PtH2 Offsh. CAPEX -15%	4.2 (0%)	17.0 (-1%)	24.6 (+3%)	2.7 (0%)	3.2 (-3%)	2.3 (0%)
PtH2 Offsh. CAPEX +15%	4.1 (-2%)	17.4 (+2%)	24.0 (+0.4%)	2.6 (-4%)	3.6 (+9%)	2.7 (+17%)
PtH2 Offsh. CAPEX +30%	3.9 (-7%)	17.2 (+1%)	24.1 (+1%)	2.4 (-11%)	3.6 (+9%)	3.4 (+48%)

Variations in the total annualised CAPEX and OPEX costs over the simulation horizon 2030-2050 are displayed in Table 4.11. Variations in the offshore electrolyser CAPEX led to marginal changes in the overall annualised CAPEX and OPEX cost, between + 0.12% (+1.8 billion €) and -0.08% (-1.2 billion €).

Table 4.11: Annualised CAPEX and OPEX costs for time horizon 2030-2050, in billion of Euros [B€$_{2020}$].

Scenario	**[B€$_{2020}$]**
Base	1484.7
PtH2 Offshore CAPEX -15%	1483.5 (- 0.08% to base)
PtH2 Offshore CAPEX +15%	1485.7 (+ 0.07% to base)
PtH2 Offshore CAPEX +30%	1486.5 (+ 0.12% to base)

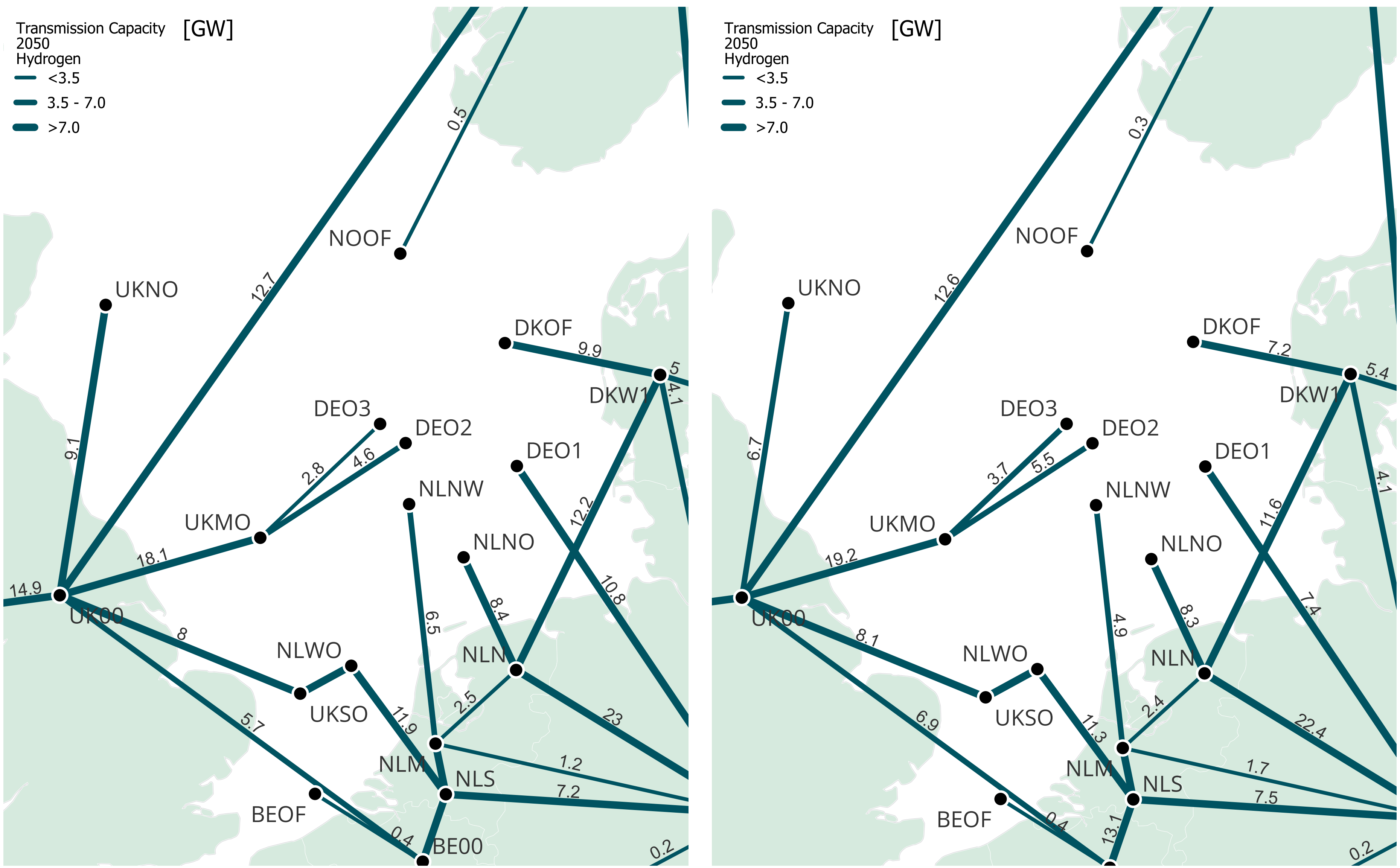

Figure 4.19: Hydrogen transmission network in 2050, in the offshore electrolyser CAPEX -15% scenario (left) and the CAPEX +30% scenario (right).

5 Discussion

The results presented in chapter 4 indicate significant expansion of an integrated offshore network in the North Sea by 2050. Considering the net energy flows, as presented in Figure 4.12, major offshore hubs in the interconnected network are UKSO, NLWO, UKMO, DEO2 and DEO3. These nodes represent the areas around OWFs East Anglia, Nederwiek, Dogger Bank, and German search areas N 17-20 respectively. These locations display interconnections for both electricity and hydrogen and are connected to several other offshore locations besides their respective radial connections to shore. Offshore nodes DKOF and DEO1 also play important roles in transporting electricity flows from Scandinavia towards central Europe. These findings are similar to those presented in [90], shown in Figure 5.1 below. Connections from the Danish offshore energy island (node DKOF), towards Germany and the Netherlands, via nodes DEO2 and NLNW are also present here [90]. Branching of the transmission network around Dutch OWF IJmuiden Ver, to connect to Belgium and the UK was reported by [90] and the same was found to be true within this project. Furthermore, the results of both studies concur on the area around node UKMO being a central point for the offshore network. This node connects both to the far-from-shore locations of the German EEZ and the North Western parts of the Dutch EEZ [90]. The significant energy flows from the three German offshore nodes into mainland Germany found in this project illustrate a similar pattern as the connection pathway known as '4' in Figure 5.1. The importance of hubs located in similar areas to UKMO, DEO1, NLNW and DKOF was also found in [34].

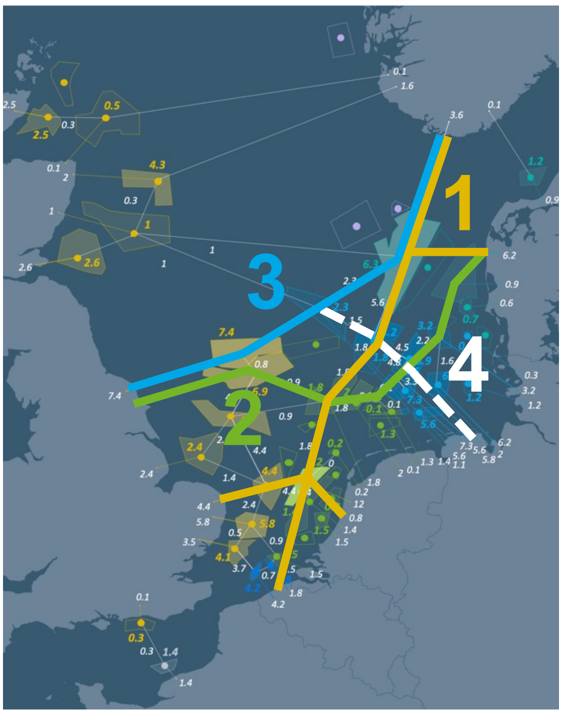

Figure 5.1: Probable power corridors identified in [90].

Within this project, LCP found it cost-effective to build out 287 GW of OWF in the North Sea by 2050, in all scenarios. This closely corresponds to the 283 GW determined in [34], when both hydrogen and power transmission infrastructure was allowed. As mentioned in chapter 4, 287 GW of OWF build-out was the maximum allowed build-out in the North Sea within the optimisation range. Together with the OWF potential allocated to other nodes around the North Sea, this means that the ambitious targets of 300 GW set by the Ostend declaration [91] will be met in 2050. The determined 491 GW of offshore wind that will be built across all of Europe by 2050 is significantly higher than the 300 GW target announced by the European Commission [92]. This could be because LCP finds OWF to be more favourable than in reality, due to the representative supply profiles. The applied selection method can lead to underestimating the full extent of OWF variability and potentially extreme behaviour subsubsection 3.1.2. It is important to note that this also applies to the reported values for curtailment (Table 4.6 and Table 4.10) that are also dictated by the representative supply profiles. Using representative days can lead to underestimating curtailment, as extreme days are not fully captured.

In all scenarios considered within this project, the results indicate that it is cost-efficient to have a significant build-out of electrolysers offshore. This can be understood by looking at the cost assumptions for electricity versus hydrogen transmission infrastructure, outlined in Table 3.12 and Table 3.13. It can be seen that constructing electricity transmission connections to transport the electricity generated at sea to shore is significantly more expensive than constructing the equivalent hydrogen connections. Despite the offshore electrolysers being more expensive than their onshore equivalents (+25% in the base scenario), LCP still determined that building them and their associated H_2 transmission was less costly than solely building out an electricity transmission network. This is particularly true for nodes located far from shore, such as DEO2 and 3, which predominantly transport their generated energy in the form of H_2 to shore to avoid transmission losses. This further explains why the nodes located closer to shore, such as DEO1 and DKOF present a higher sensitivity to offshore electrolyser CAPEX variations (see Figure 4.18). Nodes closer to shore are less affected by electricity line losses due to shorter transmission distances, meaning that it can become cost-efficient to transport the generated energy in the form of electricity. The hydrogen is then instead produced onshore if the cost of building the electrolyser offshore becomes too high. The total optimised build-out of 79.7 GW of offshore electrolysers in this project lies within the reported range of 61-96 GW found in [34].

Despite vows for significant cross-national collaborations (see e.g. [29]), it remains uncertain if citizens of one country would accept that energy hubs within their EEZ are not connected to their own mainlands. This is for example the case with hydrogen transmission from DEO2 and 3, which transports all its' produced hydrogen towards the UK. Hence the question arises as to what the benefit of developing said offshore electrolysers at these locations would be for Germany, as they might not receive any of the benefits from their production. This highlights additional challenges that remain to be solved for the successful implementation of an integrated offshore network. As discussed in [93], appropriately incorporating the offshore nodes into the electricity bidding structure across Europe could be a way to tackle such issues, by potentially developing new offshore bidding zones.

There are however several limitations to this research. Firstly, spatial limitations such as designated military areas or shipping routes in the North Sea were disregarded when considering possible infrastructure developments. Thus the resulting transmission network determined in this project may cross into areas that are unavailable for development as LCP assumes the shortest route between nodes to be available. Spatial limitations were also disregarded when optimising for the expansion of offshore electrolysers, as the space they would require was not considered. Literature states that this can be of significant size, with 8 m^2 needed per MW_e [26]. This could also be problematic when considering the size of the currently designated electrolyser area within the German EEZ that would account for roughly 900 MW according to the [69]. Expanding the research scope to consider that level of spatial detail would have required the use of Geographical Information System (GIS) software, such as performed in [94]. LCP is however not able to handle this type of data, making this level of analysis outside of the project scope. Finding ways to incorporate this level of spatial granularity in future iterations of LCP would be a suitable area for future research.

Secondly, ramping rates for all technologies were assumed to be 100%, i.e. each technology could ramp up completely within the same time step that it was deployed. Considering the long time horizon that this project investigated (31 years) this was deemed to be an acceptable simplification. Future studies can nevertheless benefit from including more detailed technology behaviour as this will lead to even more reliable results. The ramping of an electrolyser can for example be seen in Figure 4.7, where the dispatch significantly changes within a single time step and the electrolyser is turned on and off repeatedly. This can have an effect on the lifetime of the electrolyser, as the degradation may occur more rapidly if the electrolyser is experiencing significant cycling [95]. Variations in electrolyser (and other technology) lifetimes, as a consequence of operational handling, were not considered in this project, and their lifetimes were assumed to be constant.

Thirdly, the copper plate assumption applied in this project is further a limitation as it disregards inter-array cabling from the wind turbines to the hubs, as well as congestion issues present onshore. This can be particularly problematic for offshore nodes, as there are usually no alternative routes that the generated electricity can take if one cable is used at full capacity [93]. This could potentially lead to the OWF being unable to transmit its' electricity to shore if the transmission cable is already used to transmit power flows from other locations [93].

Another limitation of this study is the usage of pre-determined energy demand profiles. These energy demand profiles were static and did not capture the potential interplay between energy prices and demand, such as a high price of one fuel leading to consumers switching to an alternative fuel. Such market mechanisms are not currently possible to model in LCP. Similarly, the installed capacities of energy supply technologies onshore were fixed according to values published by TYNDP in the Distributed Energy scenario [71]. This left LCP with little ability to capture potential dynamics between offshore and onshore capacity expansions. This was a deliberate decision, as allowing all supply technologies to freely optimise would have increased the computational complexity significantly. Considering the widespread consensus around the TYNDP, the input values used for the onshore supply technologies were deemed to be of sufficient robustness. Although the Distributed Energy scenario created by [71] aims for European energy autonomy it was developed pre-Ukrainian war and thus does not consider the implications of this. Repeating this analysis on subsequent iterations of the TYNDP could hence be a suitable area for further research.

The presence and availability of depleted hydrocarbon fields to be used as long-term storage locations for hydrogen were in this project solely considered for onshore locations. Expanding the project scope to also include depleted fields located offshore would be an additional appropriate direction for further research. This could potentially provide an offshore storage location at a discounted price through re-purposing of the existing infrastructure. The potential for this has been discussed in [96] considering a UK context.

Lastly, there are several limitations to modelling network developments using linear programming. The linear nature of the optimisation means that LCP finds it cost-efficient to build out several small connections, as it is only able to judge the suitability of connections based on the route with the shortest distance. In reality, however, it is unlikely that hubs like DEO2 and DEO3 are connected to so many other nodes respectively, instead of just having one of the two nodes be the hub in the area. This could have helped to achieve economies of scale while limiting environmental disturbance and operational complications [26]. If a mixed integer programming model had been employed as opposed to a linear programming model, this could have resulted in a less cluttered offshore network. This is visualised in Figure 12 in [26].

6 Conclusion

This project has investigated what a hub-based offshore network in the North Sea will look like by 2050, by applying a linear programming methodology. The analysis was performed using the internal Guidehouse model Low Carbon Pathways (LCP). The results indicate substantial build-out of both power and hydrogen transmission infrastructure, across all modelling runs. This is built out as a consequence of the large quantities of offshore wind power and offshore electrolysers that were part of the least-cost solution. Within the optimisation, offshore and onshore electrolysers were unconstrained in their capacity expansion, while offshore wind capacities were capped in line with announced offshore wind development targets. The results of the base scenario displayed a North Sea build-out of 287 GW of offshore wind power and 80 GW of offshore electrolysers. All considered offshore locations had electrolysers placed upon them as part of the optimised solution.

The North Sea transmission network in 2050 predominantly consists of electricity connections, but hydrogen connections are also present to a smaller degree. The offshore electricity network is highly interconnected, displaying both hub-to-hub as well as hub-to-shore connectivity. Major connection points for the offshore electricity network are nodes UKMO (OWF Dogger Bank area), DKOF (Nordsøen Energy Island area), UKSO (around OWF East Anglia), NLWO (OWF Nederwiek area) together with nodes DEO2 and 3 (around German search areas N 17-20). The 2050 offshore hydrogen network is significantly less interconnected and solely exhibits hub-to-hub connections between UKSO and NLWO, and German far-from-shore nodes DEO2/DEO3 and UKMO. All other offshore nodes display radially connected hydrogen pipelines to shore. The results of the base scenario modelling run were further refined by removing infrastructure connections below 500 MW and re-running the optimisation in LCP. This yielded similar results to the base scenario, albeit less cluttered as small connections which are unlikely to be built in practice due to their poor cost-effectiveness were now nonexistent. The results show that all offshore power transmission cables are built as HVDC connections preferentially over HVAC.

A sensitivity analysis was performed by varying the CAPEX assumptions for offshore electrolysers within a -15% to +30% range. This resulted in no changes in the installed wind power capacity but did impact the quantity of offshore electrolysers installed within a -7.8% to +4.6% range in 2050. Changes in the installed capacity of offshore electrolysers led to decreased hydrogen transmission infrastructure in the North Sea, and to as much as a 48% increase in North Sea curtailment in 2050. However, on a system-wide level, the curtailment and installed infrastructure capacities remained within 2% of the base scenario results. The total annualised CAPEX and OPEX costs across the simulation horizon were estimated to be 1485 billion €$_{2020}$ for the base scenario. The sensitivity analysis led to marginal changes in the overall annualised costs, within a -0.08% to +0.12% range.

The results of this project are limited by several factors, such as spatial limitations of the

North Sea not being considered. This could have an effect on the transmission network design and limit the amount of electrolysis that could be placed offshore. Further ramping rates of all technologies were assumed to be 100%, thus leading to substantial cycling which could negatively affect technology lifetimes. Such considerations were not accounted for in this project. Moreover, the onshore energy system was largely fixed, leading the model to only being able to optimise the installed capacities of offshore wind, electrolyser (onshore and offshore), hydrogen storage and transmission infrastructure. Suggested future research directions are increasing the modelling degrees of freedom to better capture capacity expansion interactions between the onshore and offshore energy systems. Expanding the model scope to include hydrogen storage in depleted gas fields located offshore is also identified as a suitable topic for future research.

Appendices

Appendix 1

Table 1: Existing interconnection capacities between Dutch nodes, based on [57].

Node From	Node To	Type of connection	Inst. Cap (MW)	Source
NLN	NLM	AC-cable	2832.83	[57]
NLN	NLM	CH_4 pipe	190193	[57]
NLN	DE00	AC-cable	2027	[57]
NLN	DE00	CH_4 pipe	93469	[57]
NLN	NOS0	AC-cable	700	[57]
NLN	NOS0	CH_4 pipe	35958	[57]
NLN	DKW1	AC-cable	700	[57]
NLM	NLN	AC-cable	3571	[57]
NLM	NLS	AC-cable	3927	[57]
NLM	NLS	CH_4 pipe	180193	[57]
NLM	DE00	CH_4 pipe	12092	[57]
NLS	NLM	AC-cable	1314	[57]
NLS	NLWO	AC-cable	2800	[57]
NLS	BE00	AC-cable	2780	[57]
NLS	UK00	AC-cable	3000	[57]
NLWO	NLS	AC-cable	2800	[97]

Table 2: Detailed overview of all OWFs considered in this project

				OWF Capacity [GW]			
Country	**Node**	**OWF**	**Status**	**2020**	**2030**	**2040**	**2050**
NL	NLWO	Borssele		1.5025	1.5025	1.5025	0
NL	NLWO	HKZ		1.649	1.649	1.52	0
NL	NLWO	HKN		0.228	0.987	0.987	0.987
NL	NLWO	HKW		0	1.456	2.1	2.1
NL	NLNO	Ten noorden van den Waddeneilanden		0.6	0.7	0.7	0.7
NL	NLWO	Ijmuiden Ver	Tendering in 2023, operational in 2027	0	0	4	4
NL	NLWO	Nederwiek	Tendering in 25/26	0	0	6	6
NL	NLNO	Doordewind	Tendering in 27	0	0	4	4
NL	NLNW	Search area 3	Search area after 2030	0	0	2	2
NL	NLNO	Search area 4	Search area after 2030	0	0	10	10
NL	NLNW	Search area 5 (mb)	Search area after 2030	0	0	2	2
NL	NLNW	Search area 6	Search area after 2030	0	0	10	10
NL	NLNW	Search area 7	Search area after 2030	0	0	8	8
NL	NLNW	Search area 8	Search area after 2030	0	0	2	2
NL	NLWO	Rebuild of retired cap		0	0	0	3.0225
DE	DEO1		Already installed North Sea	6.636	0	0	0
DE	DEO1	N-3.5		0	0.42	0.42	0.42
DE	DEO1	N-3.6		0	0.48	0.48	0.48
DE	DEO1	N-3.7		0	0.225	0.225	0.225
DE	DEO1	N-3.8		0	0.433	0.433	0.433
DE	DEO1	N-6.6		0	0.63	0.63	0.63
DE	DEO1	N-6.7		0	0.27	0.27	0.27
DE	DEO1	N-7.2		0	0.98	0.98	0.98
DE	DEO1	N-9.1		0	2	2	2
DE	DEO1	N-9.2		0	2	2	2
DE	DEO1	N-9.3		0	1.5	1.5	1.5
DE	DEO1	N-10.1		0	2	2	2
DE	DEO1	N-10.2		0	0.5	0.5	0.5
DE	DEO1	N-11.1		0	2	2	2
DE	DEO1	N-11.2		0	1.5	1.5	1.5
DE	DEO1	N-12.1		0	2	2	2
DE	DEO1	N-12.2		0	2	2	2
DE	DEO1	N-12.3		0	1	1	1
DE	DEO1	N-13.1		0	0	0.5	0.5
DE	DEO1	N-13.2		0	0	1	1
DE	DEO1	N-13.3		0	0	2	2
DE	DEO2	N-17 b		0	0	2	2
DE	DEO2	N-18		0	0	2	2
DE	DEO3	N-19		0	0	2	2
DE	DEO2	N-20		0	0	2	2
DE	DEO1	N-21.1		0	0	2	2
UK	UKMO	Dogger bank A	First power expected in 2023	0	1.2	1.2	1.2
UK	UKMO	Dogger bank B	First power expected in 2024	0	1.2	1.2	1.2
UK	UKMO	Dogger bank C	Turbine installation starts 2025	0	1.2	1.2	1.2
UK	UKMO	Sofia	Expected to be fully operational by 2026	0	1.4	1.4	1.4
UK	UKMO	Hornsea 1	Operational by 2020	1.2	1.2	1.2	1.2
UK	UKMO	Hornsea 2	Operational by 2022	1.32	1.32	1.32	1.32
UK	UKMO	Hornsea 3	Planned	0	2.4	2.4	2.4
UK	UKMO	Hornsea 4	Planned	0	1	1	1
UK	UKMO	Outer Dowsing	Operational by 2030	0	1.5	1.5	1.5
UK	UKSO	East Anglia 1	Operational	0.714	0.714	0.714	0
UK	UKSO	East Anglia 1 North	Planned	0	0.8	0.8	0.8
UK	UKSO	East Anglia 2	Planned	0	0.9	0.9	0.9
UK	UKSO	East Anglia 3	Under contruction	0	1.4	1.4	1.4
UK	UKSO	Greater Gabbard	Operational since 2012	0.504	0.504	0.504	0
UK	UKNO	Berwick Bank		0	4.1	4.1	4.1
UK	UKNO	Seagreen	Some already operational by 2022	0	1.075	1.075	1.075
UK	UKNO	E1	Planned operational in 2028	0	2.61	2.61	2.61
UK	UKSO	Rebuilt of retired cap		0	0	0	1.218
BE	BEOF	Princess Elisabeth Zone	Planned	0	3.5	3.5	3.5
BE	BEOF	Installed	Already installed	2.261	2.261	2.261	2.261
NO	NOOF	Sørlige Nordsjø II	Planned for operational in 2030	0	3	3	3
NO	NOOF	Sørlige Nordsjø I	Search area after 2030	0	0	1.5	1.5
DK	DKOF	Nordsøen III	Tendered in 2023	0	3	10	10
DK	DKW1	Horns Rev III	Operational	0.4067	0	0	0

Appendix 2

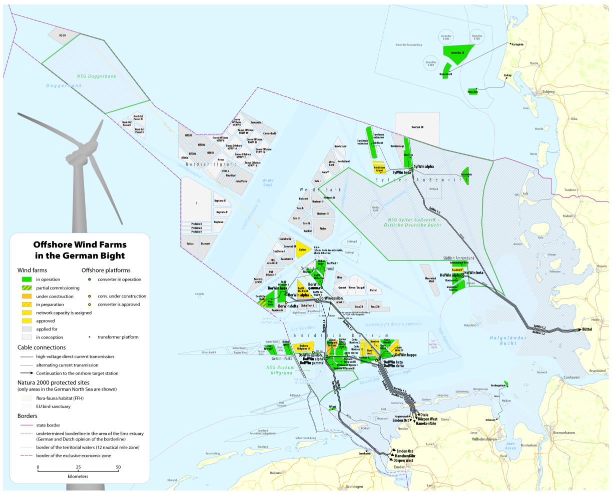

Figure 1: German offshore wind developments [98].

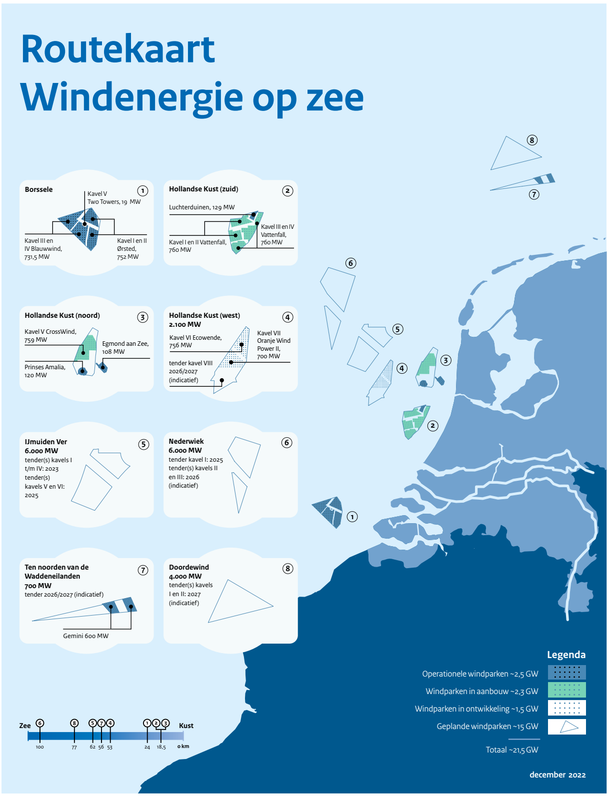

Figure 2: Planned Dutch offshore wind developments [82].

Appendix 3

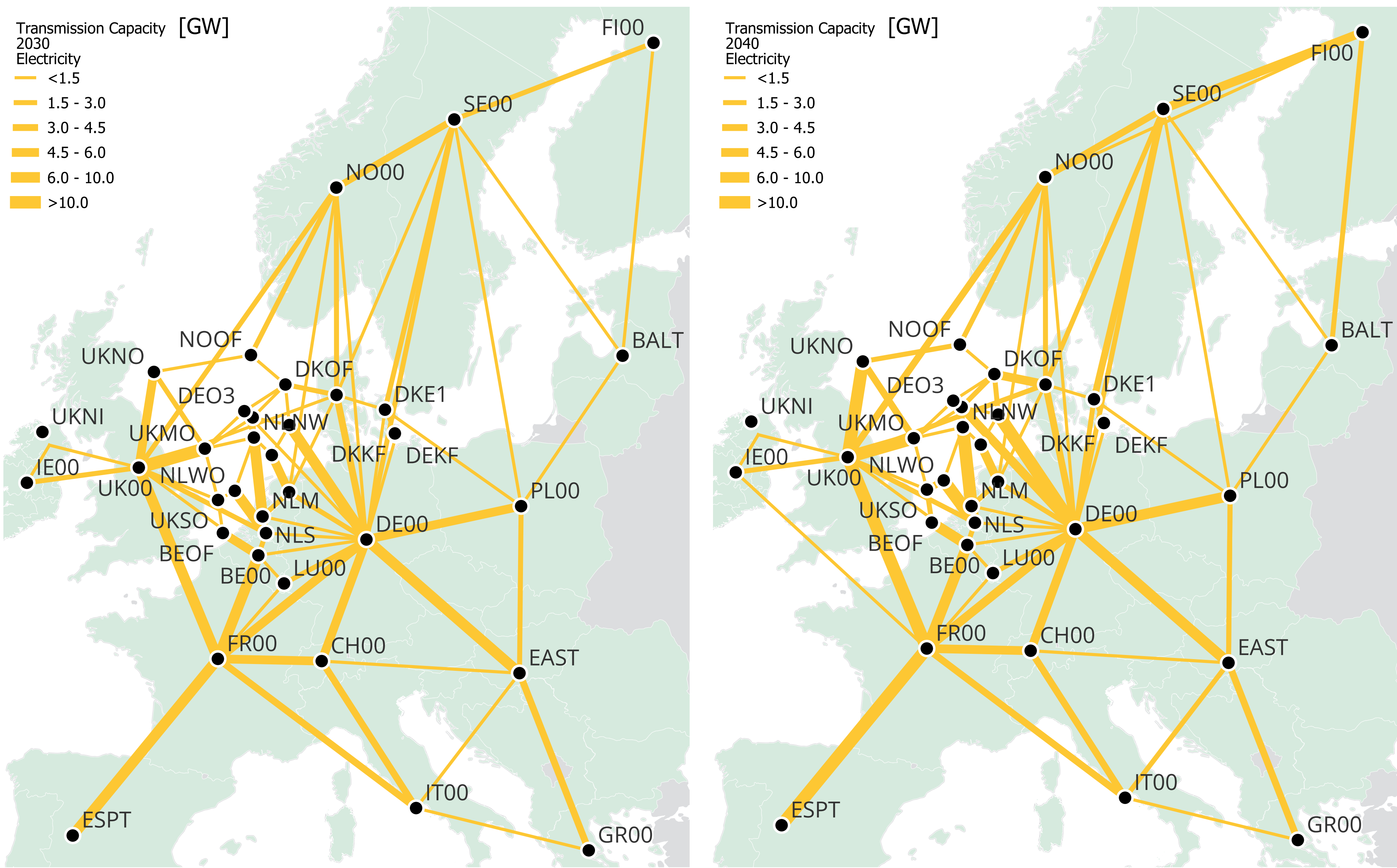

Figure 3: European wide electricity transmission network in 2030 (left) and 2040 (right), base scenario

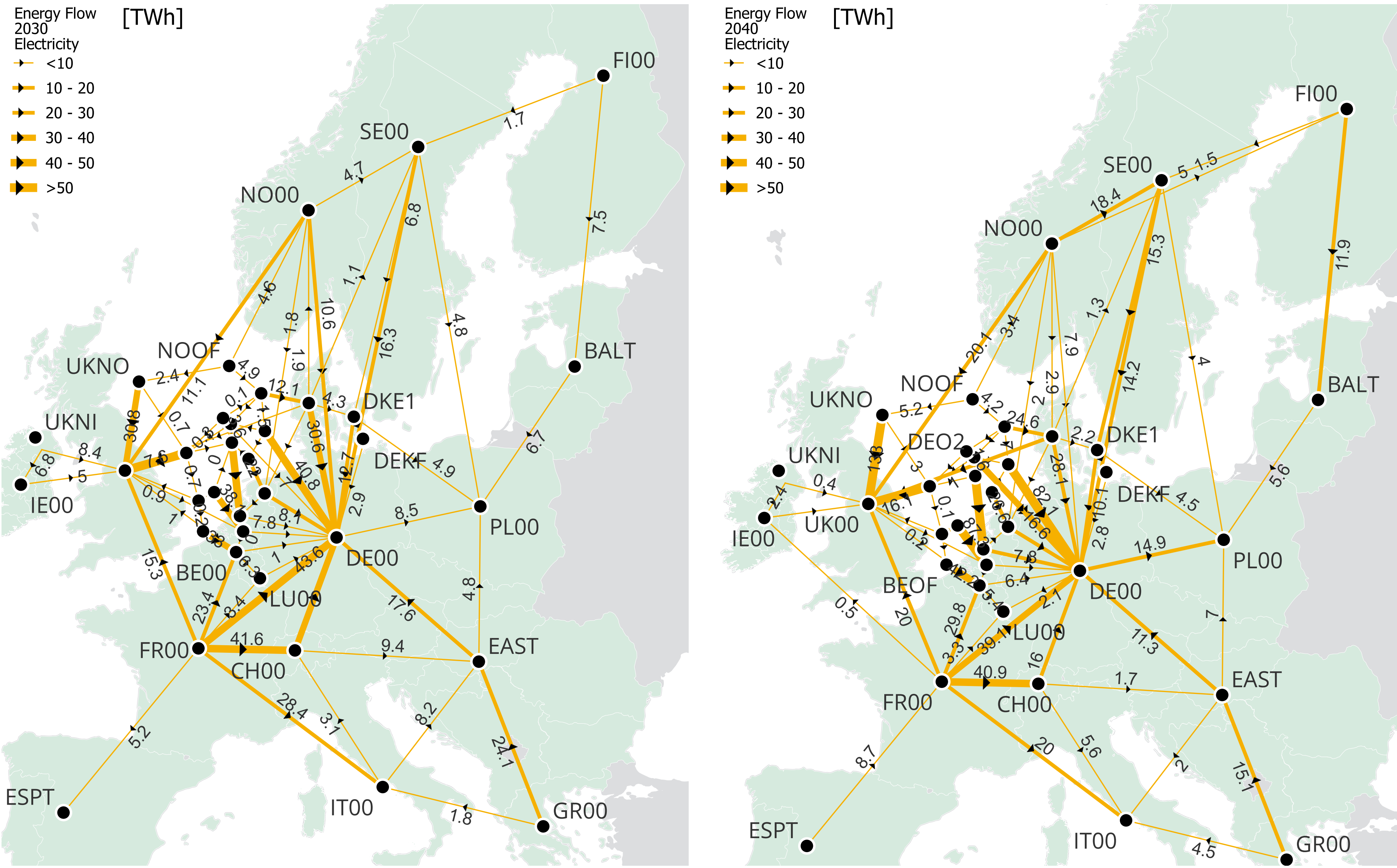

Figure 4: European net electricity energy flows in 2030 (left) and 2040 (right), base scenario.

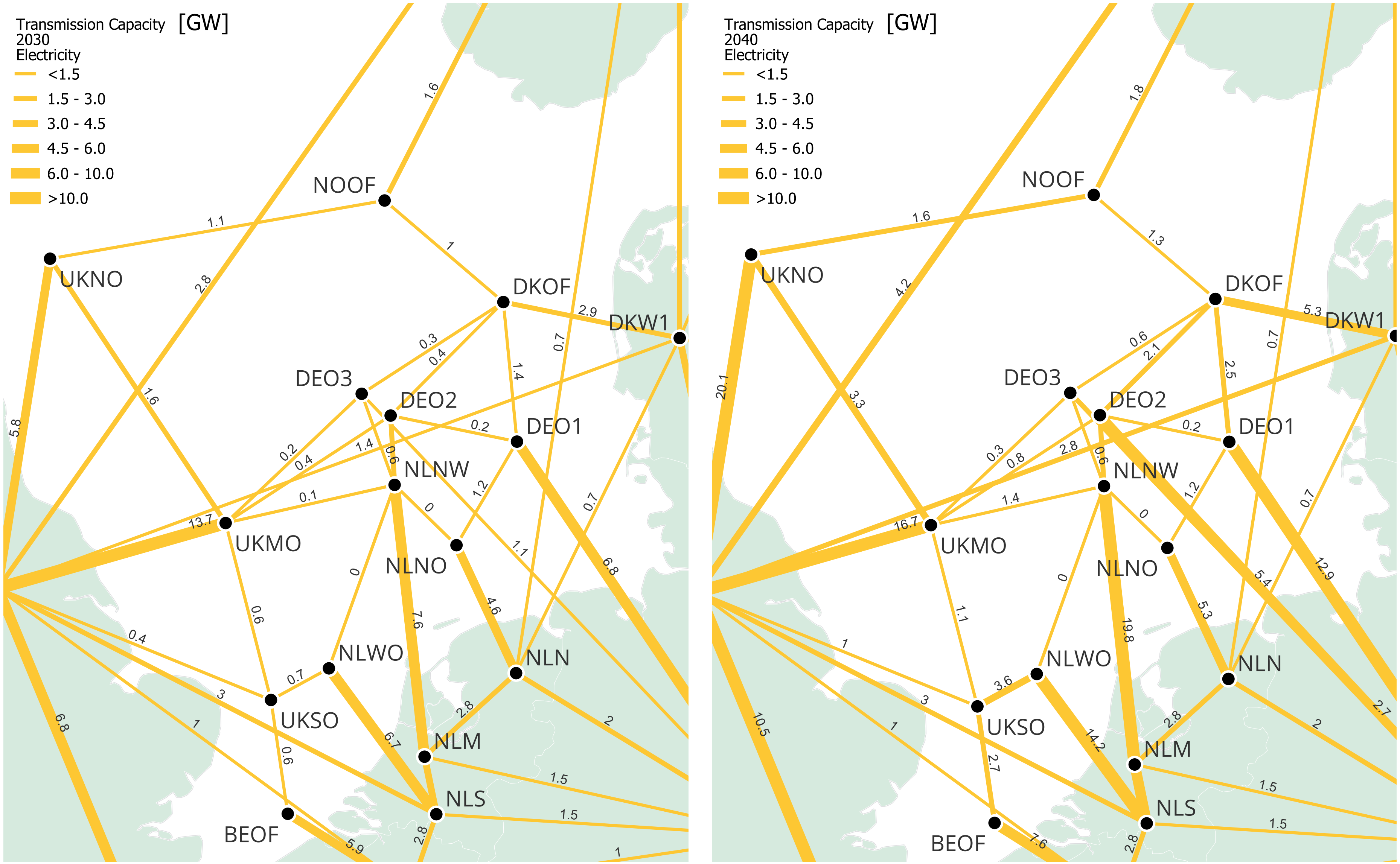

Figure 5: North Sea electricity transmission network in 2030 (left) and 2040 (right), base scenario.

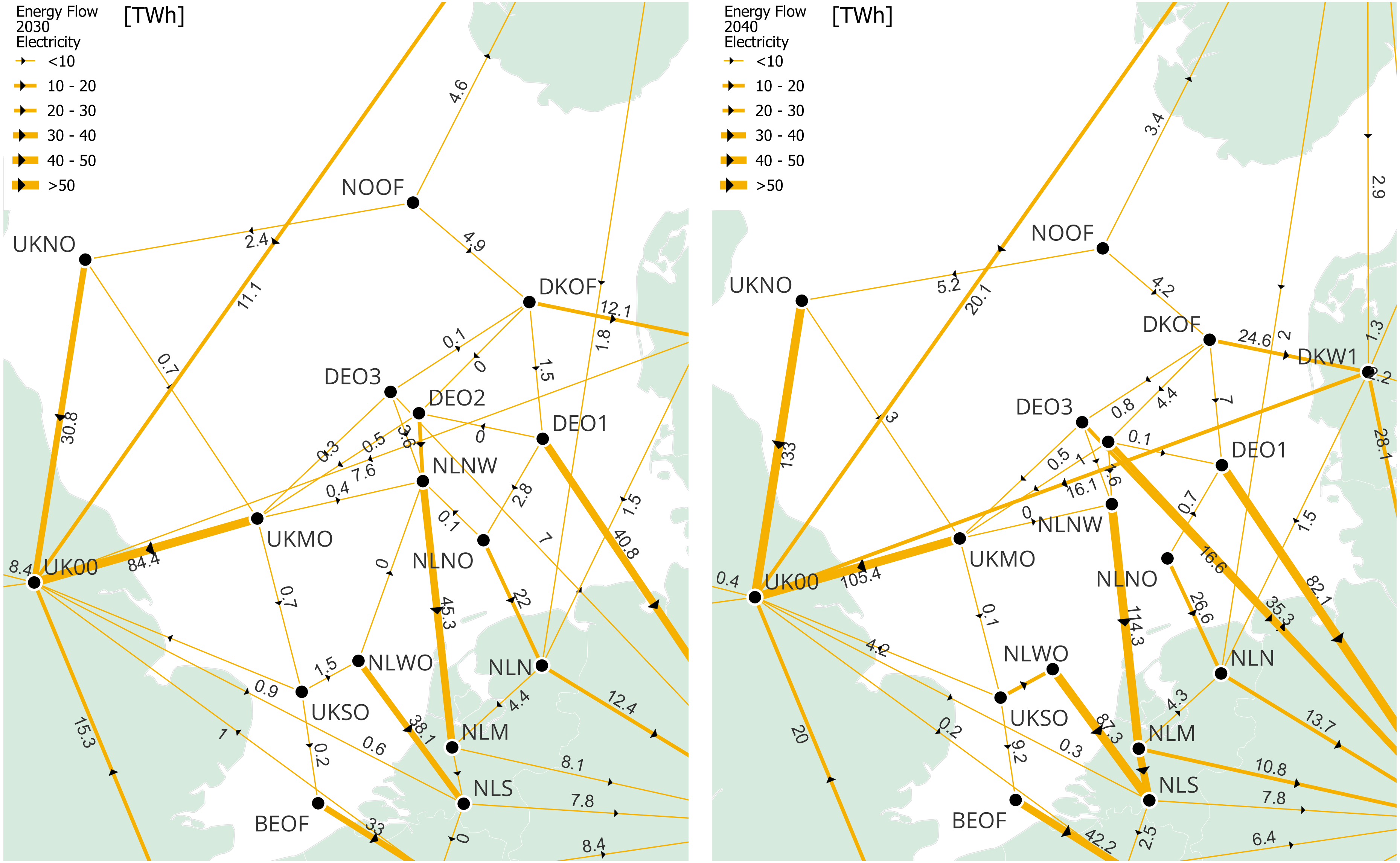

Figure 6: North Sea net electricity energy flows in 2030 (left) and 2040 (right), base scenario.

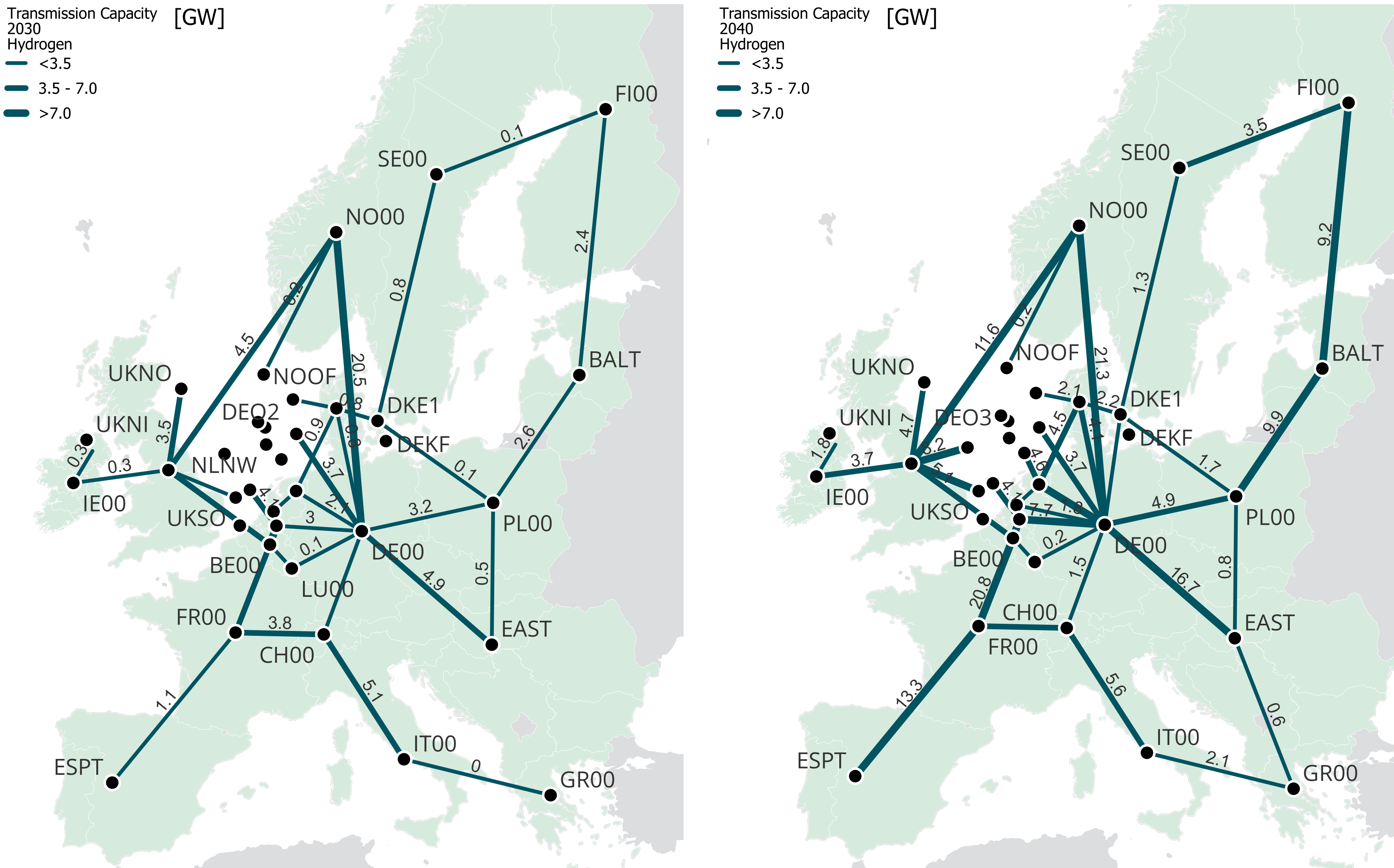

Figure 7: European hydrogen transmission network in 2030 (left) and 2040 (right), base scenario.

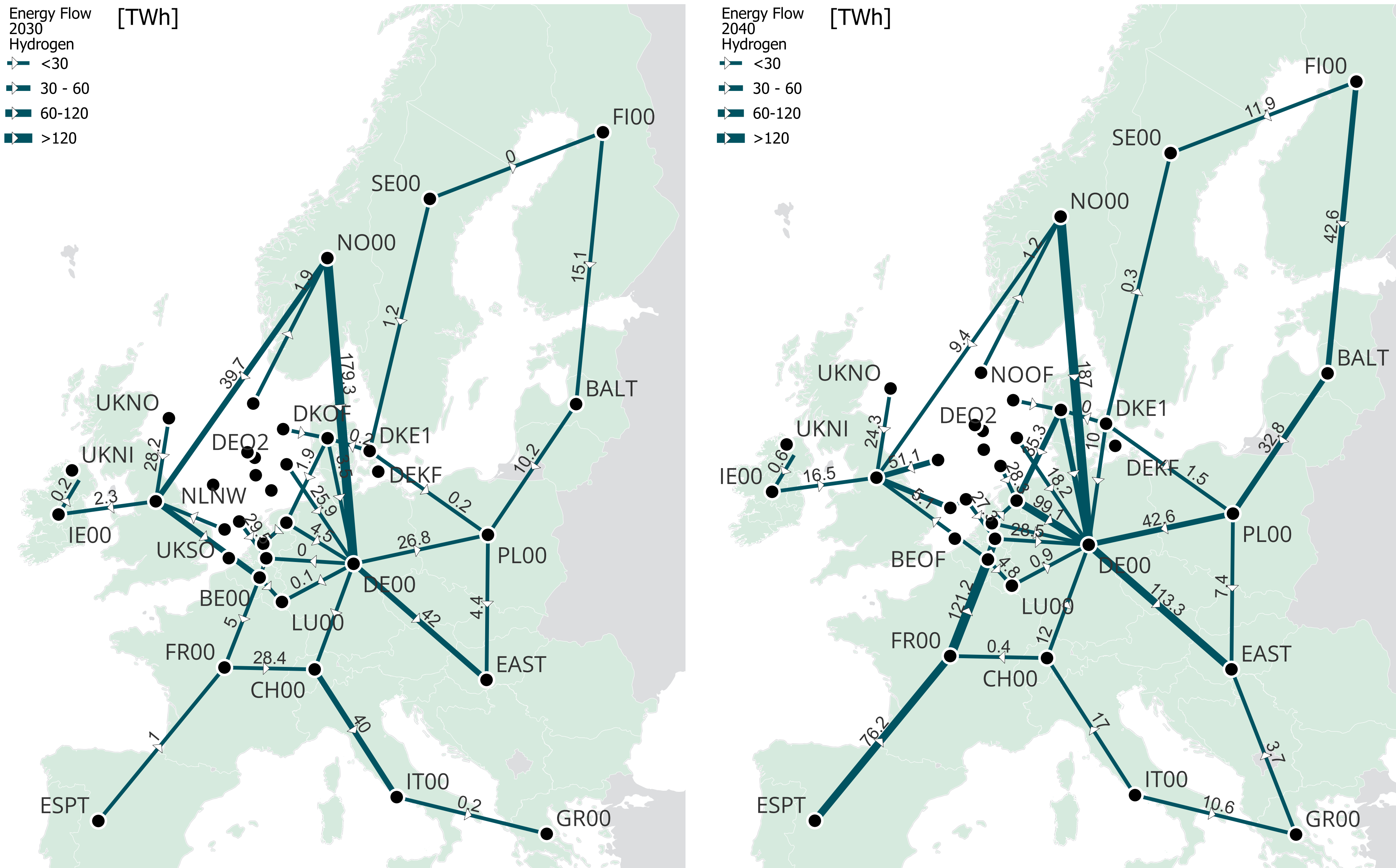

Figure 8: European hydrogen net flows in 2030 (left) and 2040 (right), base scenario.

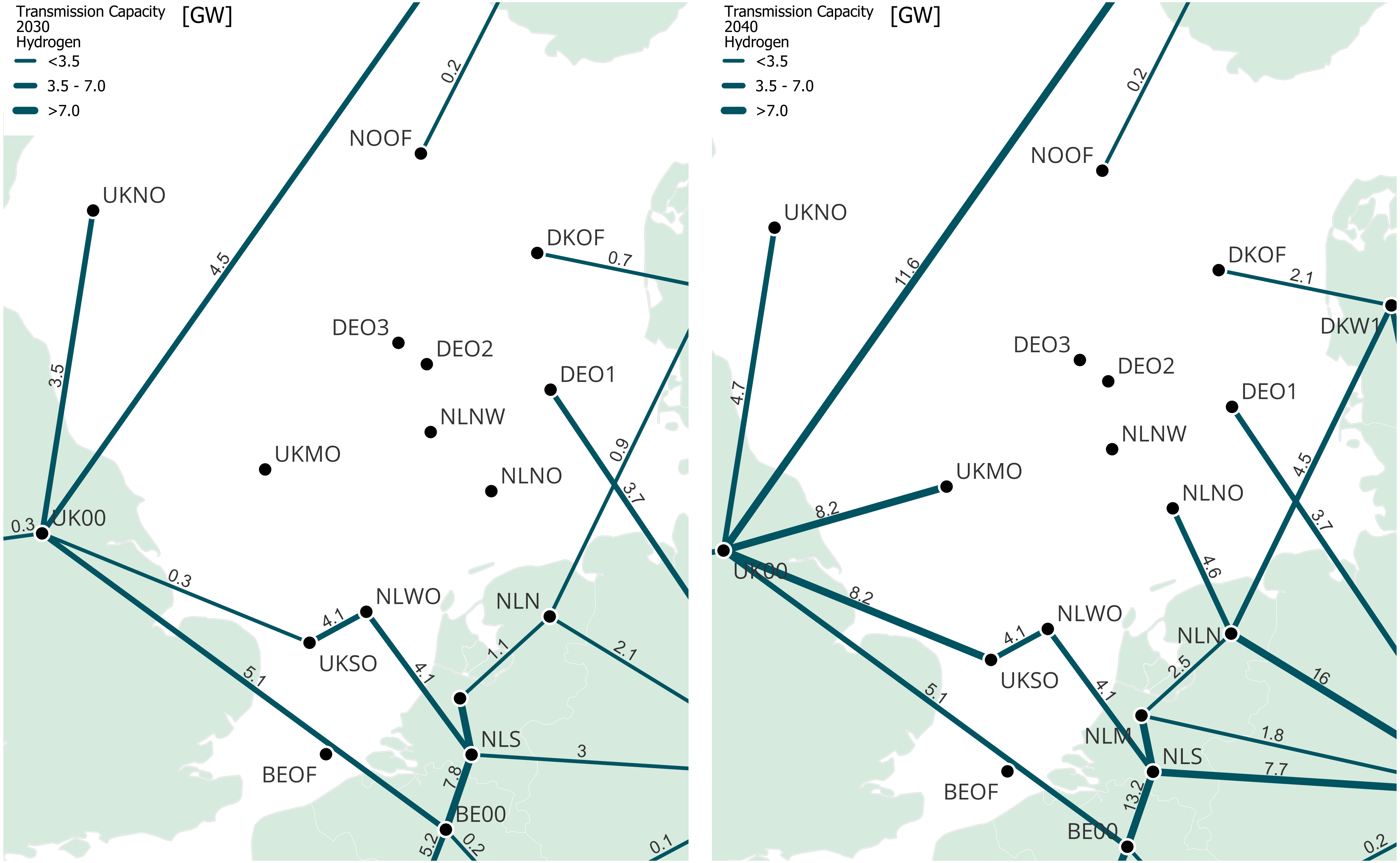

Figure 9: North Sea hydrogen transmission network in 2030 (left) and 2040 (right), base scenario.

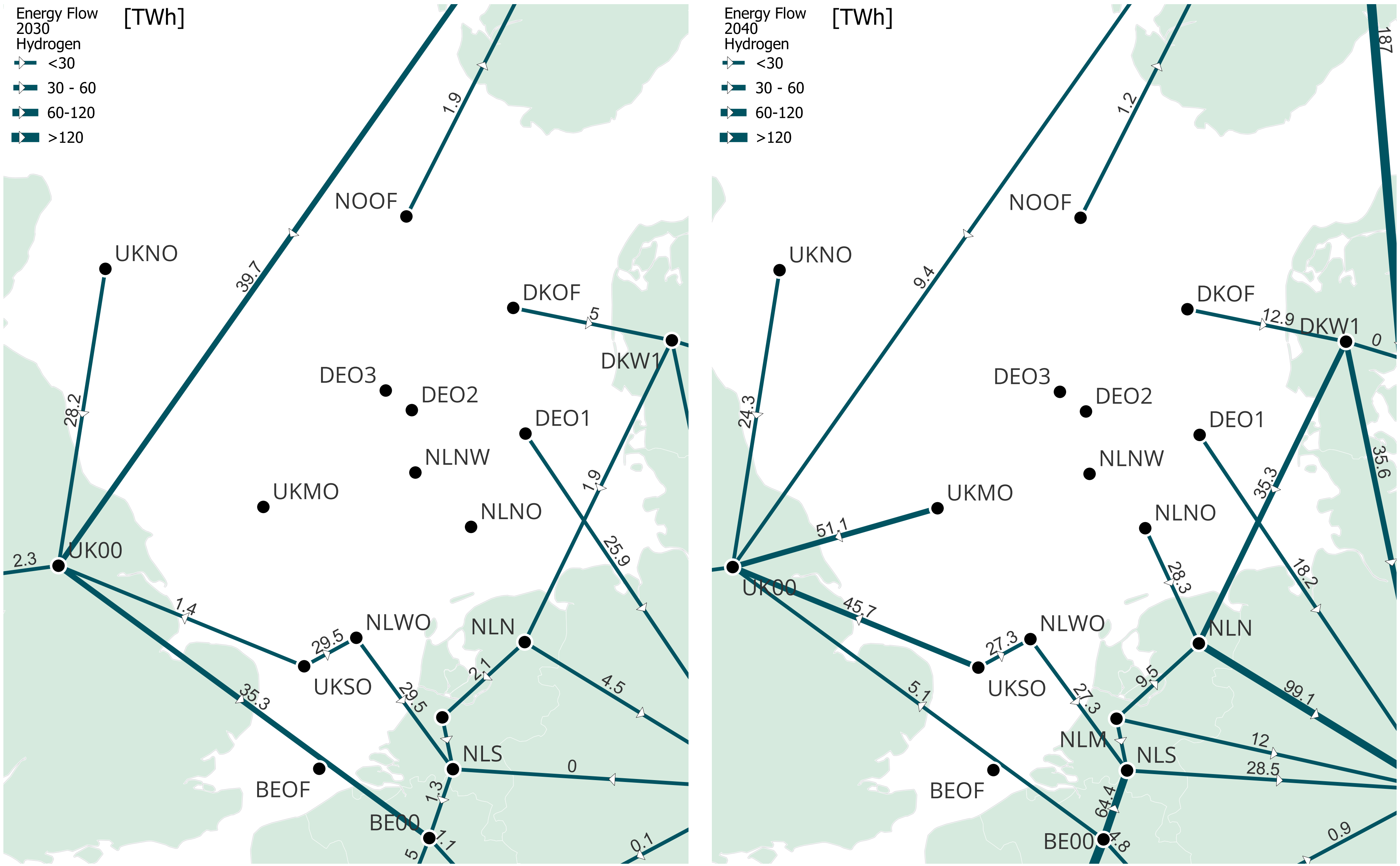

Figure 10: North Sea hydrogen net flows in 2030 (left) and 2040 (right), base scenario.

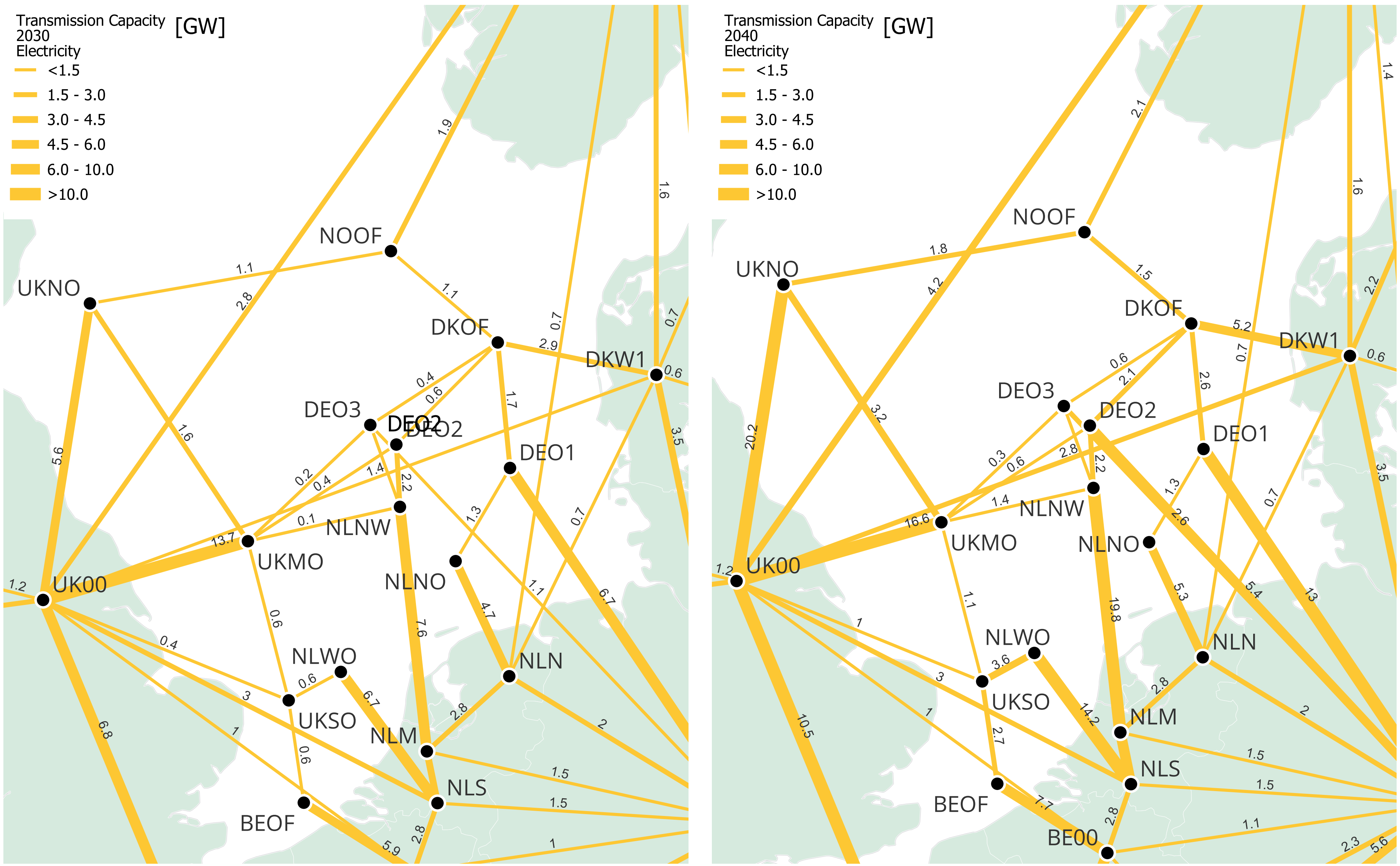

Figure 11: North Sea electricity network in 2030 (left) and 2040 (right), **Infra500 scenario**.

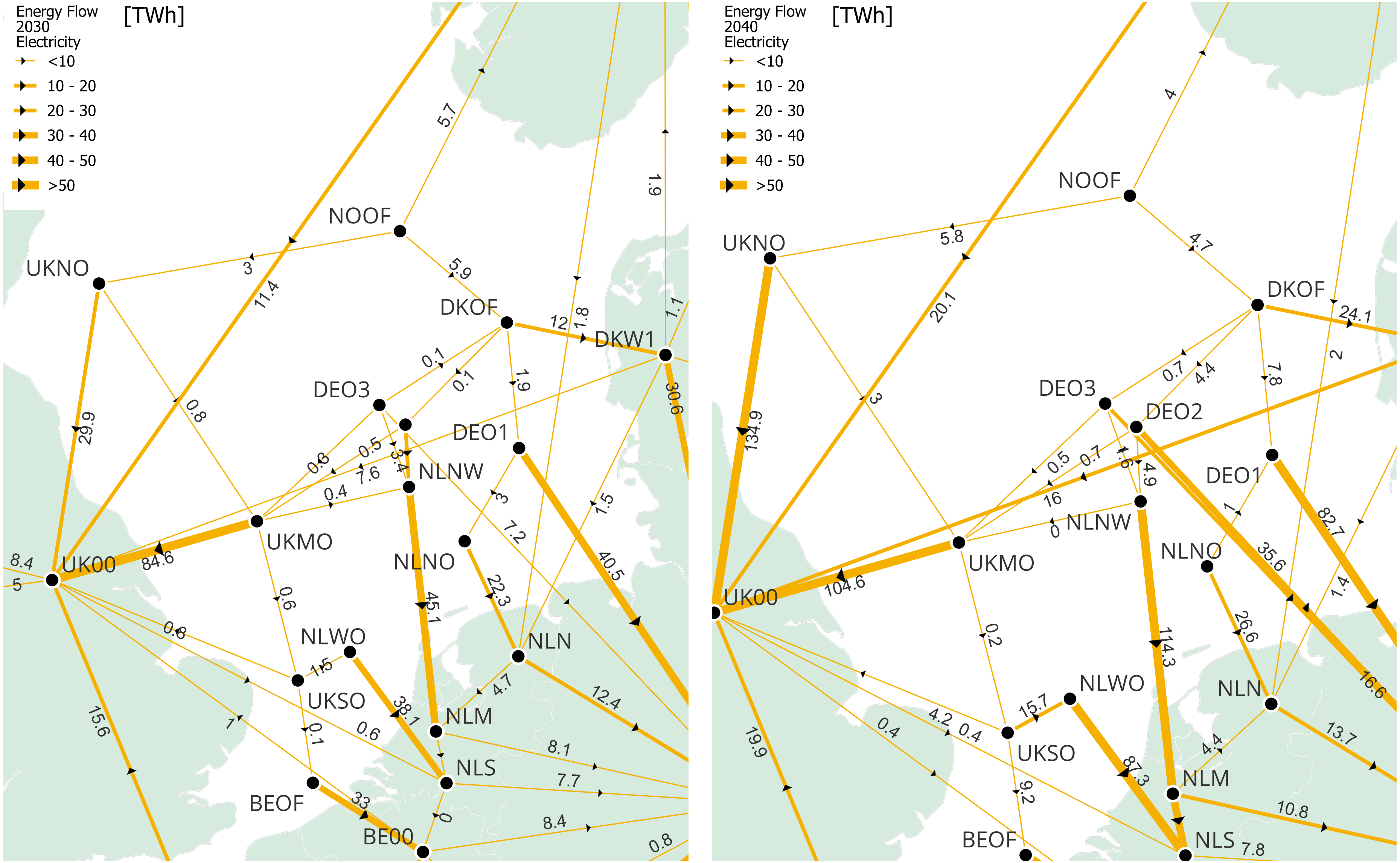

Figure 12: North Sea net electricity flows in 2030 (left) and 2040 (right), **Infra500 scenario**.

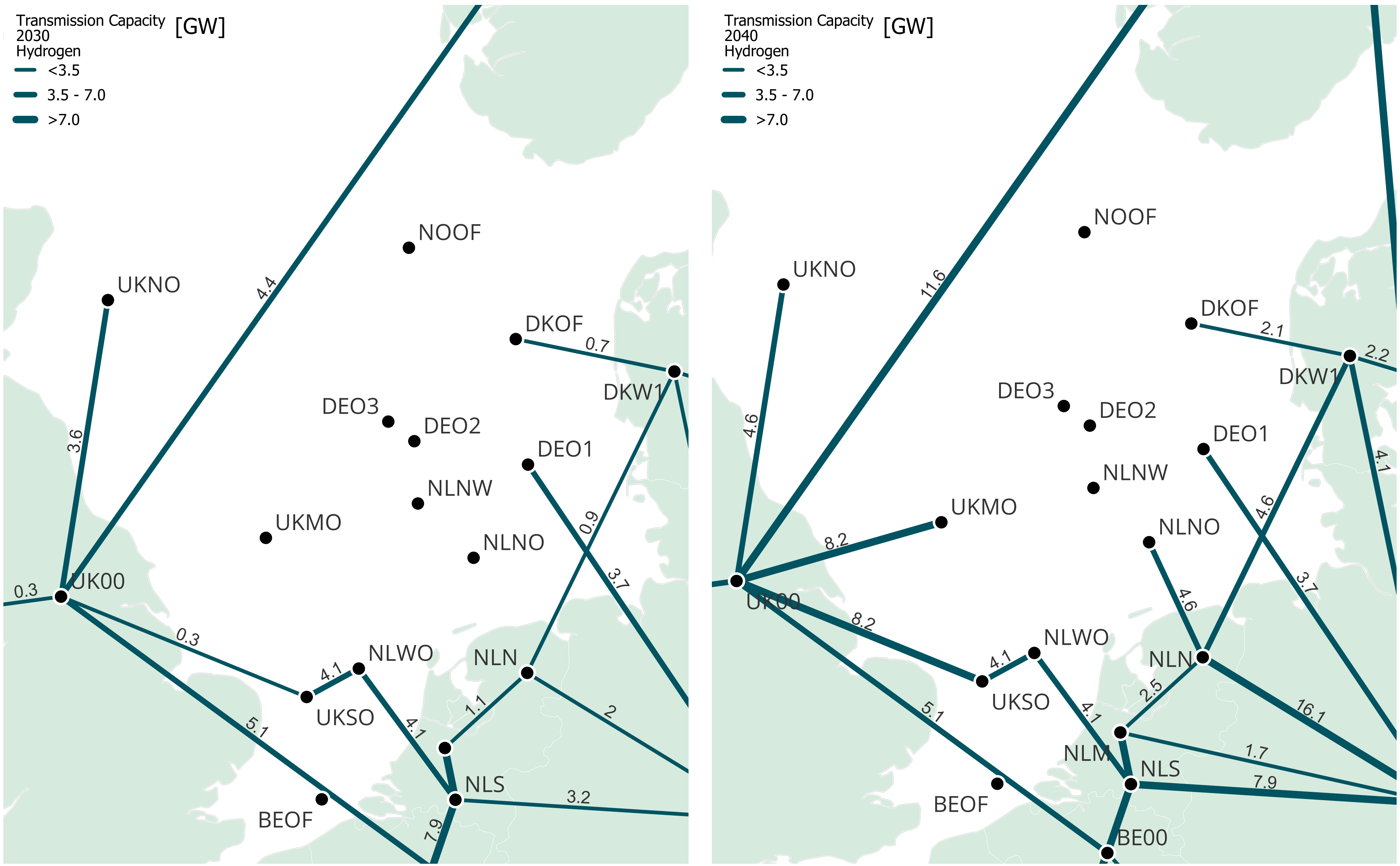

Figure 13: North Sea hydrogen network in 2030 (left) and 2040 (right), **Infra500 scenario**.

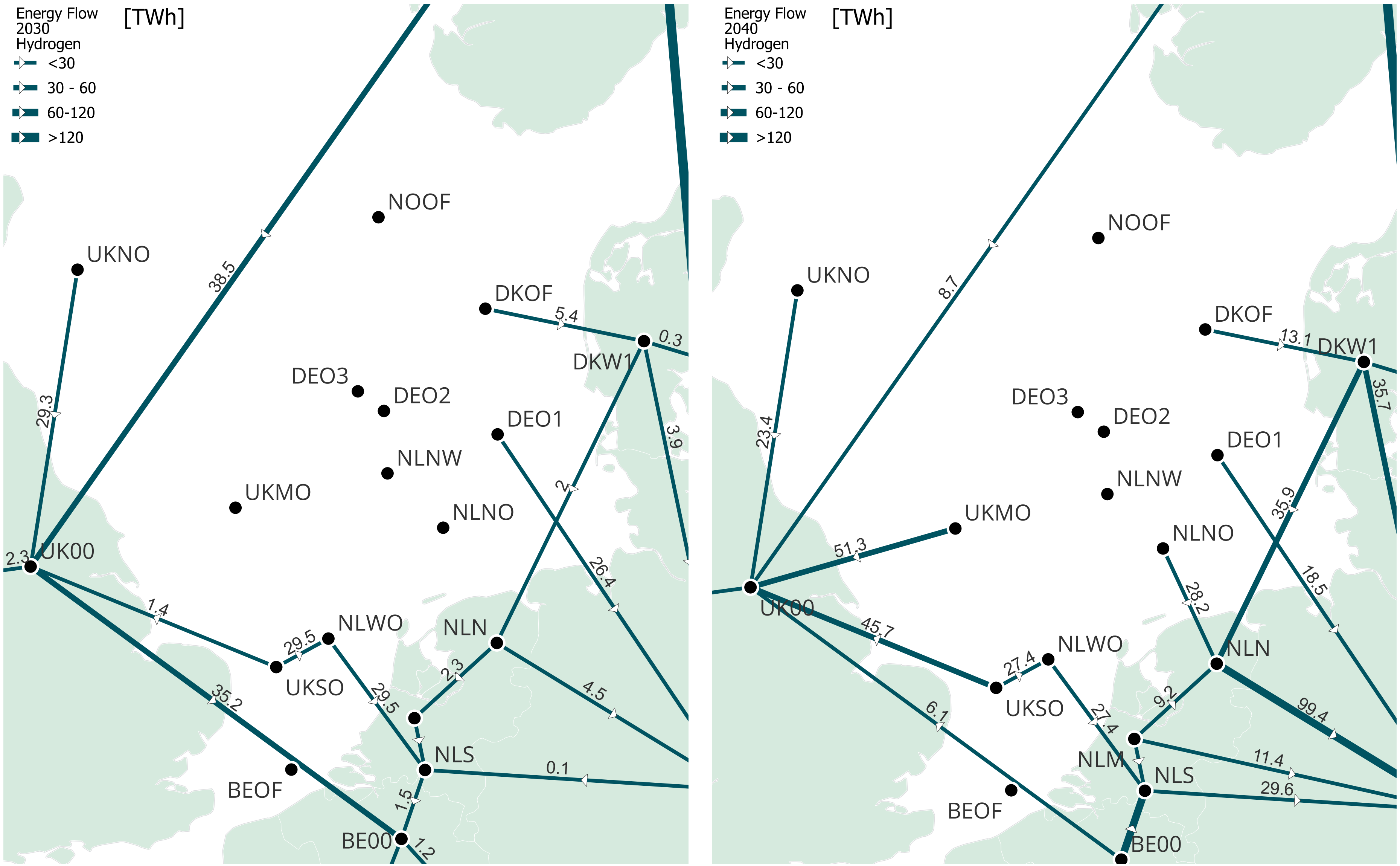

Figure 14: North Sea net hydrogen flows in 2030 (left) and 2040 (right), **Infra500 scenario**.

Bibliography

[1] United Nations Framework Convention on Climate Change. *Paris Agreement*. Tech. rep. 2015.

[2] European Council. *Fit for 55*. URL: https://www.consilium.europa.eu/en/policies/green-deal/fit-for-55-the-eu-plan-for-a-green-transition/.

[3] International Energy Agency. "Renewables 2021 - Analysis and forecast to 2026". In: (2021). URL: www.iea.org/t&c/.

[4] Eurostat. *Electricity production, consumption and market overview*. 2023. URL: https://ec.europa.eu/eurostat/statistics-explained/index.php?title=Electricity_production,_consumption_and_market_overview#Electricity_generation.

[5] IEA. *Heating - Fuels & Technologies*. Tech. rep. 2022. URL: https://www.iea.org/fuels-and-technologies/heating.

[6] IEA. *Transport*. URL: https://www.iea.org/reports/transport.

[7] European Commission. "REPowerEU plan". In: (2022).

[8] IEA. *Coping with the Crisis: Increasing Resilience in Small Businesses in Europe through Energy Efficiency Proposed Energy Saving Strategies*. Tech. rep. 2022. URL: www.iea.org.

[9] A Lawson, C Skopeliti, and J Otte. *Small businesses warn they may not survive winter due to UK energy bills*. 2022. URL: https://www.theguardian.com/business/2022/aug/25/sleepless-nights-business-owners-energy-bills-quadruple.

[10] European Commission. *Energy Poverty in the EU*. URL: https://energy.ec.europa.eu/topics/markets-and-consumers/energy-consumer-rights/energy-poverty-eu_en#:~:text=Energy%20poverty%20occurs%20when%20energy,their%20health%20and%20well%2Dbeing..

[11] IEA. *A 10-Point Plan to Reduce the European Union's Reliance on Russian Natural Gas*. Tech. rep. 2022. URL: www.iea.org/t&c/.

[12] Ana Fernández-Guillamón, Kaushik Das, Nicolaos A. Cutululis, et al. "Offshore wind power integration into future power systems: Overview and trends". In: *Journal of Marine Science and Engineering* 7.11 (2019). ISSN: 20771312. DOI: 10.3390/jmse7110399.

[13] International Energy Agency. *Offshore Wind Outlook 2019: World Energy Outlook Special Report*. Tech. rep. 2019. URL: www.iea.org/t&c/.

[14] Panit Potisomporn and Christopher R. Vogel. "Spatial and temporal variability characteristics of offshore wind energy in the United Kingdom". In: *Wind Energy* 25.3 (Mar. 2022), pp. 537–552. ISSN: 10991824. DOI: 10.1002/we.2685.

[15] DNV. *Development of offshore wind turbines*. 2019. URL: https://www.dnv.com/expert-story/maritime-impact/Offshore-wind-power-expands-globally.html.

[16] The Dutch Government. *Offshore wind enery*. URL: https://www.government.nl/topics/renewable-energy/offshore-wind-energy#:~:text=The%20North%20Sea%20is%20a,and%20(industrial)%20energy%20consumers..

[17] North Sea Energy. *Energy Atlas*. URL: https://north-sea-energy.eu/en/energy-atlas/.

[18] Netbeheer Nederland. *Capacity map electricity grid*. 2022. URL: https://capaciteitskaart.netbeheernederland.nl/.

[19] Mehdi Attar, Sami Repo, and Pierre Mann. "Congestion management market design-Approach for the Nordics and Central Europe". In: *Applied Energy* 313 (May 2022). ISSN: 03062619. DOI: 10.1016/j.apenergy.2022.118905.

[20] Fabio Monforti-Ferrario and Marta Poncela Blanco. "The impact of power network congestion, its consequences and mitigation measures on air pollutants and greenhouse gases emissions. A case from Germany". In: *Renewable and Sustainable Energy Reviews* 150 (Oct. 2021). ISSN: 18790690. DOI: 10.1016/j.rser.2021.111501.

[21] North Sea Energy. *North Sea Energy 2020-2022: Energy Hubs and Transport Infrastructure*. Tech. rep. 2022.

[22] Ioannis Konstantelos, Danny Pudjianto, Goran Strbac, et al. "Integrated North Sea grids: The costs, the benefits and their distribution between countries". In: *Energy Policy* 101 (Feb. 2017), pp. 28–41. ISSN: 03014215. DOI: 10.1016/j.enpol.2016.11.024.

[23] IEEE Staff. *The European North- Sea Countries Offshore Grid Initiatives*. IEEE, 2013. ISBN: 9781479913039.

[24] João Gorenstein Dedecca, Sara Lumbreras, Andrés Ramos, et al. "Expansion planning of the North Sea offshore grid: Simulation of integrated governance constraints". In: *Energy Economics* 72 (May 2018), pp. 376–392. ISSN: 01409883. DOI: 10.1016/j.eneco.2018.04.037.

[25] Ioannis Konstantelos, Rodrigo Moreno, and Goran Strbac. "Coordination and uncertainty in strategic network investment: Case on the North Seas Grid". In: *Energy Economics* 64 (May 2017), pp. 131–148. ISSN: 01409883. DOI: 10.1016/j.eneco.2017.03.022.

[26] Juan Gea Bermúdez, Rasmus Bo Bramstoft Pedersen, Matti Juhani Koivisto, et al. "Going offshore or not: Where to generate hydrogen in future". In: (2021). DOI: 10.36227/techrxiv.14806647.v2. URL: https://doi.org/10.36227/techrxiv.14806647.v2.

[27] Interreg North Sea Region. *Transnational energy cooperation between North Sea countries*. URL: https://northsearegion.eu/northsee/e-energy/transnational-energy-cooperation-between-north-sea-countries/#:~:text=The%20North%20Seas%20Energy%20Cooperation%20was%20formed%20in%202016%20where,of%20offshore%20wind%20energy%20in.

[28] European Commission. *The North Seas Energy Cooperation*. URL: https://energy.ec.europa.eu/topics/infrastructure/high-level-groups/north-seas-energy-cooperation_en#:~:text=of%20regional%20cooperation.-,NSEC%20members,EU%20on%2031%20January%202020..

[29] Alexander De Croo, Mette Frederiksen, Emmanuel Macron, et al. *Prime Ministers: Ostend Declaration On The North Seas As Europe's Green Power Plant Delivering Cross-Border Projects and Anchoring The Renewable Offshore Industry in Europe*. 2023.

[30] Mette Frederiksen, Mark Rutte, Alexander De Croo, et al. *THE ESBJERG DECLARATION on The North Sea as a Green Power Plant of Europe*. Tech. rep. 2022.

[31] North Sea Wind Power Hub Programme. *Unlocking the North Sea as a Green Powerplant An ambitious next step for the North Sea*. Tech. rep. URL: www.northseawindpowerhub.eu..

[32] L. M. Andreasson, J. E. H. Kusters, J. F. Wiegner, et al. "Interdisciplinary perspectives on offshore energy system integration in the North Sea: A systematic literature review". In: (2023).

[33] Juan Gea-Bermúdez, Lise Lotte Pade, Matti Juhani Koivisto, et al. "Optimal generation and transmission development of the North Sea region: Impact of grid architecture and planning horizon". In: *Energy* 191 (Jan. 2020). ISSN: 03605442. DOI: 10.1016/j.energy.2019.116512.

[34] Rafael Martínez-Gordón, Laura Gusatu, Germán Morales-España, et al. "Benefits of an integrated power and hydrogen offshore grid in a net-zero North Sea energy system". In: *Advances in Applied Energy* 7 (Sept. 2022). ISSN: 26667924. DOI: 10.1016/j.adapen.2022.100097.

[35] Rafael Martínez-Gordón, Manuel Sánchez-Diéguez, Amirhossein Fattahi, et al. "Modelling a highly decarbonised North Sea energy system in 2050: A multinational approach". In: *Advances in Applied Energy* 5 (Feb. 2022). ISSN: 26667924. DOI: 10.1016/j.adapen.2021.100080.

[36] Matti Koivisto, Juan Gea-Bermúdez, and Poul Sørensen. "North Sea offshore grid development: Combined optimisation of grid and generation investments towards 2050". In: *IET Renewable Power Generation*. Vol. 14. 8. Institution of Engineering and Technology, June 2020, pp. 1259–1267. DOI: 10.1049/iet-rpg.2019.0693.

[37] Guidehouse and Berenschot. *Offshore wind system integration 2030-2040*. Tech. rep.

[38] Manuel Sánchez Diéguez, Amirhossein Fattahi, Jos Sijm, et al. "Modelling of decarbonisation transition in national integrated energy system with hourly operational resolution". In: *Advances in Applied Energy* 3 (Aug. 2021). ISSN: 26667924. DOI: 10.1016/j.adapen.2021.100043.

[39] Alessandro Singlitico, Jacob Østergaard, and Spyros Chatzivasileiadis. "Onshore, offshore or in-turbine electrolysis? Techno-economic overview of alternative integration designs for green hydrogen production into Offshore Wind Power Hubs". In: *Renewable and Sustainable Energy Transition* 1 (Aug. 2021), p. 100005. ISSN: 2667095X. DOI: 10.1016/j.rset.2021.100005.

[40] J. van Stralen, J. Sipma, and J. Gerdes. *An analysis of the value of offshore hydrogen production in relation to alternatives*. Tech. rep. 2020. URL: http://www.h2data.de/.

[41] TNO. *Offshore hydrogen for unlocking the full energy potential of the North Sea*. Tech. rep. 2022. URL: https://energy.ec.europa.eu/system/files/2022-09/220912_NSEC_Joint_Statement_Dublin_Ministerial.pdf.

[42] ENTSOG and ENTSO-E. *TYNDP 2022 Scenario Report — Version. April 2022*. Tech. rep. 2022.

[43] Henrik Lund, Jakob Zinck Thellufsen, Poul Alberg Østergaard, et al. "EnergyPLAN – Advanced analysis of smart energy systems". In: *Smart Energy* 1 (Feb. 2021). ISSN: 26669552. DOI: 10.1016/j.segy.2021.100007.

[44] Alessandro Chiodi, J Paul Deane, Maurizio Gargiulo, et al. *Modelling Electricity Generation-Comparing Results: From a Power Systems Model and an Energy Systems Model*. Tech. rep.

[45] M Sánchez Diéguez, A Fattahi, and J Sijm. "Linear programing formulation of a high temporal and technological resolution integrated energy system model for the energy transition Method name: Optimisation energy system model". In: *MethodsX* 9 (2022), p. 101732. DOI: 10.1016/j.adapen.2021.10. URL: http://creativecommons.org/licenses/by/4.0/.

[46] Machteld van den Broek, Evelien Brederode, Andrea Ramírez, et al. "Designing a cost-effective CO2 storage infrastructure using a GIS based linear optimization energy model". In: *Environmental Modelling and Software* 25.12 (Dec. 2010), pp. 1754–1768. ISSN: 13648152. DOI: 10.1016/j.envsoft.2010.06.015.

[47] A. Fattahi, J. Sijm, and A. Faaij. *A systemic approach to analyze integrated energy system modeling tools: A review of national models*. Nov. 2020. DOI: 10.1016/j.rser.2020.110195.

[48] Christina Kockel, Lars Nolting, Jan Priesmann, et al. "Does renewable electricity supply match with energy demand? – A spatio-temporal analysis for the German case". In: *Applied Energy* 308 (Feb. 2022). ISSN: 03062619. DOI: 10.1016/j.apenergy.2021.118226.

[49] Eurostat. *NUTS- Nomenclature of Territorial Units for Statistics*. URL: https://ec.europa.eu/eurostat/web/nuts/nuts-maps.

[50] Entsog and Entso-e. *TYNDP 2022 Scenario Building Guidelines — Version. April 2022*. Tech. rep. 2022.

[51] Lukas Weimann and Matteo Gazzani. "A novel time discretization method for solving complex multi-energy system design and operation problems with high penetration of renewable energy". In: *Computers and Chemical Engineering* 163 (July 2022). ISSN: 00981354. DOI: 10.1016/j.compchemeng.2022.107816.

[52] Paul Nahmmacher, Eva Schmid, Lion Hirth, et al. "Carpe diem: A novel approach to select representative days for long-term power system modeling". In: *Energy* 112 (Oct. 2016), pp. 430–442. ISSN: 03605442. DOI: 10.1016/j.energy.2016.06.081.

[53] Ana Roxana Ciupuliga. *Transmission expansion planning under increased uncertainties towards efficient and sustainable power systems*. Tech. rep. 2013.

[54] K Poncelet, H Höschle, E Delarue, et al. *Selecting representative days for investment planning models*. Tech. rep. 2015. URL: http://www.mech.kuleuven.be/tme/research/1.

[55] James H. Merrick. "On representation of temporal variability in electricity capacity planning models". In: *Energy Economics* 59 (Sept. 2016), pp. 261–274. ISSN: 01409883. DOI: 10.1016/j.eneco.2016.08.001.

[56] F. Cebulla and T. Fichter. "Merit order or unit-commitment: How does thermal power plant modeling affect storage demand in energy system models?" In: *Renewable Energy* 105 (2017), pp. 117–132. ISSN: 18790682. DOI: 10.1016/j.renene.2016.12.043.

[57] Sander Meerman. *The role of interconnection and storage for the integration of renewable energy in the Netherlands*. Tech. rep. 2022.

[58] RVO. *Roadmap offshore wind*. Tech. rep. 2022. URL: https://www.rvo.nl/onderwerpen/windenergie-op-zee/plannen-windenergie-op-zee.

[59] Rijksdienst voor Ondernemend Nederland (RVO) and Ministerie van Economische Zaken en Klimaat (EZK). *Tendering document: European tender according to the public procedure for drawing up advice for the Energy Infrastructure Plan North Sea 2050*. Tech. rep. 2023.

[60] National Grid. *Pathway to 2030*. Tech. rep. 2022. URL: https://www.nationalgrideso.com/future-energy/pathway-2030-holistic-network-design.

[61] SSE Renewables. *Dogger Bank Wind Farm - Building the world's largest offshore wind farm*. 2022. URL: https://www.sserenewables.com/offshore/projects/dogger-bank/.

[62] RWE. *Sofia Wind Farm*. URL: https://sofiawindfarm.com/.

[63] ScottishPower Renewables. *East Anglia Offshore Wind*. URL: https://www.scottishpowerrenewables.com/pages/east_anglia.aspx.

[64] East Suffolk Council. *East Anglia One North and East Anglia Two*. URL: https://www.eastsuffolk.gov.uk/planning/national-infrastructure-and-energy-projects/offshore-windfarms/east-anglia/.

[65] East Suffolk Council. *East Anglia One and East Anglia Three*. URL: https://www.eastsuffolk.gov.uk/planning/national-infrastructure-and-energy-projects/offshore-windfarms/east-anglia-one-and-east-anglia-three/.

[66] Ørsted. *Hornsea Projects*. URL: https://hornseaprojects.co.uk/.

[67] Belgian Federal Public Service Government. *Belgian Offshore Wind*. 2023. URL: https://economie.fgov.be/en/themes/energy/belgian-offshore-wind-energy.

[68] Energistyrelsen (Danish Department of Energy). *Energiø Nordsøen*. URL: https://ens.dk/ansvarsomraader/energioeer/energioe-nordsoeen.

[69] German Federal Maritime and Hydrographic Agency (BSH). *Area Development Plan 2023 for the German North Sea and Baltic Sea*. Tech. rep. 2023.

[70] Norwegian Department of Water and Energy. *Map of Norwegian Offshore Planned Wind Farms*. URL: https://temakart.nve.no/link/?link=havvind.

[71] ENTSO-E. *ENTSO-E High-Level Report TYNDP 2022*. Tech. rep.

[72] Adriaan van der Welle, Ricardo Hernandez, German Morales-Espana, et al. *Effects of more available interconnection capacity on the energy transition*. Tech. rep. 2022.

[73] NREL Turbine models power curve archive. *IEA 10 MW turbine key parameters*. 2020. URL: https://nrel.github.io/turbine-models/IEA_10MW_198_RWT.html.

[74] NREL Turbine models power curve archive. *IEA 15 MW turbine key parameters*. 2020. URL: https://nrel.github.io/turbine-models/IEA_15MW_240_RWT.html.

[75] windturbinemodels.com. *Siemens SWT- 2.3- 108*. URL: https://en.wind-turbine-models.com/turbines/647-siemens-swt-2.3-108.

[76] windturbinemodels.com. *Siemens SWT- 3.6-130*. URL: https://en.wind-turbine-models.com/turbines/1468-siemens-swt-3.6-130.

[77] Liam Hayes and Andrew Blakers. *Windatlas.xyz*. URL: http://windatlas.xyz/download/.

[78] Liam Hayes, Matthew Stocks, and Andrew Blakers. "Accurate long-term power generation model for offshore wind farms in Europe using ERA5 reanalysis". In: *Energy* 229 (Aug. 2021). ISSN: 03605442. DOI: 10.1016/j.energy.2021.120603.

[79] Bowen Li, Sukanta Basu, Simon J. Watson, et al. "A brief climatology of dunkelflaute events over and surrounding the north and baltic sea areas". In: *Energies* 14.20 (Oct. 2021). ISSN: 19961073. DOI: 10.3390/en14206508.

[80] Masamichi Ohba, Yuki Kanno, and Shigeru Bando. "Effects of meteorological and climatological factors on extremely high residual load and possible future changes". In: *Renewable and Sustainable Energy Reviews* 175 (Apr. 2023). ISSN: 18790690. DOI: 10.1016/j.rser.2023.113188.

[81] Energistyrelsen (Danish Energy Agency). *Technology Data*. URL: https://ens.dk/en/our-services/projections-and-models/technology-data.

[82] Nordzeeloket. *Map of North Sea Search Areas 2022-2027*. 2022. URL: https://www.noordzeeloket.nl/beleid/programma-noordzee-2022-2027/.

[83] TNO. *Huge worldwide potential for floating wind turbines*. URL: https://www.tno.nl/en/sustainable/renewable-electricity/technology-wind/worldwide-potential-floating-wind/.

[84] Zhongjie Guo, Wei Wei, Mohammad Shahidehpour, et al. *Optimisation methods for dispatch and control of energy storage with renewable integration*. June 2022. DOI: 10.1049/stg2.12063.

[85] European Network of Transmission System Operators for Gas (ENTSO-G). *Transmission Capacity and System Development Map*. 2021. URL: https://www.entsog.eu/sites/default/files/2021-11/ENTSOG_CAP_2021_A0_1189x841_FULL_066_FLAT.pdf.

[86] Anthony Wang, Jaro Jens, David Mavins, et al. *Analysing future demand, supply, and transport of hydrogen EUROPEAN HYDROGEN BACKBONE Executive summary*. Tech. rep. 2021.

[87] Gas for Climate and Guidehouse. *Assessing the benefits of a pan-European hydrogen transmission network*. Tech. rep. 2023. URL: www.istockphoto.com.

[88] TenneT. *Grid Map Onshore The Netherlands*. 2023.

[89] European Network of Transmission System Operators for Electricity ENTSO-E. *HVDC UTILISATION AND UNAVAILABILITY STATISTICS 2021 From: DISTAC Subgroup*. Tech. rep. 2022.

[90] North Sea Wind Power Hub Programme. *Pathway Study- Key messages from the study*. Tech. rep. 2022.

[91] Tinne Van der Straeten, Lars Aagaard, Agnes Pannier-Runacher, et al. "Ostend Declaration of Energy Ministers on the North Sea as Europe's Green Power Plant". In: ().

[92] European Commission. *Offshore renewable energy*. URL: https://energy.ec.europa.eu/topics/renewable-energy/offshore-renewable-energy_en.

[93] C. T. Nieuwenhout. "Dividing the sea into small bidding zones? The legal challenges of connecting offshore wind farms to multiple countries". In: *Journal of Energy and Natural Resources Law* 40.3 (2022), pp. 315–335. ISSN: 23764538. DOI: 10.1080/02646811.2021.2011034.

[94] Steffan Brosschot. *Comparing hydrogen networks and electricity grids for transporting offshore wind energy to shore in the North Sea region. A spatial network optimisation approach*. Tech. rep. 2022.

[95] Matthew Little, Murray Thomson, and David Infield. "Electrical integration of renewable energy into stand-alone power supplies incorporating hydrogen storage". In: *International Journal of Hydrogen Energy* 32.10-11 (July 2007), pp. 1582–1588. ISSN: 03603199. DOI: 10.1016/j.ijhydene.2006.10.035.

[96] Anna Peecock, Katriona Edlmann, Julien Mouli-Castillo, et al. "Mapping hydrogen storage capacities of UK offshore hydrocarbon fields and exploring potential synergies with offshore wind". In: (2022). DOI: 10.6084/m9.figshare.c.6150395. URL: https://doi.org/10.6084/m9.figshare.c.6150395.

[97] Tennet. *Offshore Projects Netherlands*. URL: https://www.tennet.eu/projects/offshore-projects-netherlands#9618.

[98] Maximilian Dörrbecker. *Map of the offshore wind power farms in the German bight*. URL: https://en.wikipedia.org/wiki/List_of_offshore_wind_farms_in_Germany#/media/File:Map_of_the_offshore_wind_power_farms_in_the_German_Bight.png.